

# **Design and Implementation of a Maximum Power Point Tracking (MPPT) Charge Controller for a Standalone Photovoltaic System**

A Thesis

Submitted to the Department of Electrical and Electronic Engineering

Of

**Bangladesh University of Engineering and Technology**

By

Farhat Binte Azam - 1406135

Saraf Mahnaz – 1406160

Supervised by

**Dr. Kazi Mujibur Rahman**

Professor,

Department of Electrical and Electronic Engineering,  
Bangladesh University of Engineering and Technology, Dhaka

## **Declaration**

We hereby declare that this thesis report on ‘Design of a Maximum Power Point Tracking (MPPT) Solar Charge Controller’ has been written based only on the works and results found by us. Any material of the works or research or thesis used by researchers has been mentioned along with their references. This thesis, neither in whole nor in part, has been previously submitted for any degree by anyone else. This report is purely based on our research findings and is being submitted to the Department of Electrical and Electronic Engineering of Bangladesh University of Engineering and Technology.

### **Signature of Supervisor Signature of Authors**

-----  
Dr. Kazi Mujibur Rahman

Professor,

Department of Electrical and Electronics Engineering,  
Bangladesh University of Engineering and Technology,  
Dhaka – 1000

-----  
Farhat Binte Azam

Student ID: 1406135

-----  
Saraf Mahnaz

Student ID: 1406160

**Date of Submission:** 21/04/19

## **Acknowledgement**

We would firstly like to acknowledge our thesis supervisor Dr. Kazi Mujibur Rahman, Professor of Department of Electrical & Electronic Engineering, Bangladesh University of Engineering and Technology, for his guidance and kind advice in helping us decide on our topic of interest. He not only monitored our work all the way through but also taught us the basics of power electronics. Whenever we faced any challenge while building the hardware of the project, he always suggested better alternatives and great solutions.

We would like to convey our gratitude to our parents. They have been the encouragement behind our every successful endeavor. This thesis work is not an exception and this would not have been completed without their constant support and inspiration.

Finally, we put forward our humble gratitude to all our friends and well-wishers for their help, support and words of encouragement during the research work.

## **Abstract**

The world is experiencing a fast growth of renewable energy sector to combat global warming and reducing fossil fuel storage. Solar Power was the fastest-growing source of renewable energy worldwide last year, outstripping the growth in all other forms of power generation for the first time. Today it is one of the biggest concerns of researchers to reduce cost and increase efficiency of PV systems in order to make it more affordable and longer lasting. Hence the idea of Maximum Power Point Tracking (MPPT) system emerged to provide a maximized power output. An MPPT, or maximum power point tracker is an electronic DC to DC converter that optimizes the match between the solar array (PV panels), and the battery bank or utility grid. The main objective of the thesis was to track the maximum power point of a photovoltaic module so that the maximum possible power can be extracted from the PV system by varying certain conditions in algorithm and set up mechanism.

With a view to increasing the efficiency of the MPPT algorithm, we used incremental conductance method to track the maximum power point and were able to charge two 12V batteries in a time efficient manner successfully. Arduino Uno was used to implement incremental conductance algorithm and to generate pwm signal. A DC-DC boost converter was implemented with the help of a MOSFET driver circuit with high switching frequency. Two 12V batteries were used as loads and were charged at instantaneous maximum power points of the standalone PV system.

## **Table of Contents**

<b>Declaration.....</b>	1
<b>Acknowledgement.....</b>	2
<b>Abstract.....</b>	3
<b>Table of Contents .....</b>	4
<b>List of Tables .....</b>	7
<b>List of Figures.....</b>	8
<b>Glossary .....</b>	12
<b>Chapter 1 .....</b>	13
<b>Introduction.....</b>	13
1.1 Solar Energy in Bangladesh.....	13
1.2 Atmospheric Effects.....	18
1.3 Air Mass.....	19
1.4 Motion of the sun .....	19
1.5 Elevation Angle .....	20
1.6 Solar Radiation on a Tilted Surface .....	20
1.7 Solar Cell Efficiency.....	21
1.8 Solar Module type Used.....	22
Polycrystalline Silicon Solar PV:.....	22
1.9 MPPT Solar Charge Controller.....	23
1.10 Battery.....	24
<b>Chapter 2 .....</b>	25
<b>Solar Cell.....</b>	25
2.1 Structure of a Solar Cell.....	25
2.2 Construction of a Solar Panel .....	27
Glass:.....	28
Frame: .....	29
EVA Film:.....	30
Back Sheet: .....	30
Junction Box: .....	31
Bypass diodes: .....	32

2.3 Equivalent Circuit of Solar Cell.....	33
2.4 Solar Cell I-V Characteristics .....	35
2.5 Fill Factor.....	37
2.6 Effect of Temperature.....	39
2.7 Effect of Series Resistance.....	41
2.8 Effect of Shunt Resistance .....	43
2.9 Effect of Parasitic Resistance.....	45
2.10 Effect of Light Intensity.....	46
Concentrators: .....	47
Low Light Intensity: .....	47
2.11 Ideality Factor .....	48
2.12 Losses.....	49
2.12.1 Optical Losses.....	49
2.12.2 MOSFET Losses.....	50
2.12.3 Inductor Losses .....	50
2.12.4 Core Losses .....	50
2.12.5 Switching Loss.....	50
<b>Chapter 3 .....</b>	<b>51</b>
<b>Maximum Power Point Tracking Algorithms.....</b>	<b>51</b>
3.1 Introduction.....	51
3.2 Maximum Power Point Tracking.....	51
3.3 Methods of MPPT algorithms.....	52
3.3.1 Constant Voltage Method .....	52
3.3.2 Open Circuit Voltage Method.....	53
3.3.3 Short Circuit Current Method .....	54
3.3.4 Perturb and Observe Method .....	55
3.3.5 Incremental Conductance Method .....	57
<b>Chapter 4 .....</b>	<b>60</b>
<b>System Overview .....</b>	<b>60</b>
4.1 Panel Specifications .....	61
4.2 Voltage Sensor .....	61
4.3 Current Sensor .....	62
4.4 MOSFET Driver Circuit .....	66
4.5 Boost Converter .....	68

4.5.1 Inductor .....	72
4.5.2 Capacitor .....	73
4.5.3 Diode .....	73
4.5.4 MOSFET (IRF250) .....	74
4.6 Arduino Uno .....	75
4.6.1 Characteristics of Arduino Uno .....	75
4.7 Battery .....	77
<b>Chapter 5 .....</b>	<b>78</b>
<b>Experimentation for MPPT .....</b>	<b>78</b>
5.1 Searching MPP Using Nichrome Heater Coil .....	78
5.2 Searching MPP Using 24V Lead Acid Battery as a Load .....	81
5.3 Full System Software Simulation .....	88
5.4 Printed Circuit Board (PCB) Design.....	92
5.5 Experimental Setup.....	95
5.6 Result Analysis .....	96
<b>Chapter 6 .....</b>	<b>104</b>
<b>Conclusion .....</b>	<b>104</b>
6.1 Summary .....	104
6.2 Future Prospects.....	104
<b>Bibliography .....</b>	<b>105</b>
<b>Appendix A .....</b>	<b>107</b>
Code implemented in Incremental Conductance Method.....	107
SignalGenerator Library (.h file): .....	107
SignalGenerator Library (.cpp file): .....	109
Main Code:.....	112
<b>Appendix B .....</b>	<b>116</b>
Circuit implementation in PCB (Printed Circuit Board).....	116
<b>Appendix C .....</b>	<b>117</b>
Abbreviations .....	117
<b>Appendix D .....</b>	<b>118</b>
Solar Panel Characteristics .....	118

## **List of Tables**

<b>Table 1.1.1:</b> Monthly Solar Insolation at different locations of Bangladesh (in kWh/m <sup>2</sup> /day) Source: Dr. Shahida Rafique, Dhaka University, recorded from 1988 to 1998, printed 14.07.2007 -----	(14)
<b>Table 1.1.2:</b> Solar Radiation Data (1985-2005) -----	(15)
<b>Table 2.10.1:</b> Ideality Factor of different types of recombination -----	(48)
<b>Table 4.1:</b> Current sensor test results with comparison to actual value-----	(65)
<b>Table 4.5.1:</b> The list of components of DC-DC Boost Converter-----	(70)
<b>Table 5.1.1:</b> Data Sheet of MPPT testing using Nichrome Wire -----	(79)
<b>Table 5.2.1:</b> Data Sheet of MPPT testing using 24V Lead Acid Battery as a Load -----	(82)
<b>Table 5.2.2:</b> Data Sheet of MPPT testing using 24V Lead Acid Battery as a Load -----	(84)
<b>Table 5.2.3:</b> Data Sheet of MPPT testing using 24V Lead Acid Battery as a Load -----	(86)
<b>Table 5.6.1:</b> Collected data from full hardware when initial duty cycle was 30% -----	(96)
<b>Table 5.6.2:</b> Collected data from full hardware when initial duty cycle was 35% -----	(98)
<b>Table 5.6.3:</b> Collected data from full hardware when initial duty cycle was 40% -----	(100)
<b>Table 5.6.4:</b> Collected data from full hardware when initial duty cycle was 45% -----	(102)

## List of Figures

- Figure 1.1.1:** Monthly solar irradiation in different locations in Bangladesh ----- (16)
- Figure 1.3.1:** Air mass ratio of solar radiation ----- (17)
- Figure 2.1.1:** Solar Cell ----- (25)
- Figure 2.1.2:** PV Cells, Module and Array ----- (26)
- Figure 2.2.1:** Solar Panel Assembly ----- (27)
- Figure 2.2.2:** Front Glass Sheet of a Solar Panel ----- (28)
- Figure 2.2.3:** Frame of a Solar Panel ----- (29)
- Figure 2.2.4:** Junction Box of a Solar Panel ----- (31)
- Figure 2.2.5:** Bypass diodes of a Solar Panel ----- (32)
- Figure 2.3.1:** Equivalent Circuit of Solar PV Cell ----- (32)
- Figure 2.4.1:** I-V and P-V graphs showing the characteristic of a PV Module ----- (35)
- Figure 2.4.2:** I-V and P-V graphs of a Solar Panel ----- (36)
- Figure 2.5.1:** Fill Factor of a Solar Cell ----- (37)
- Figure 2.6.1:** Effect of Temperature on I-V graph of Solar Panel----- (39)
- Figure 2.7.1:** Schematic of a solar cell with series resistance ----- (41)
- Figure 2.7.2:** The effect of the series resistance on the I-V curve of Solar cell ----- (42)
- Figure 2.8.1:** Circuit diagram of a solar cell including the shunt resistance ----- (43)
- Figure 2.8.2:** The effect of the shunt resistance on the I-V curve ----- (43)
- Figure 2.9.1:** Parasitic series and shunt resistances in a solar cell circuit ----- (45)
- Figure 2.10.1:** The effect of concentration on the I-V characteristics of a solar cell ----- (46)
- Figure 2.12.1.1:** Optical Loss in a Solar Cell ----- (49)
- Figure 3.3.4.1:** Power versus Voltage curve for Perturb and Observe algorithm ----- (55)

<b>Figure 3.3.4.2:</b> Flowchart of Perturb and Observe algorithm -----	(56)
<b>Figure 3.3.5.1:</b> Flowchart of Incremental Conductance Method algorithm -----	(59)
<b>Figure 4.1:</b> Block Diagram of the system -----	(60)
<b>Figure 4.2.1:</b> Voltage divider circuit for voltage sensing -----	(62)
<b>Figure 4.3.1:</b> Hall Effect current sensor ACS712 -----	(62)
<b>Figure 4.3.2:</b> Pin configuration -----	(63)
<b>Figure 4.3.3:</b> Pin out diagram of ACS712 -----	(63)
<b>Figure 4.3.4:</b> Testing Current Sensor ACS712-----	(64)
<b>Figure 4.3.5:</b> Test Results of ACS712 -----	(65)
<b>Figure 4.4.1:</b> Pin out diagram of TLP250 -----	(66)
<b>Figure 4.4.2:</b> TLP250 IC -----	(66)
<b>Figure 4.4.3:</b> Schematic of MOSFET driver circuit -----	(67)
<b>Figure 4.4.4:</b> Input PWM Signal (5V Amplitude - blue) & Output PWM Signal (12V Amplitude -yellow) -----	(67)
<b>Figure 4.4.5:</b> MOSFET Driver circuit during experimentation-----	(68)
<b>Figure 4.5.1:</b> Circuit diagram of Boost Converter -----	(69)
<b>Figure 4.5.2:</b> Boost converter circuit -----	(71)
<b>Figure 4.5.3:</b> Output Voltage of Boost Converter (28V DC- blue line) when the input voltage was 12V and duty cycle 0.57 -----	(71)
<b>Figure 4.5.1.1:</b> Measuring inductance using LCR meter -----	(72)
<b>Figure 4.5.3.1:</b> MUR1560 IC -----	(73)
<b>Figure 4.5.3.2:</b> Pin out diagram of MUR1560 -----	(73)
<b>Figure 4.5.4.1:</b> Pin out diagram of IRF250 -----	(74)
<b>Figure 4.6.1:</b> Arduino Uno board -----	(75)

<b>Figure 4.6.2:</b> Pin out diagram of Arduino Uno board-----	(76)
<b>Figure 4.7.1:</b> 12V lead acid battery used in the thesis -----	(77)
<b>Figure 5.1.1:</b> Block Diagram of Setup -----	(78)
<b>Figure 5.1.2:</b> I-V graph of MPPT testing using Nichrome Wire -----	(80)
<b>Figure 5.1.3:</b> P-V Graph of MPPT testing using Nichrome Wire -----	(80)
<b>Figure 5.2.1:</b> Block Diagram of Setup -----	(81)
<b>Figure 5.2.1:</b> I-V Graph of MPPT testing using 24V Lead Acid Battery as a Load -----	(83)
<b>Figure 5.2.2:</b> P-V Graph of MPPT testing using 24V Lead Acid Battery as a Load -----	(83)
<b>Figure 5.2.3:</b> I-V Graph of MPPT testing using 24V Lead Acid Battery as a Load -----	(85)
<b>Figure 5.2.4:</b> P-V Graph of MPPT testing using 24V Lead Acid Battery as a Load -----	(85)
<b>Figure 5.2.5:</b> I-V Graph of MPPT testing using 24V Lead Acid Battery as a Load -----	(87)
<b>Figure 5.2.6:</b> P-V Graph of MPPT testing using 24V Lead Acid Battery as a Load -----	(87)
<b>Figure 5.3.1:</b> Schematic of the system using a fixed voltage DC source -----	(88)
<b>Figure 5.3.2:</b> Schematic of the system with a current controlled voltage source -----	(89)
<b>Figure 5.3.3</b> Output of the Serial Monitor -----	(89)
<b>Figure 5.3.4</b> Output of the PWM from Arduino UNO -----	(90)
<b>Figure 5.3.5</b> Output of the PWM from Optocoupler -----	(90)
<b>Figure 5.3.6</b> Output Voltage -----	(91)
<b>Figure 5.3.7</b> Output of the Current from Current Transfor -----	(92)
<b>Figure 5.4.1:</b> Schematic Design of PCB Board -----	(92)
<b>Figure 5.4.2:</b> Top of the PCB Board -----	(93)
<b>Figure 5.4.3:</b> Bottom of the PCB Board -----	(93)
<b>Figure 5.4.4:</b> PCB Board with the components -----	(94)
<b>Figure 5.5.1:</b> Full Experimental Setup -----	(95)

**Figure 5.6.1:** Current vs. Voltage (Blue) and Power vs. Voltage (Orange) Graph - Initial duty cycle – 30% ----- (97)

**Figure 5.6.2:** Current vs. Voltage (Blue) and Power vs. Voltage (Orange) Graph - Initial duty cycle – 35% ----- (99)

**Figure 5.6.3:** Current vs. Voltage (Blue) and Power vs. Voltage (Orange) Graph - Initial duty cycle – 40% ----- (101)

**Figure 5.6.4:** Current vs. Voltage (Blue) and Power vs. Voltage (Orange) Graph - Initial duty cycle – 45% ----- (103)

**Figure B.1:** Top Silk of PCB Board ----- (116)

**Figure B.2:** Bottom Copper of PCB Board ----- (116)

## Glossary

### **MPPT:**

Maximum Power Point Tracking (MPPT) is a technique used commonly with wind turbines and photovoltaic solar systems to maximize power extraction under all conditions.

### **V<sub>MPP</sub>:**

Voltage at Maximum Power Point

### **Light Generated Current:**

The generation of current in a solar cell is known as the “light-generated current”. The process is the absorption of incident photons to create electron-hole pairs.

### **Parasitic:**

Habitually relying on or exploiting other.

### **Ideality Factor:**

Factorization of Ideal Diode

### **Lead Acid Battery:**

The battery which contains compounds of lead such as lead-sulfate as electrodes and acid.

### **E Shape Core:**

Inductor core that looks like English alphabet E.

# Chapter 1

## Introduction

### **1.1 Solar Energy in Bangladesh**

Meeting the ever increasing demand is a challenge the world is facing and Bangladesh is no different. With a large population and huge potential as a nation, the growth of the country largely depends on the electricity. To tackle this problem, we have to look for different means of generating electricity. The problem we face while doing so is the environmental issues which have been acting up. Government has set up the goal of providing electricity to all by 2020 and to ensure reliable and quality supply of electricity at a reasonable and affordable price. Sustainable social and economic development depends on adequate power generation capacity of a country. There is no other way for accelerating development except to increase the power generation by fuel diversification. Development of Renewable Energy is one of the important strategies adopted as part of Fuel Diversification Program. In line with the Renewable Energy policy 2009, the Government is committed to facilitate both public and private sector investment in Renewable Energy projects to substitute indigenous non-renewable energy supplies and scale up contributions of existing Renewable Energy based electricity productions. The Renewable Energy Policy envisions that 5% of total energy production will have to be achieved by 2015 and 10% by 2020. The government introduced a scheme known as solar home systems (SHS) to provide electricity to households with no grid access. The program reached 3 million households as of late 2014 and, with more than 50,000 systems being added per month since 2009, the World Bank has called it "the fastest growing solar home system program in the world." The government is also presently focusing on net-metering to boost solar power generation and popularize it among the masses hoping the renewable energy's stake will leap to 1,000MW by the year 2020.

There are mainly two ways in which the solar to electrical conversion can be done, solar thermal and solar photovoltaic. In terms of Solar thermal, it is the conventional AC electricity generation produced by steam turbine; heat extracted from intense solar ray is used to produce steam and apart is stored in thermally insulated tanks for usage during lack of sunshine or night time. Solar photovoltaic use cells made of silicon or certain types of semiconductor materials which convert the light energy absorbed from incident sunshine into

DC electricity. To make up for intermittency and night time storage of the generated electricity into battery is needed.

### **Some of the Major Solar Power Ongoing Projects in Bangladesh -**

- 650 KW<sub>p</sub> (400 kW load) Solar Mini Grid Power Plant at remote haor area of Sullahupazila in Sunamgonj district under Climate Change Trust Fund (CCTF) on turnkey basis.
- 8 MW<sub>p</sub> Grid Connected Solar PV Power Plant at Kaptai Hydro Power Station, at Rangamati on turnkey basis.
- 3 MW<sub>p</sub> Grid Connected Solar PV Power Plant at Sharishabari, Jamalpur on IPP basis.
- 30 MW<sub>p</sub> Solar Park Project adjacent to new Dhorola Bridge, Kurigram on IPP basis.
- Solar Street Lighting Projects in seven City Corporations of the country.

Month	Dhaka	Rajshahi	Sylhet	Bogra	Barisal	Jessore
January	4.03	3.96	4	4.01	4.17	4.25
February	4.78	4.47	4.63	4.69	4.81	4.85
March	5.33	5.88	5.2	5.68	5.3	4.5
April	5.71	6.24	5.24	5.87	5.94	6.23
May	5.71	6.17	5.37	6.02	5.75	6.09
June	4.8	5.25	4.53	5.26	4.39	5.12
July	4.41	4.79	4.14	4.34	4.2	4.81
August	4.82	5.16	4.56	4.84	4.42	4.93
September	4.41	4.96	4.07	4.67	4.48	4.57
October	4.61	4.88	4.61	4.65	4.71	4.68
November	4.27	4.42	4.32	4.35	4.35	4.24
December	3.92	3.82	3.85	3.87	3.95	3.97
Average	4.73	5	4.54	4.85	4.71	4.85

**Table 1.1.1:** Monthly Solar Insolation at different locations of Bangladesh (in kWh/m<sup>2</sup>/day)

Source: Dr. Shahida Rafique, Dhaka University, recorded from 1988 to 1998, printed

14.07.2007.

### NREL, DRL and RERC values of GHI for Dhaka:

Month	NREL(1985-91)	RERC(1987-89)	RERC(1992)	DLR(2002-2003)	RERC(2003-2005)
January	4.18	4.29	3.34	4.58	3.16
February	4.68	4.86	4.05	4.81	4.46
March	5.55	5.53	5.24	5.31	4.88
April	5.65	5.23	6.02	5.84	5.28
May	5.58	5.67	5.76	5.21	5.46
June	4.48	5.13	5.39	3.85	4.22
July	3.9	3.87	4.2	3.76	4.48
August	4.12	3.92	4.87	4.11	4.12
September	3.96	4.5	5.38	3.76	3.78
October	4.7	4.61	4.93	4.19	3.57
November	4.25	4.22	3.72	4.47	3.92
December	4.06	3.89	3.39	4.34	3.19
Annual Average (KWh/m <sup>2</sup> -day)	4.59	4.64	4.69	4.52	4.21
Annual Average (KWh/m <sup>2</sup> -year)	1676	1695	1712	1649	1536

**Table 1.1.2:** Solar Radiation Data (1985-2005)

#### Source:

<http://lib.buet.ac.bd:8080/xmlui/bitstream/handle/123456789/870/Full%20%20Thesis%20.pdf?sequence=1&isAllowed=y>

From the above table it is seen that maximum solar radiation is available from March to May whereas minimum solar radiation is available during the month of December and January. These numbers are very much promising if we are looking to harness solar energy for electricity. With the future of solar energy so promising, the engineers and the researchers of our country should be looking to invest more and more time to develop new technology to

make this a major mean of power generation. Among many hurdles designing a solar panel, perhaps the most challenging task is to make it operate at the maximum power point, thus making it the most efficient. The possibility of solar power hinges on it. Also another point to reconsider is how fast the operation is done to reach maximum power point, as the condition randomly changes, thus requiring advanced technology to attain the desired output condition. Lack of work on this field has led to many poor performing controllers which do not operate smoothly. In turn, it is creating a negative impact about solar power in people's mind.

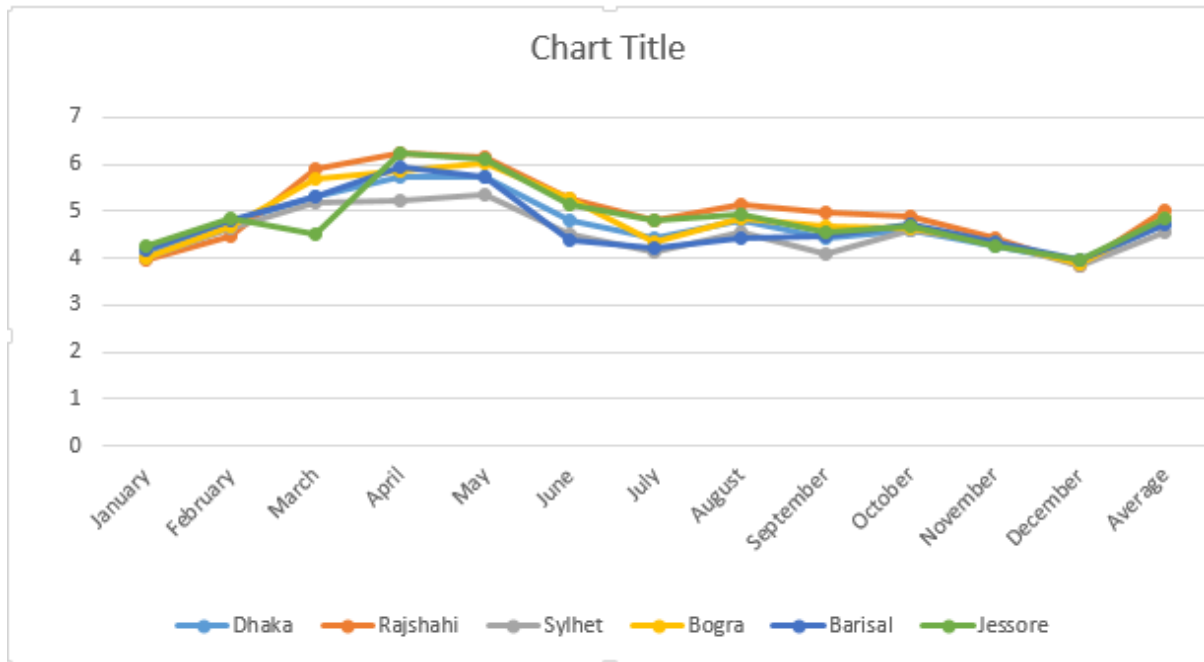


**Figure1.1.1:** Monthly solar irradiation in different locations in Bangladesh

The new era of solar power begins from achieving the maximum power point even so quickly under all circumstances. Tracking the maximum power point is the utmost priority. The method implemented here is the incremental conductance method. It is a simple method, but has a very promising output. Another execution of solar energy is to charge the battery, which can be used even after the sun has set. Solar energy is the basic form of nearly all the forms of energy on the earth. Photovoltaic (PV) is a simple and elegant method of harnessing the solar energy. A solar cell is a PV device. A solar cell is, in principle, a simple semiconductor device that converts light into electric energy. The conversion is accomplished by absorbing light and ionizing crystal atoms, thereby creating free and negatively charged electrons and positively charged ions. If these ions are created from the basic crystal atoms then their ionized state can be exchanged readily to a neighbor, from which it can be exchanged to another neighbor and so forth; that is, this ionized state is mobile; it behaves

like an electron, and it is called a hole. It has properties similar to a free electron except that it has the opposite charge. It does the conversion with no noise, pollution or moving parts, making them robust, reliable and long lasting. The pollution-free process makes it an important method for power production in the future, despite being a comparatively new technology. It hopefully will pave the way for sustainable environment for future generation.

There are several key characteristics of the incident solar energy which are critical in determining how the incident sunlight interacts with a photovoltaic converter or any other object. The important characteristics of the incident solar energy are

- The spectral content of the incident light
- The radiant power density from the sun
- The angle at which the incident solar radiation strikes a photovoltaic module
- The radiant energy from the sun throughout a year or day for a particular surface

While the solar radiation incident on the Earth's atmosphere is relatively constant, the radiation at the Earth's surface varies widely due to:

- Atmospheric effects, including absorption and scattering
- Local variations in the atmosphere, such as water vapor, clouds and pollution
- Latitude of the location
- The season of the year and the time of day

The above effects have several impacts on the solar radiation received at the Earth's Surface. These changes include variations in overall power received, the spectral content of the light and the angle from which light is incident on a surface. In addition, a key change is that the variability of the solar radiation at a particular location changes dramatically. The variability is due to both local effects such as clouds and seasonal variations, as well as other effects such as the length of the day at particular latitude. Desert regions tend to have lower variations due to local atmospheric phenomena such as clouds. Equatorial regions have low variability between seasons.

## **1.2 Atmospheric Effects**

The solar radiation destined to Earth's surface is modified by three atmospheric processes. This is basically caused by the interaction with the gas and other suspended particles found in the atmosphere. Small particles and gas molecules diffuse a portion of the incoming solar radiation in different random directions but do not cause any change in the wave length of the electromagnetic energy. But eventually it does reduce the total amount of incoming radiation towards earth's surface. A significant amount of scattered shortwave radiation is redirected back to the space. These scattering events are dependent on two factors – wavelength of the incoming radiation and the size of the scattering particles or have molecules. A particle with a size about 0.5 microns which is abundant in our atmosphere scatters short wave lengths. This is the reason of the blue color of the sky as the corresponding color and wave lengths are affected. The sky in daytime would be black unless this scattering event took place.

Atmospheric effects have several impacts on the solar radiation at the earth's surface. The major effects of photo voltaic effects are -

- A reduction in the power of solar radiation due to absorption, scattering and reflection in the atmosphere.
- A change in the spectral content of the solar radiation due to the greater absorption or scattering of the waves of varying wave length.
- Diffusion as well as indirect components into solar radiation are introduced
- Local variations in the atmosphere (such as water vapor, clouds and pollution) which have additional effects on the incident power, spectrum and directionality.

### 1.3 Air Mass

The air mass is the pathway that light has to travel through the atmosphere and this path is normalized to the shortest possible path length in case of sun being directly over head. The air Mass quantifies the power of lights passing through the atmosphere and being absorbed by air and dust.

$$\text{Air Mass} = \frac{1}{\cos\theta}$$

Here,

$\theta$ = angle from the vertical (Zenith Angle)

When Sun is directly overhead,  $\theta=0^\circ$ , Air mass is 1

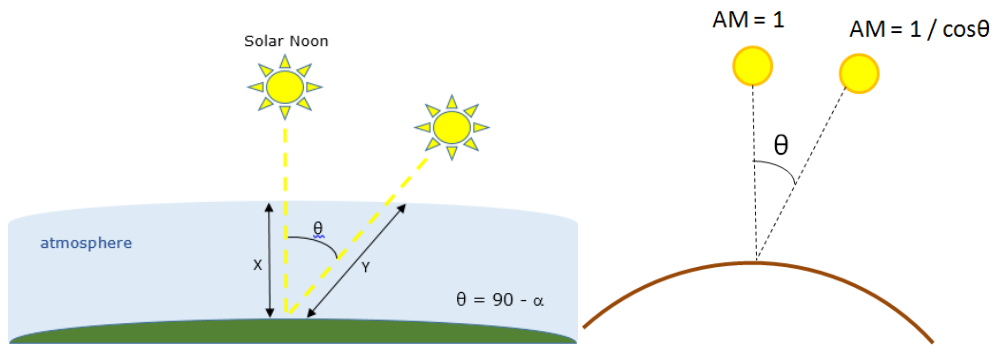


**Figure 1.3.1:** Air mass ratio of solar radiation

### 1.4 Motion of the sun

The apparent motion of the sun is a very influential factor in terms of the total received amount of power by a solar collector. When the absorbing surface is perpendicular to the sun's incident rays, the power density is as the same as the incident power density of the incoming radiation. In case of the alteration of angles between the sun and the absorbing surface, intensity on the surface is altered and generally - reduced. When the module is parallel to the sun's rays, the total applicative intensity of lights is practically zero. For intermediate angles, the relative power density is  $\cos\theta$  and  $\theta$  is the angle between the sun's rays and the module normal.

## **1.5 Elevation Angle**

The elevation angle (used interchangeably with altitude angle) is the angular height of the sun in the sky measured from the horizontal. Confusingly, both altitude and elevation are also used to describe the height in meters above sea level. The elevation is  $0^\circ$  angle at sunrise and  $90^\circ$  when the sun is directly overhead (which occurs for example at the equator on the spring and fall equinoxes). The elevation angle varies throughout the day. It also depends on the latitude of a particular location and the day of the year.

## **1.6 Solar Radiation on a Tilted Surface**

The power incident on a PV module depends not only on the power contained in the sunlight, but also on the angle between the module and the sun. When the absorbing surface and the sunlight are perpendicular to each other, the power density on the surface is equal to that of the sunlight (in other words, the power density will always be at its maximum when the PV module is perpendicular to the sun). However, as the angle between the sun and a fixed surface is continually changing, the power density on a fixed PV module is less than that of the incident sunlight.



## **1.8 Solar Module type Used**

### **Polycrystalline Silicon Solar PV:**

Polycrystalline solar is made by pouring molten silicon into a cast. However, because of this construction method, the crystal structure will form imperfectly, creating boundaries where the crystal formation breaks. This gives the polycrystalline silicon its distinctive, grainy appearance as the gemstone type pattern highlights the boundaries in the crystal. Because of these impurities in the crystal, polycrystalline silicon is less efficient when compared to monocrystalline. However, this manufacturing process uses less energy and materials giving it a significant cost advantage over monocrystalline silicon.

#### **Merits:**

The process used to make polycrystalline silicon is simpler and cost less. The amount of waste silicon is less compared to monocrystalline.

Polycrystalline solar panels tend to have slightly lower heat tolerance than monocrystalline solar panels. This technically means that they perform slightly worse than monocrystalline solar panels in high temperatures. Heat can affect the performance of solar panels and shorten their lifespans. However, this effect is minor, and most homeowners do not need to take it into consideration.

#### **Disadvantages:**

The efficiency of polycrystalline-based solar panels is typically 13-16%. Because of lower silicon purity polycrystalline solar panels are not quite as efficient as monocrystalline solar panels.

Lower space efficiency, One generally need to cover larger surface to output the same electrical power as he/she would with a solar panel made of monocrystalline silicon. However, this does not mean every monocrystalline solar panel perform better than those based on polycrystalline.

## **1.9 MPPT Solar Charge Controller**

The core function of a charge controller is to maintain the battery at highest possible state of charge so when the PV module charges the battery the charge controller shields the battery from overcharge and detaches the load to prevent deep or full discharging. In other words it simply performs the necessary function of ensuring that the batteries cannot be damaged by overcharging by effectively cutting off the current from the PV panels when the battery voltage reaches a certain level. So basically a Maximum Power Point Tracking Solar Charge Controller performs an extra function to improve the system efficiency. The efficiency loss in a basic system is due to a miss-match between voltage produced by the PV panels and that required to charge the batteries under certain conditions. Ideally, charge controller directly controls the state of charge of the battery. Without charge control, the current from the module will flow into a battery proportional to the ‘IRRADIANCE’ (the radiant power received by a surface per unit area), whether the battery needs to be charging or not. If the battery is fully charged, unregulated charging will cause the battery voltage to reach exceedingly high levels, causing electrolyte loss, internal heating and also might lead to grid corrosion. So we can basically say that a charge controller maintains the health and extends the lifetime of the battery. Hence the necessity of having such a type of charge controller has immense advantage while using solar panels. This work done by the controller has a very complex mechanism where the main components are a converter and sensor. There are certain algorithms assigned to the system in order to compare and decide on that right voltage and power which makes the whole system a truly smart and further efficient. So from the sunlight captured by the PV panels are then turned into current which is later sent to these controllers for further modifications.

## **1.10 Battery**

The battery's main responsibility is to store the charge modified from the solar charge controller for later use. Since solar energy is concerned selecting the right type of battery is the most important thing. So in this case the deep cycle type battery is preferred for its efficiency. Basically deep cycle batteries are energy storing units in which chemical reactions occurs that generates voltage hence generates electricity. The reason it is called deep cycled because it works in two cycles.

1) Charging cycle

2) Discharging cycle.

The methodology followed by the deep cycle batteries is very interesting. While a car battery is designed to supply an instant bulk of energy to start up, a deep cycle battery is designed to provide power at a balanced rate slowly powering up the load. Again there are different types of deep cycle batteries which are categorized more vividly for more efficient using in different climatic condition. They are as follows,

- Flooded batteries
- Gel batteries
- AGM (absorbed glass mat)
- Lithium ion

As long as conventional scenario is concerned flooded batteries are mostly used in the standalone PV systems. Other types are also used in off-grid connections. Lithium-ion batteries are preferably used in grid-connected systems in many households but are not that much popular for not being cost efficient.

## Chapter 2

### Solar Cell

#### 2.1 Structure of a Solar Cell

A solar cell, or photovoltaic cell, is an electrical device that converts the energy of light directly into electricity by the photovoltaic effect, which is a physical and chemical phenomenon. It is a form of photoelectric cell, defined as a device whose electrical characteristics, such as current, voltage, or resistance, vary when exposed to light. Individual solar cell devices can be combined to form modules, otherwise known as solar panels. In basic terms a single junction silicon solar cell can produce a maximum open-circuit voltage of approximately 0.5 to 0.6 volts.

A solar cell is essentially a PN junction with a large surface area. The N-type material is kept thin to allow light to pass through to the PN junction.

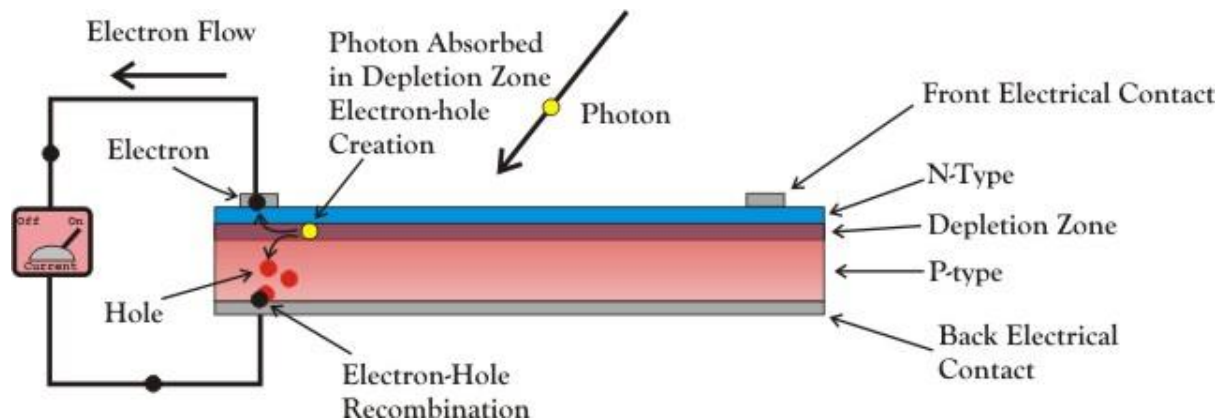


**Figure 2.1.1:** Solar Cell

Light travels in packets of energy called photons. The generation of electric current happens inside the depletion zone of the PN junction. The depletion region as explained previously with the diode is the area around the PN junction where the electrons from the N-type silicon, have diffused into the holes of the P-type material. When a photon of light is absorbed by one of these atoms in the N-Type silicon it will dislodge an electron, creating a free electron and a hole. The free electron and hole has sufficient energy to jump out of the depletion zone. If a wire is connected from the cathode (N-type silicon) to the anode (P-type silicon) electrons

will flow through the wire. The electron is attracted to the positive charge of the P-type material and travels through the external load (meter) creating a flow of electric current. The hole created by the dislodged electron is attracted to the negative charge of N-type material and migrates to the back electrical contact. As the electron enters the P-type silicon from the back electrical contact it combines with the hole restoring the electrical neutrality.

To increase their utility, a number of individual PV cells are interconnected together in a sealed, weatherproof package called a Panel (Module). For example, a 12 V Panel (Module) will have 36 cells connected in series and a 24 V Panel (Module) will have 72 PV Cells connected in series. To achieve the desired voltage and current, Modules are wired in series and parallel into what is called a PV Array. The flexibility of the modular PV system allows designers to create solar power systems that can meet a wide variety of electrical needs. Fig. 2.1.2 shows PV cell, Panel (Module) and Array.

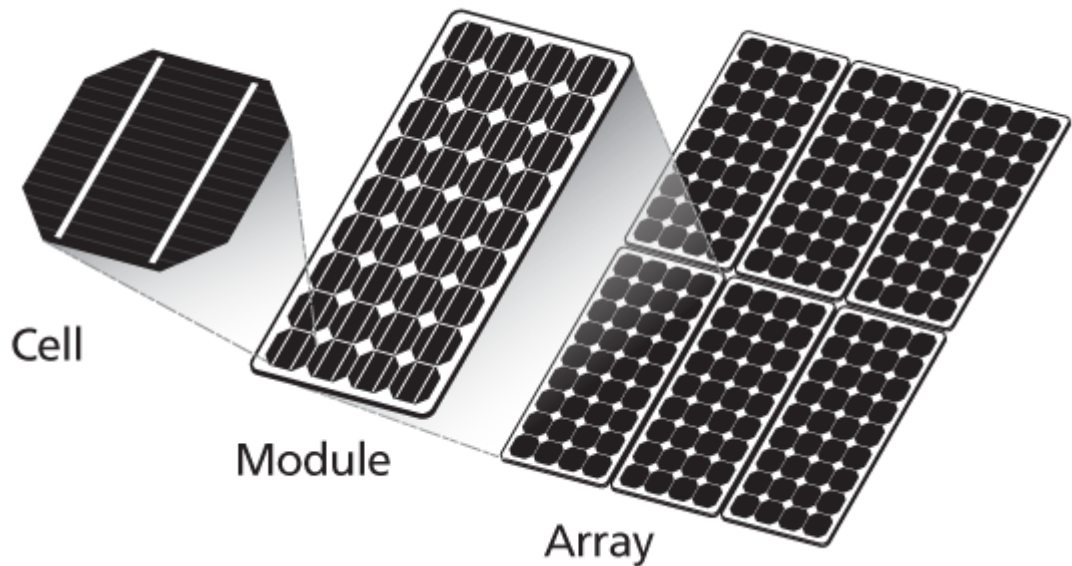


**Figure 2.1.2:** PV Cells, Module and Array

## 2.2 Construction of a Solar Panel

Solar photovoltaic or ‘PV’ panels are made using the 6 main components described below and assembled in advanced manufacturing facilities with extreme accuracy. In this article we will focus on panels made using silicon crystalline solar cells which are by far the most common and highest performing solar technology available today. There are other solar PV technologies available such as thin film and screen printed cells but we will not be discussing these as they have limited use or are still in development.

The main components of a solar panel:

- Extruded Aluminum frame
- Tempered Glass - 3 to 4mm thick
- Silicon PV cells
- Encapsulation - EVA film layers
- Polymer rear backsheet
- Junction box - diodes and connectors

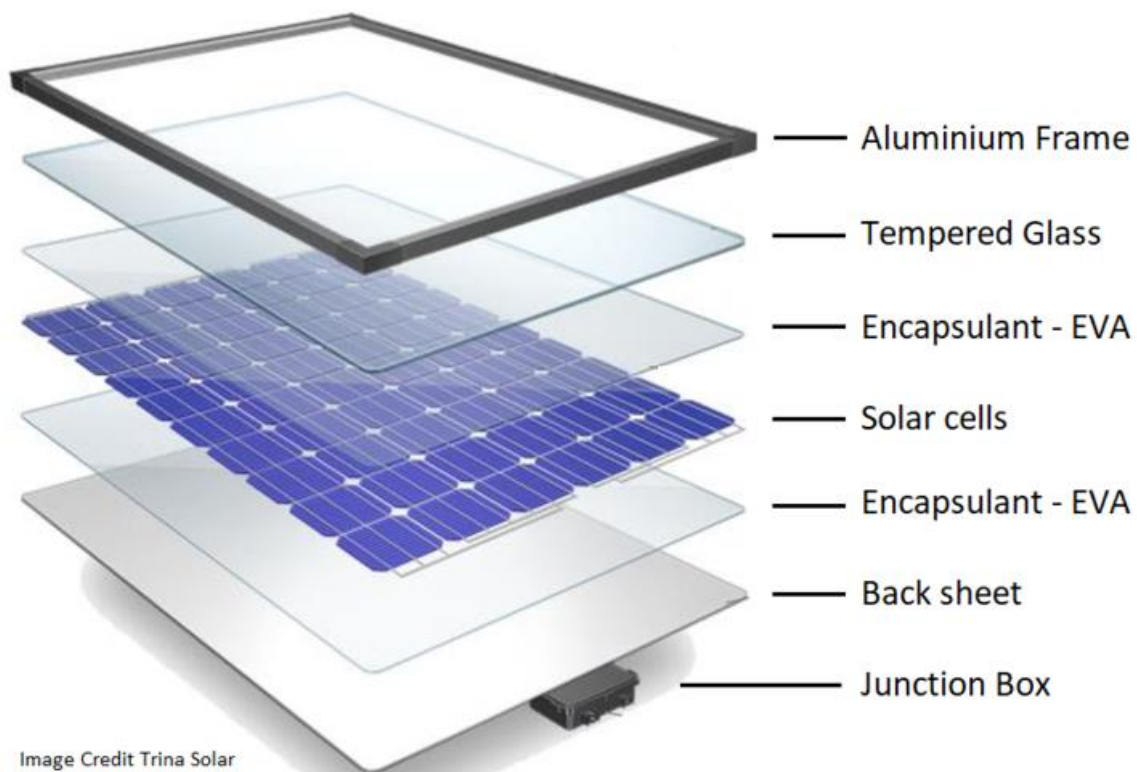


Image Credit Trina Solar

**Figure 2.2.1:** Solar Panel Assembly

Many well-known solar panel manufacturers are ‘vertically integrated’ which means the one company supplies and manufactures all the main components including the silicon ingots and wafers used to make the solar PV cells. However, many panel manufacturers assemble solar panels using externally sourced parts including cells, polymer back sheet and encapsulation EVA material. These manufacturers can be more selective about which components they chose but they do not always have control over the quality of the products so they should be sure they use the best suppliers available.

### Glass:

The front glass sheet protects the PV cells from the weather and impact from hail or airborne debris. The glass is typically high strength tempered glass which is 3.0 to 4.0mm thick and is designed resist mechanical loads and extreme temperature changes. The IEC minimum standard impact test requires solar panels to withstand an impact of hail stones of 1 inch (25 mm) diameter traveling up to 60 mph (27 m/s). In the event of an accident or severe impact tempered glass is also much safer than standard glass as it shatters into tiny fragments rather than sharp jagged sections. To improve efficiency and performance high transmissive glass is used by most manufacturers which have very low iron content and an anti-reflective coating on the rear side to reduce losses and improve light transmission.



**Figure 2.2.2:** Front Glass Sheet of a Solar Panel

**Frame:**

The aluminum frame plays a critical role by both protecting the edge of the laminate section housing the cells and providing a solid structure to mount the solar panel in position. The extruded aluminum sections are designed to be extremely lightweight, stiff and able to withstand extreme stress and loading from high wind and external forces.

The aluminum frame can be silver or anodized black and depending on the panel manufacturer the corner sections can either be screwed, pressed or clamped together providing different levels of strength and stiffness.



**Figure 2.2.3:** Frame of a Solar Panel

### **EVA Film:**

EVA stands for ‘ethylene vinyl acetate’ which is a specially designed polymer highly transparent (plastic) layer used to encapsulate the cells and hold them in position during manufacture. The EVA material must be extremely durable and tolerant of extreme temperature and humidity; it plays an important part in the long term performance by preventing moisture and dirt ingress.

The lamination either side of the PV cells provides some shock absorption and helps protect the cells and interconnecting wires from vibrations and sudden impact from hail stones and other objects. A high quality EVA film with a high degree of what is known as ‘cross-linking’ can be the difference between a long life or a panel failure due to water ingress. During manufacture the cells are first encapsulated with the EVA before being assembled within the glass and back sheet.

### **Back Sheet:**

The backsheet is the rear most layer of common solar panels which acts as a moisture barrier and final external skin to provide both mechanical protection and electrical insulation. The backsheet material is made of various polymers or plastics including PP, PET and PVF which offer different levels of protection, thermal stability and long term UV resistance. The backsheet layer is typically white in color but is also available as clear or black depending on the manufacturer and module. ‘Tedlar’ PVF material from Dupont is known as one the leading high performance back sheets for PV module manufacturing.

Some panels such as bifacial and frameless panels use a rear glass panel instead of a polymer backsheet. The rear side glass is more durable and longer lasting than most backsheet materials and so some manufacturers offer a 30year performance warranty on dual glass panels.

### **Junction Box:**

The junction box is a small weather proof enclosure located near the top on the rear side of the panel. It is needed to securely attach the cables required to interconnect the panels. The junction box is important as it is the central point where all the cells sets interconnect and must be protected from moisture and dirt.



**Figure 2.2.5:Junction Box of a Solar Panel**

### **Bypass diodes:**

The junction box also houses the bypass diodes which are needed to prevent back current which occurs when some cells are shaded or dirty. Diodes only allow current to flow in one direction and a typical 60 cell panel has 3 rows of 20 PV cells and in turn there are 3 bypass diodes, one for preventing reverse current to each of the 3 sets of cells. Unfortunately bypass diodes can fail over time and may need to be replaced, so the cover of the junction box is usually possible to remove for servicing, although many modern solar panels now use more advanced long lasting diodes and non-serviceable junction boxes.

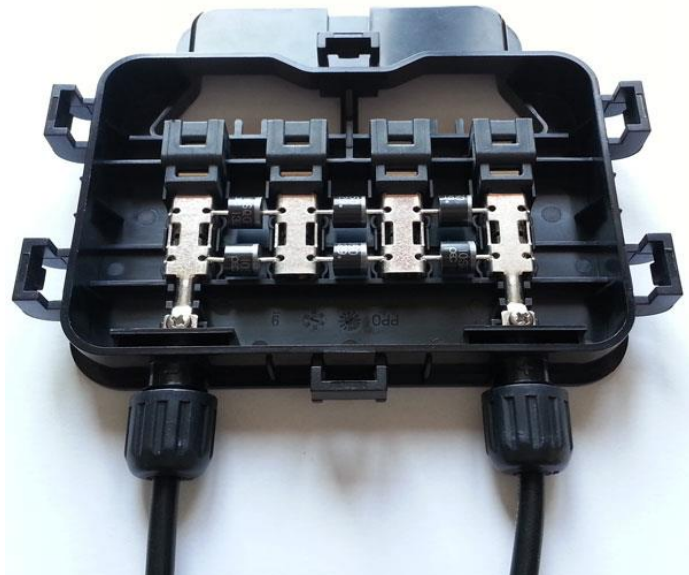


**Figure 2.2.6:** Bypass diodes of a Solar Panel

## 2.3 Equivalent Circuit of Solar Cell

The characteristics of a PV cell can be further explained using an equivalent circuit shown in the Figure: 2.3.1. The PV model consists of a current source, a diode and a series resistance. The effect of parallel resistance represents the leakage resistance of the cell which is very small in a single module. The current source represents the current which is generated by the photons, and its output is constant under constant temperature and constant incident radiation of light.

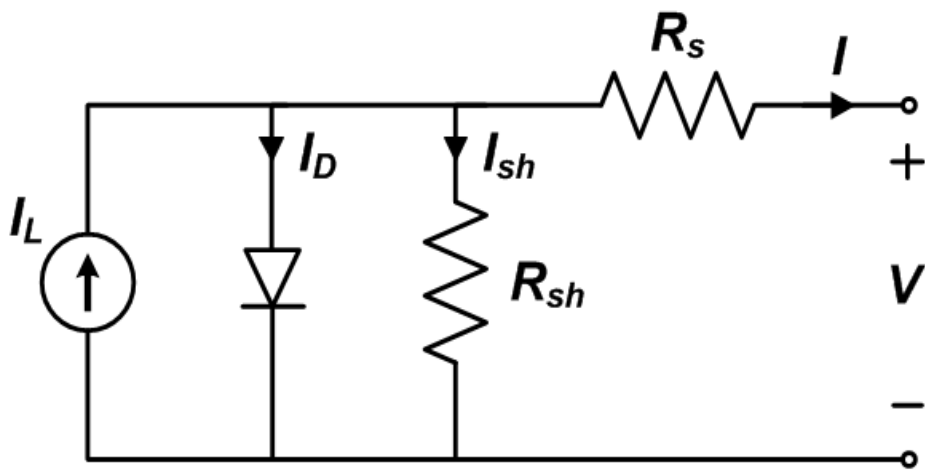


**Figure 2.3.1:** Equivalent Circuit of Solar PV Cell

Current-voltage (I-V) curves are obtained by exposing the cell to a constant level of light, while maintaining a constant cell temperature, varying the resistance of the load, and measuring the produced current. When an I-V curve is drawn it normally passes through two points:

- **Short-circuit current ( $I_{sc}$ ):** This is the current produced when the positive and negative terminals of the cell are short-circuited (i.e., when the solar cell is short circuited), and the voltage between the terminals is zero, which corresponds to zero load resistance.

- **Open-circuit voltage ( $V_{oc}$ ):** This is the voltage across the positive and negative terminals under open-circuit conditions, when the current is zero, which corresponds to infinite load resistance.



## 2.4 Solar Cell I-V Characteristics

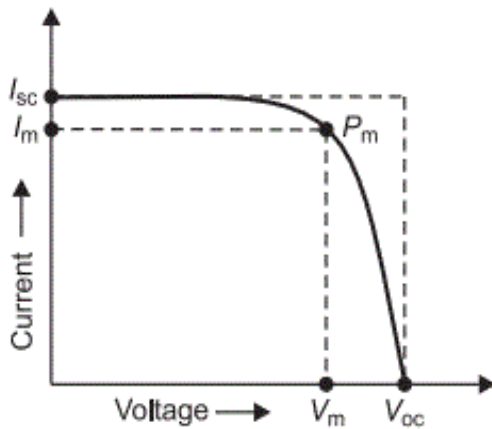


**Figure 2.4.1:** I-V and P-V graphs showing the characteristic of a solar cell

Figure: 2.4.1 shows the current-voltage (I-V) characteristics of a typical silicon PV cell operating under normal conditions. The power delivered by a solar cell is the product of current and voltage (I-V). If the multiplication is done, point for point, for all voltages from short-circuit to open-circuit conditions, the power curve above is obtained for a given radiation level.

With the solar cell open-circuited that is not connected to any load, the current will be at its minimum (zero) and the voltage across the cell is at its maximum, known as the solar cells open circuit voltage, or  $V_{oc}$ . At the other extreme, when the solar cell is short circuited, that is the positive and negative leads connected together, the voltage across the cell is at its minimum (zero) but the current flowing out of the cell reaches its maximum, known as the solar cells short circuit current, or  $I_{sc}$ .

Then the span of the solar cell I-V characteristics curve ranges from the short circuit current ( $I_{sc}$ ) at zero output volts, to zero current at the full open circuit voltage ( $V_{oc}$ ). In other words, the maximum voltage available from a cell is at open circuit, and the maximum current at closed circuit. Of course, neither of these two conditions generates any electrical power, but there must be a point somewhere in between the solar cell generates maximum power. However, there is one particular combination of current and voltage for which the power reaches its maximum value, at  $I_{mp}$  and  $V_{mp}$ . In other words, the point at which the cell generates maximum electrical power and this is shown at the top right area of the green

rectangle. This is the “maximum power point” or MPP. Therefore the ideal operation of a photovoltaic cell (or panel) is defined to be at the maximum power point.

Thus far we have looked at Solar Cell I-V Characteristic Curve for a single solar cell or panel. But many photovoltaic arrays are made up of smaller PV panels connected together. Then the I-V curve of a PV array is just a scaled up version of the single solar cell I-V characteristic curve as shown in Figure: 2.4.2.

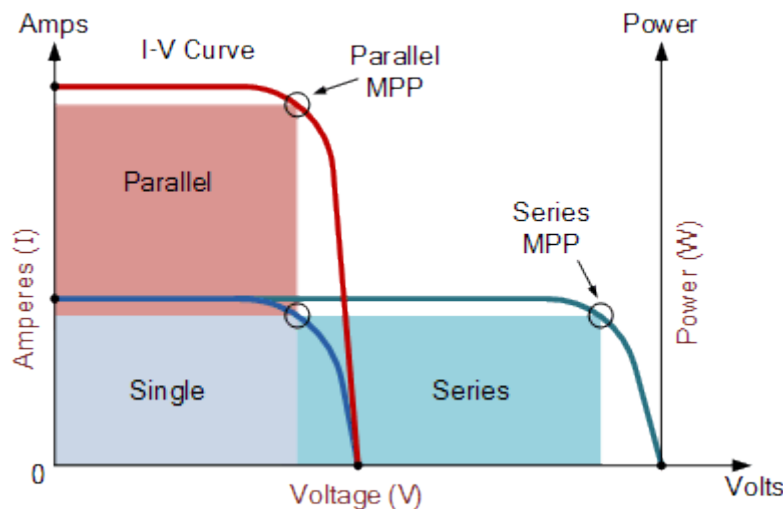


**Figure 2.4.2:** I-V and P-V graphs of a Solar Panel

Photovoltaic panels can be wired or connected together in either series or parallel combinations, or both to increase the voltage or current capacity of the solar array. If the array panels are connected together in a series combination, then the voltage increases. If connected together in parallel then the current increases. The electrical power in Watts, generated by these different photovoltaic combinations will still be the product of the voltage times the current, ( $P = V \times I$ ). However the solar panels are connected together, the upper right hand corner will always be the maximum power point (MPP) of the array.

## 2.5 Fill Factor

The short-circuit current and the open-circuit voltage are the maximum current and voltage respectively from a solar cell. However, at both of these operating points, the power from the solar cell is zero. The “fill factor”, more commonly known by its abbreviation “FF”, is a parameter which, in conjunction with  $V_{oc}$  and  $I_{sc}$ , determine the maximum power from a solar cell. The FF is defined as the ratio of the maximum power from the solar cell to the product of  $V_{oc}$  and  $I_{sc}$ . Graphically, the FF is a measure of the “squareness” of the solar cell and is also the area of the largest rectangle which will fit in the I-V Curve. The FF is illustrated below.

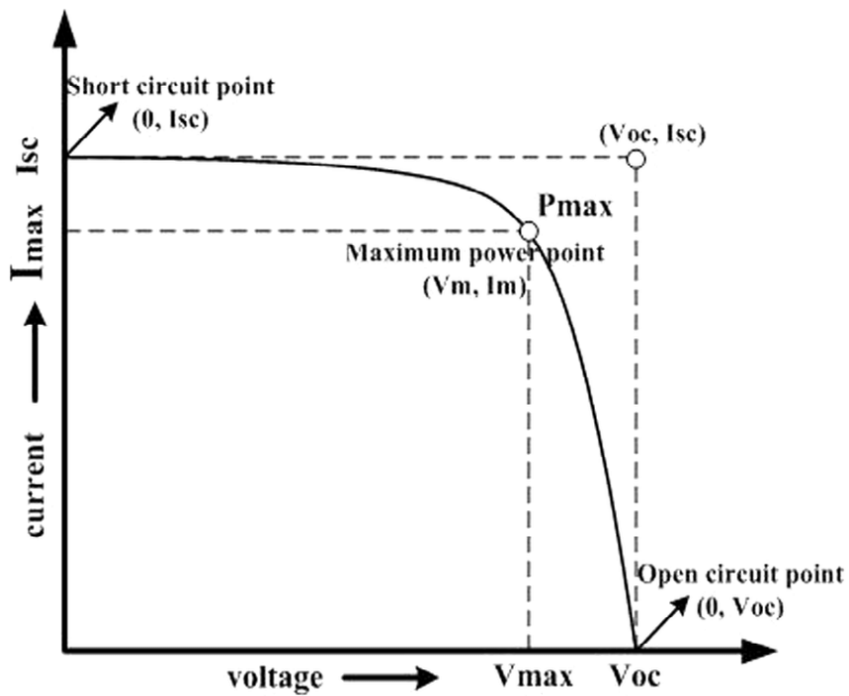


**Figure 2.5.1:** Fill Factor of a Solar Cell

As FF is a measure of the "squareness" of the IV curve, a solar cell with a higher voltage has a larger possible FF since the "rounded" portion of the IV curve takes up less area. The maximum theoretical FF from a solar cell can be determined by differentiating the power from a solar cell with respect to voltage and finding where this is equal to zero. Hence:

$$\frac{d(IV)}{dV} = 0$$

Giving:

$$V_{MP} = V_{OC} - \frac{nKT}{q} \ln\left(\frac{qV_{MP}}{nKT} + 1\right)$$

The equation above requires Lambert functions to solve (see below) but a simpler approach is to use iteration to calculate  $V_{MP}$ . The equation above only relates  $V_{OC}$  to  $V_{MP}$  and extra equations are needed to find  $I_{MP}$  and FF. A more commonly used expression for the FF can be determined empirically as:

$$FF = \frac{V_{OC} - \ln(V_{OC} + 0.72)}{V_{OC} + 1}$$

Where  $v_{oc}$  is defined as a "normalized  $V_{oc}$ ":

$$V_{OC} = \frac{q}{nKT} V_{oc}$$

The above equations show that a higher voltage will have a higher possible FF. However, large variations in open-circuit voltage within a given material system are relatively uncommon. For example, at one sun, the difference between the maximum open-circuit voltage measured for a silicon laboratory device and a typical commercial solar cell is about 120 mV, giving maximum FF's respectively of 0.85 and 0.83. However, the variation in maximum FF can be significant for solar cells made from different materials. For example, a GaAs solar cell may have a FF approaching 0.89.

The above equation also demonstrates the importance of the ideality factor, also known as the "n-factor" of a solar cell. The ideality factor is a measure of the junction quality and the type of recombination in a solar cell. For the simple recombination mechanisms discussed in Types of Recombination, the n-factor has a value of 1. However, some recombination mechanisms, particularly if they are large, may introduce recombination mechanisms of 2. A high n-value not only degrades the FF, but since it will also usually signal high recombination, it gives low open-circuit voltages. A key limitation in the equations described above is that they represent a maximum possible FF, although in practice the FF will be lower due to the presence of parasitic resistive losses, which are discussed in Effects of Parasitic Resistances. Therefore, the FF is most commonly determined from measurement of the IV curve and is defined as the maximum power divided by the product of  $I_{SC}$  and  $V_{OC}$ , i.e.:

$$FF = \frac{V_{MP} I_{MP}}{V_{OC} I_{SC}}$$

## 2.6 Effect of Temperature

Like all other semiconductor devices, solar cells are sensitive to temperature. Increases in temperature reduce the band gap of a semiconductor, thereby effecting most of the semiconductor material parameters. The decrease in the band gap of a semiconductor with increasing temperature can be viewed as increasing the energy of the electrons in the material. Lower energy is therefore needed to break the bond. In the bond model of a semiconductor band gap, reduction in the bond energy also reduces the band gap. Therefore increasing the temperature reduces the band gap.

In a solar cell, the parameter most affected by an increase in temperature is the open-circuit voltage. The impact of increasing temperature is shown in the Figure: 2.6.1.

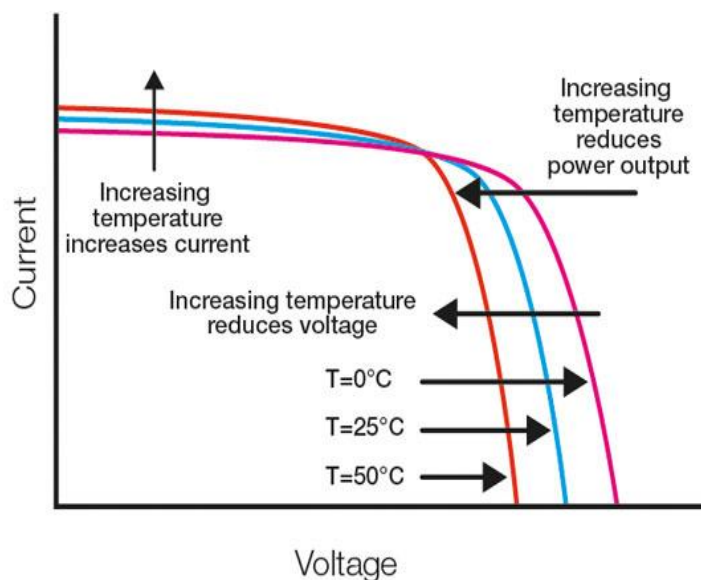


**Figure 2.6.1:** Effect of Temperature

The open-circuit voltage decreases with temperature because of the temperature dependence of  $I_0$ . The equation for  $I_0$  from one side of a p-n junction is given by,

$$I_0 = qA \frac{Dn_i^2}{LN_D}$$

Where,

- q is the electronic charge given in the constants page;
- A is the area;
- D is the diffusivity of the minority carrier given for silicon as a function of doping in the Silicon Material Parameters page;
- L is the minority carrier diffusion length;
- $N_D$  is the doping;
- $n_i$  is the intrinsic carrier concentration given for silicon in the Silicon Material Parameters page.

In the above equation, many of the parameters have some temperature dependence, but the most significant effect is due to the intrinsic carrier concentration,  $n_i$ . The intrinsic carrier concentration depends on the band gap energy (with lower band gaps giving a higher intrinsic carrier concentration), and on the energy which the carriers have (with higher temperatures giving higher intrinsic carrier concentrations). The equation for the intrinsic carrier concentration is,

$$n_i^2 = 4\left(\frac{2\pi kT}{h^2}\right)^3 (m_e^* m_h^*)^{3/2} \exp\left(-\frac{E_{G0}}{kT}\right) = BT^3 \exp\left(-\frac{E_{G0}}{kT}\right)$$

Where:

T is the temperature;

$h$  and  $K$  are constants given in the constants page;

$m_e$  and  $m_h$  are the effective masses of electrons and holes respectively;

$E_{G0}$  is the band gap linearly extrapolated to absolute zero;

B is a constant which is essentially independent of temperature.

## 2.7 Effect of Series Resistance

Series resistance in a solar cell has three causes: firstly, the movement of current through the emitter and base of the solar cell; secondly, the contact resistance between the metal contact and the silicon; and finally the resistance of the top and rear metal contacts. The main impact of series resistance is to reduce the fill factor, although excessively high values may also reduce the short-circuit current.

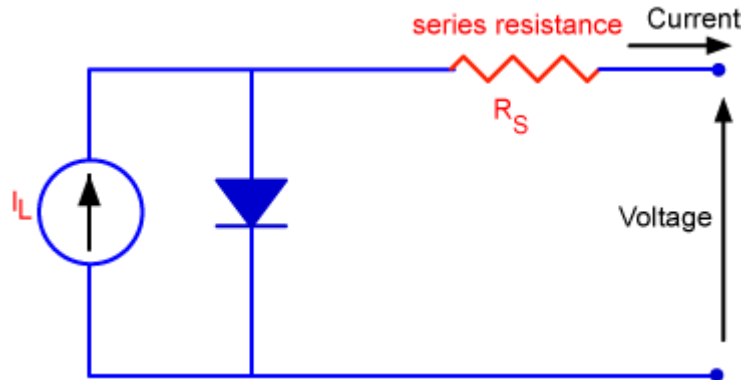


**Figure 2.7.1:** Schematic of a solar cell with series resistance

$$I = I_L - I_0 \left[ e^{\frac{q(V+IR_S)}{nKT}} \right]$$

Where:

$I$  is the cell output current,

$I_L$  is the light generated current,

$V$  is the voltage across the cell terminals,

$T$  is the temperature;

$q$  and  $k$  are constants,

$n$  is the ideality factor,

$R_S$  is the cell series resistance.

The formula is an example of an implicit function due to the appearance of the current,  $I$ , on both sides of the equation and requires numerical methods to solve.

The effect of the series resistance on the IV curve is shown in Figure 2.6.2. To generate the plot the voltage across the diode is varied thereby avoiding the need to solve an implicit equation.

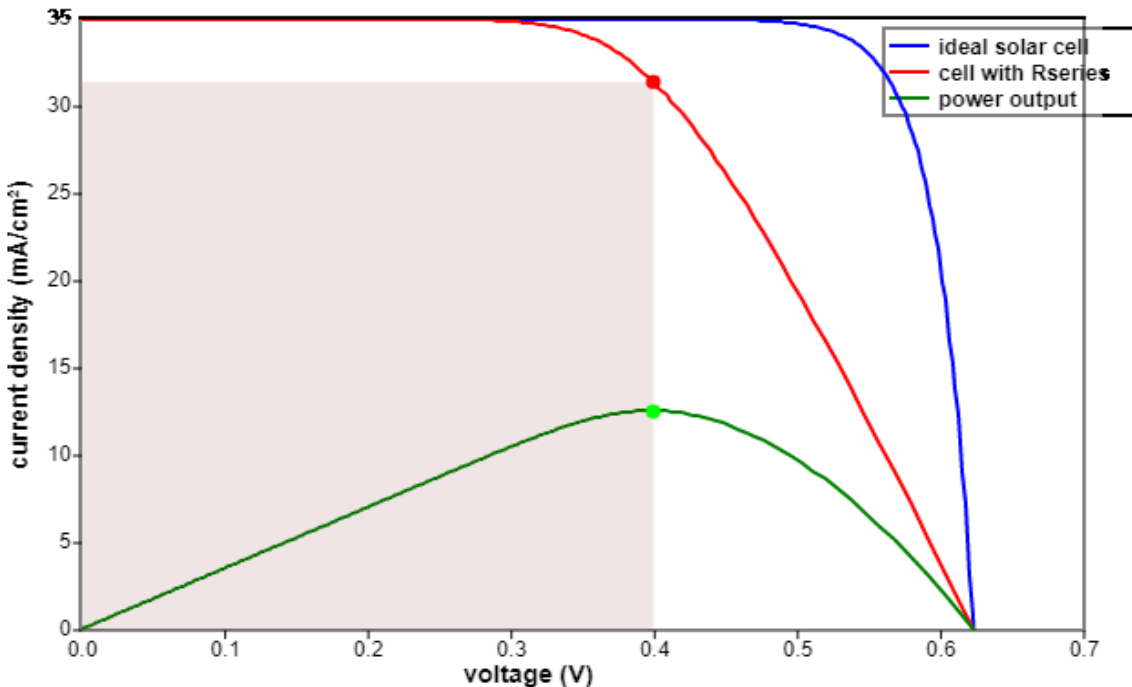


**Figure 2.7.2:** The effect of the series resistance on the IV curve

Series resistance does not affect the solar cell at open-circuit voltage since the overall current flow through the solar cell, and therefore through the series resistance is zero. However, near the open-circuit voltage, the I-V curve is strongly affected by the series resistance. A straightforward method of estimating the series resistance from a solar cell is to find the slope of the I-V curve at the open-circuit voltage point.

## 2.8 Effect of Shunt Resistance

Significant power losses caused by the presence of a shunt resistance,  $R_{SH}$ , are typically due to manufacturing defects, rather than poor solar cell design. Low shunt resistance causes power losses in solar cells by providing an alternate current path for the light-generated current. Such a diversion reduces the amount of current flowing through the solar cell junction and reduces the voltage from the solar cell. The effect of a shunt resistance is particularly severe at low light levels, since there will be less light-generated current. The loss of this current to the shunt therefore has a larger impact. In addition, at lower voltages where the effective resistance of the solar cell is high, the impact of a resistance in parallel is large.

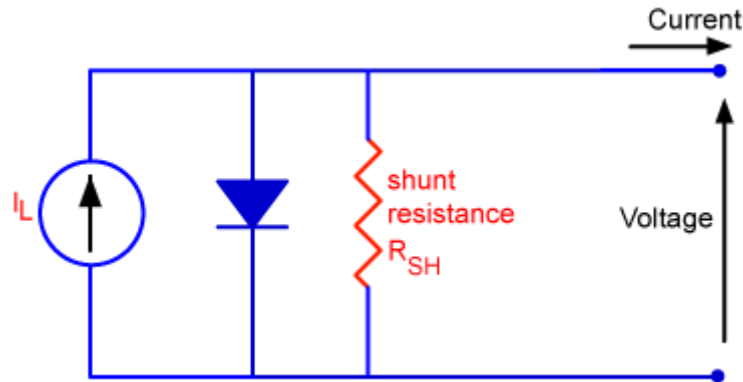


**Figure 2.8.1:** Circuit diagram of a solar cell including the shunt resistance

The equation for a solar cell in presence of a shunt resistance is:

$$I = I_L - I_0 \left[ e^{\frac{qV}{nKT}} \right] - \frac{V}{R_{SH}}$$

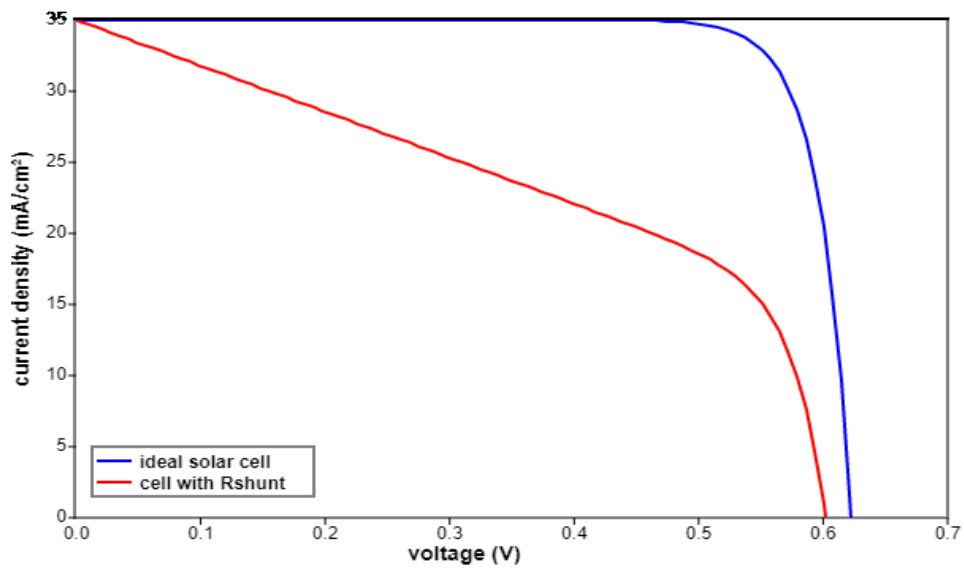


**Figure 2.8.2:**The effect of the shunt resistance on the IV curve

An estimation of the value of the shunt resistance of a solar cell can be determined from the slope of the IV curve near short-circuit current point.

## 2.9 Effect of Parasitic Resistance

Resistive effects in solar cells reduce the efficiency of the solar cell by dissipating power in the resistances. The most common parasitic resistances are series resistance and shunt resistance. The inclusion of the series and shunt resistance on the solar cell model is shown in the Figure: 2.9.1.

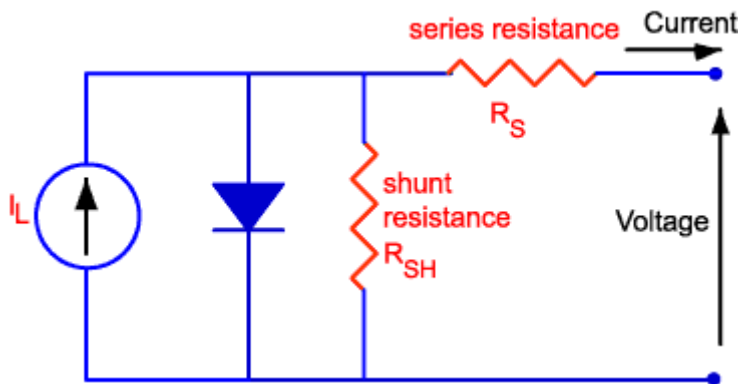


**Figure 2.9.1:** Parasitic series and shunt resistances in a solar cell circuit

In most cases and for typical values of shunt and series resistance, the key impact of parasitic resistance is to reduce the fill factor. Both the magnitude and impact of series and shunt resistance depend on the geometry of the solar cell, at the operating point of the solar cell. Since the value of resistance will depend on the area of the solar cell, when comparing the series resistance of solar cells which may have different areas, a common unit for resistance is in  $\Omega\text{cm}^2$ . This area-normalized resistance results from replacing current with current density in Ohm's law as shown below,

$$R'(\Omega\text{cm}^2) = \frac{V}{J}$$

## 2.10 Effect of Light Intensity

Changing the light intensity incident on a solar cell changes all solar cell parameters, including the short-circuit current, the open-circuit voltage, the FF, the efficiency and the impact of series and shunt resistances. The light intensity on a solar cell is called the number of suns, where 1 sun corresponds to standard illumination at AM1.5, or  $1 \text{ kW/m}^2$ . For example a system with  $10 \text{ kW/m}^2$  incident on the solar cell would be operating at 10 suns, or at 10X. A PV module designed to operate under 1 sun conditions is called a "flat plate" module while those using concentrated sunlight are called "concentrators".

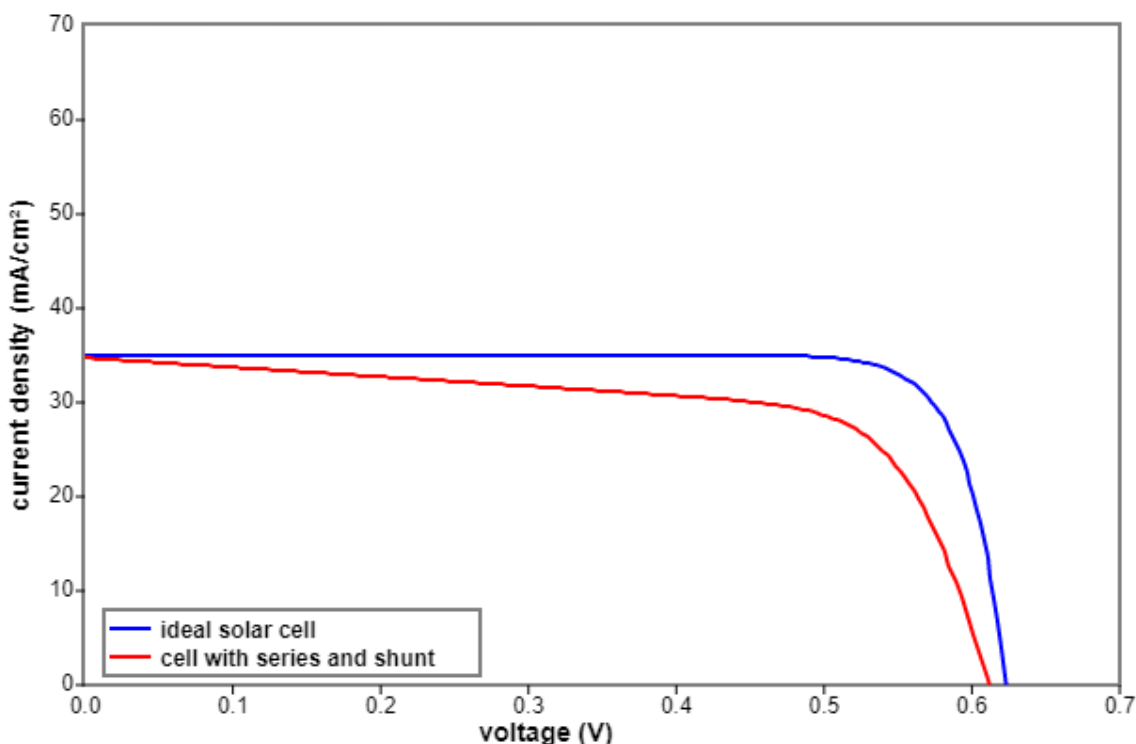


**Figure 2.10.1:** The effect of concentration on the IV characteristics of a solar cell

### **Concentrators:**

A concentrator is a solar cell designed to operate under illumination greater than 1 sun. The incident sunlight is focused or guided by optical elements such that a high intensity light beam shines on a small solar cell. Concentrators have several potential advantages, including a higher efficiency potential than a one-sun solar cell and the possibility of lower cost. The short-circuit current from a solar cell depends linearly on light intensity, such that a device operating under 10 suns would have 10 times the short-circuit current as the same device under one sun operation. However, this effect does not provide an efficiency increase, since the incident power also increases linearly with concentration. Instead, the efficiency benefits arise from the logarithmic dependence of the open-circuit voltage on short circuit. Therefore, under concentration,  $V_{oc}$  increases logarithmically with light intensity.

The cost of a concentrating PV system may be lower than a corresponding flat-plate PV system since only a small area of solar cells is needed. The efficiency benefits of concentration may be reduced by increased losses in series resistance as short-circuit current increases and also by the increased temperature operation of the solar cell. As losses due to short-circuit current depend on the square of the current, power loss due to series resistance increases as the square of the concentration.

### **Low Light Intensity:**

Solar cells experience daily variations in light intensity, with the incident power from the sun varying between 0 and 1 kW/m<sup>2</sup>. At low light levels, the effect of the shunt resistance becomes increasingly important. As the light intensity decreases, the bias point and current through the solar cell also decreases and the equivalent resistance of the solar cell may begin to approach the shunt resistance. When these two resistances are similar, the fraction of the total current flowing through the shunt resistance increases, thereby increasing the fractional power loss due to shunt resistance. Consequently, under cloudy conditions, a solar cell with a high shunt resistance retains a greater fraction of its original power than a solar cell with a low shunt resistance.

## 2.11 Ideality Factor

The ideality factor of a diode is a measure of how closely the diode follows the ideal diode equation. The derivation of the simple diode equation uses certain assumption about the cell. In practice, there are second order effects so that the diode does not follow the simple diode equation and the ideality factor provides a way of describing them.

Recombination mechanisms

The ideal diode equation assumes that all the recombination occurs via band to band or recombination via traps in the bulk areas from the device (i.e. not in the junction). Using that assumption the derivation produces the ideal diode equation below and the ideality factor, n, is equal to one.

$$I = I_L - I_0 \left[ e^{\frac{qV}{nKT}} - 1 \right]$$

However recombination does occur in other ways and in other areas of the device. These recombinations produce ideality factors that deviate from the ideal. Deriving the ideal diode equation by considering the number of carriers the need to come together during the process produces the results in the table below.

Recombination Type	Ideality factor	Description
SRH, band to band (low level injection)	1	Recombination limited by minority carrier.
SRH, band to band (high level injection)	2	Recombination limited by both carrier types.
Auger	2/3	Two majority and one minority carriers required for recombination.
Depletion region (junction)	2	Two carriers limit recombination.

**Table 2.10.1:** Ideality Factor of different types of recombination

## 2.12 Losses

### 2.12.1 Optical Losses

Optical losses chiefly effect the power from a solar cell by lowering the short-circuit current. Optical losses consist of light which could have generated an electron-hole pair, but does not, because the light is reflected from the front surface, or because it is not absorbed in the solar cell. For the most common semiconductor solar cells, the entire visible spectrum (350 - 780 nm) has enough energy to create electron-hole pairs and therefore all visible light would ideally be absorbed.

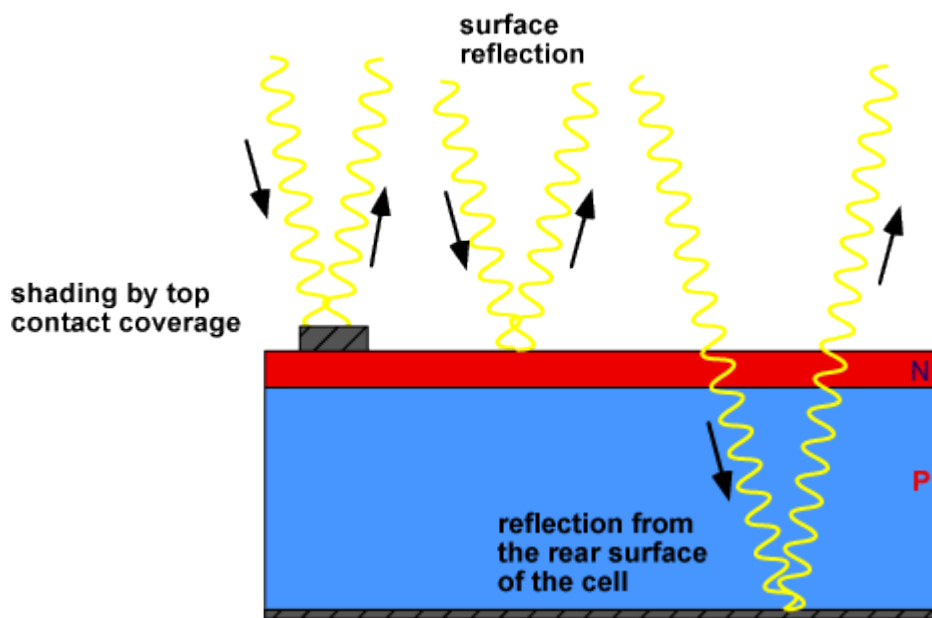


**Figure 2.12.1.1:** Optical Loss in a Solar Cell

There are a number of ways to reduce the optical losses:

- Top contact coverage of the cell surface can be minimized (although this may result in increased series resistance). This is discussed in more detail in Series Resistance;
- Anti-reflection coatings can be used on the top surface of the cell.
- Reflection can be reduced by surface texturing.

- The solar cell can be made thicker to increase absorption (although light that is absorbed more than a diffusion length from the junction has a low collection probability and will not contribute to the short circuit current).
- The optical path length in the solar cell may be increased by a combination of surface texturing and light trapping.

### **2.12.2 MOSFET Losses**

Power losses (PI) in any component operating in the switch-mode can be divided in three groups:

- a) Conduction losses ( $P_C$ )
- b) Switching losses ( $P_{SW}$ )
- c) Blocking (leakage) losses ( $P_b$ ), normally being neglected

Therefore,

$$\begin{aligned} PI &= P_C + P_{SW} + P_b \\ &\approx P_C + P_{SW} \end{aligned}$$

### **2.12.3 Inductor Losses**

The power loss of an inductor is defined by the basic formula,

$$P_{loss}(inductor) = P_{Core} + P_{dcr} + P_{acr}$$

### **2.12.4 Core Losses**

Core loss is due to hysteresis loss and eddy current loss in the inductor. A formula can be used to calculate the core loss. Measuring core loss and getting repeatable results can be a tedious task depending on the test frequency.

### **2.12.5 Switching Loss**

In the ideal switching, the current is zero when the switch is open and the power loss is zero. When the switch is closed, the voltage across it is zero and the power loss is also zero. But in practical switching there occurs some power loss.

## **Chapter 3**

### **Maximum Power Point Tracking Algorithms**

#### **3.1 Introduction**

In a (Power-Voltage or current-voltage) curve of a solar panel, there is an optimum operating point such that the PV delivers the maximum possible power to the load. This unique point is the maximum power point (MPP) of solar panel. Because of the photovoltaic nature of solar panels, their current-voltage, or IV, curves depend on temperature and irradiance levels. Therefore, the operating current and voltage which maximize power output will change with environmental conditions. As the optimum point changes with the natural conditions so it is very important to track the maximum power point (MPP) for a successful PV system. So in PV systems a maximum power point tracker (MPPT) is very much needed. In most PV systems a control algorithm, namely maximum power point tracking algorithm is utilized to have the full advantage of the PV systems. In this chapter, we attempt to design a charge controller's MPPT by presenting algorithms for different MPPT methods and comparing their advantages and drawbacks.

#### **3.2 Maximum Power Point Tracking**

For any given set of operational conditions, cells have a single operating point where the values of the current (I) and voltage (V) of the cell result in a maximum power output. These values correspond to a particular load resistance,  $R = V/I$ , as specified by Ohm's Law. The power P is given by  $P = V*I$ . From basic circuit theory, the power delivered from or to a device is optimized where the derivative of the I-V curve is equal and opposite the I/V ratio. This is known as the maximum power point (MPP) and corresponds to the "knee" of the curve. The load with resistance  $R=V/I$ , which is equal to the reciprocal of this value and draws the maximum power from the device is sometimes called the characteristic resistance of the cell. This is a dynamic quantity which changes depending on the level of illumination, 24 as well as other factors such as temperature and the age of the cell. If the resistance is lower or higher than this value, the power drawn will be less than the maximum available, and thus the cell will not be used as efficiently as it could be.

### **3.3 Methods of MPPT algorithms**

Maximum Power Point Tracking (MPPT) is used to obtain the maximum power from these systems. In these applications, the load can demand more power than the PV system can deliver. There are many different approaches to maximizing the power from a PV system, this range from using simple voltage relationships to more complexes multiple sample based analysis. MPPT Methods There are some conventional methods for MPPT. Seven of them are listed here. These methods include:

- Constant Voltage method
- Open Circuit Voltage method
- Short Circuit Current method
- Perturb and Observe method
- Incremental Conductance method
- Temperature method
- Temperature Parametric method
- Fuzzy Logic
- Neural Network

#### **3.3.1 Constant Voltage Method**

The constant voltage method is the simplest method. This method simply uses single voltage to represent the  $V_{MP}$ . In some cases this value is programmed by an external resistor connected to a current source pin of the control IC.

In this case, this resistor can be part of a network that includes a NTC thermistor so the value can be temperature compensated. For the various different irradiance variations, the method will collect about 80% of the available maximum power. The actual performance will be determined by the average level of irradiance. In the cases of low levels of irradiance the results can be better.

### **3.3.2 Open Circuit Voltage Method**

An improvement on this method uses  $V_{oc}$  to calculate  $V_{mp}$ . Once the system obtains the  $V_{oc}$  value,  $V_{mp}$  is calculated by,

$$V_{mp} = k * V_{oc}$$

The  $k$  value is typically between 0.7 to 0.8. It is necessary to update  $V_{oc}$  occasionally to compensate for any temperature change. Sampling the  $V_{oc}$  value can also help correct for temperature changes and to some degree changes in irradiance. Monitoring the input current can indicate when the  $V_{oc}$  should be re-measured. The  $k$  value is a function of the logarithmic function of the irradiance, increasing in value as the irradiance increases. An improvement to the  $V_{oc}$  method is to also take this into account.

#### **Benefits:**

- Relatively lower cost.
- Very simple and easy to implement.

#### **Drawbacks:**

- Not accurate and may not operate exactly at MPP.
- Slower response as  $V_{mp}$  is proportional to the  $V_{oc}$ .

### **3.3.3 Short Circuit Current Method**

The short circuit current method uses a value of  $I_{sc}$  to estimate  $I_{mp}$ . This method uses a short load pulse to generate a short circuit condition. During the short circuit pulse, the input voltage will go to zero, so the power conversion circuit must be powered from some other source. One advantage of this system is the tolerance for input capacitance compared to the  $V_{oc}$  method. The  $k$  values are typically close to 0.9 to 0.98.

#### **Benefits:**

- It is simple and low cost to implement.
- This method does not require an input.
- In low insulation conditions, it is better than others.

#### **Drawbacks:**

- Irradiation is never exactly at the MPP due to variations on the array that are not considered (it is not always accurate).
- Data varies under different weather conditions and locations.
- It has low efficiency. In these two methods we have to choose the right constant  $k$  value carefully, to accurately calibrate the solar panel.

### 3.3.4 Perturb and Observe Method

This algorithm uses simple feedback arrangement and little measured parameters. In this approach, the module voltage is periodically given a perturbation and the corresponding output power is compared with that at the previous perturbing cycle. In this algorithm a slight perturbation is introduced to the system. This perturbation causes the power of the solar module to vary. If the power increases due to the perturbation then the perturbation is continued in the same direction. After the peak power is reached the power at the MPP is zero and next instant decreases and hence after that the perturbation reverses as shown below.

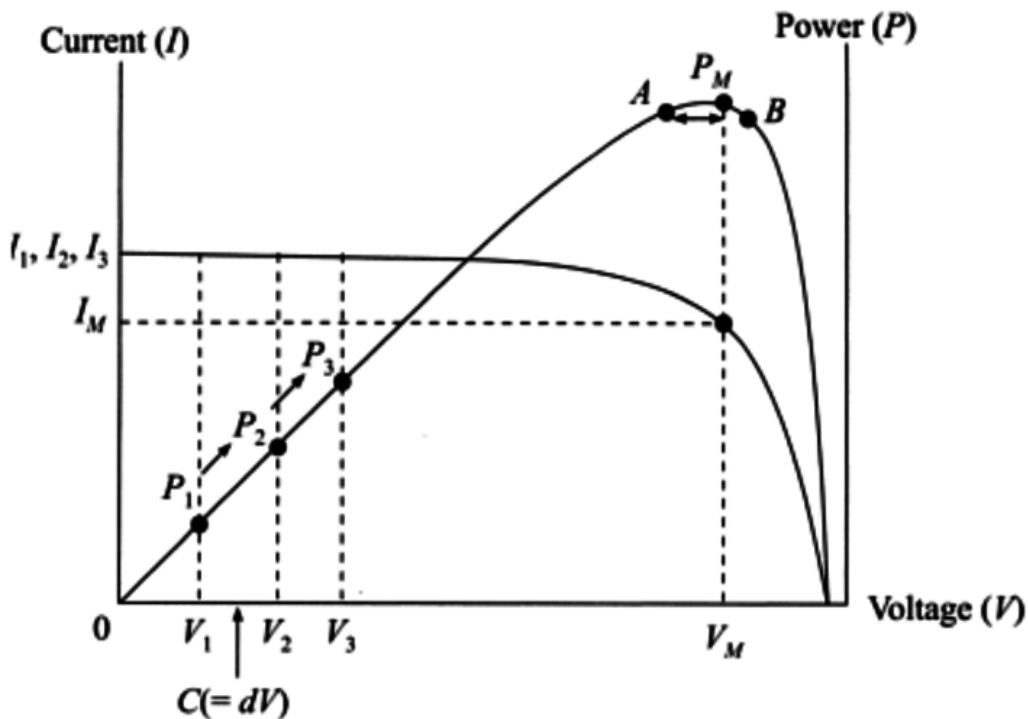


**Figure 3.3.4.1:** Power versus Voltage curve for Perturb and Observe algorithm

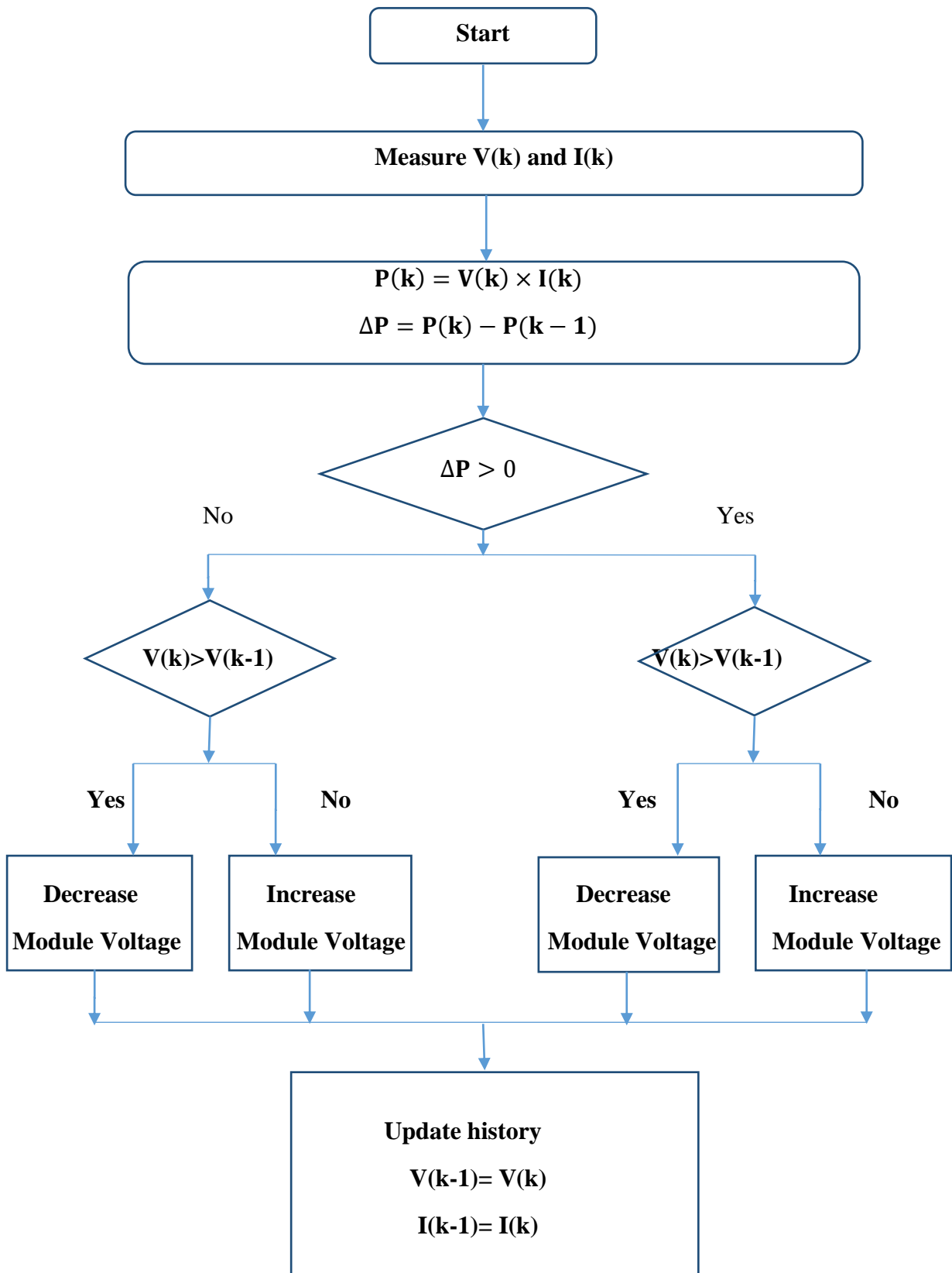


**Figure 3.3.4.2:** Flowchart of Perturb and Observe algorithm

### 3.3.5 Incremental Conductance Method

An observation based on a P-V characteristic curve the Incremental Conductance Method was planned. In 1993 when this algorithm was made it was intended to overcome some drawbacks of the P&O algorithm. The MPP can be calculated with the help of the relation between  $dI/dV$  and  $I/V$ . The incremental conductance method is based on the fact that, the slope of the PV array of the power curve is zero at the MPP, positive on the left of the MPP and negative on the right on the MPP. This can be given by,

$$\begin{aligned}\frac{dP}{dV} &= \frac{d(V \cdot I)}{dV} = I \frac{dV}{dV} + V \frac{dI}{dV} \\ &= I + V \frac{dI}{dV}\end{aligned}$$

MPP is reached when  $\frac{dP}{dV} = 0$  and

$$\frac{dI}{dV} = -\frac{I}{V}$$

$$\frac{dP}{dV} > 0 \text{ then } V_p < V_{mpp}$$

$$\frac{dP}{dV} = 0 \text{ then } V_p = V_{mpp}$$

$$\frac{dP}{dV} < 0 \text{ then } V_p > V_{mpp}$$

So if the MPP lies on right side,  $< -I/V$  and then the Photo Voltaic voltage must be reduced to reach the MPP. In order to find the MPP IC method can be used, it has been known to improve the PV efficiency, reduce power loss and also the system cost. When IC method is implemented in a microcontroller it is seen to produce a much more stable performance compared to P&O method. The procedure starts with measuring the present values of PV module voltage and current. Then, it computes the incremental changes,  $dI$  (change in current) and  $dV$  (change in voltage), which uses the present and previous values of the voltage and current. With the help of the relationships in the equations mentioned above the main check is then done.

If the condition satisfies the inequality equation shown above, it is assumed that the operating point is at the left side of the MPP thus must be moved to the right by increasing the module voltage. Similarly, if the condition satisfies the inequality equation, it is assumed that the operating point is at the right side of the MPP, thus must be moved to the left by decreasing the module voltage.

**Benefits:**

- It is able to successfully detect any changes in the irradiation and shift its MPP value by adjusting the duty cycle.
- It has a good tracking efficiency.
- This method reduces oscillation around the MPP point.
- It is able to reduce power loss and system cost as well.

**Drawbacks:**

- The computational time is increased due to slowing down of the sampling frequency resulting from the higher complexity of the algorithm compared to the P&O method.

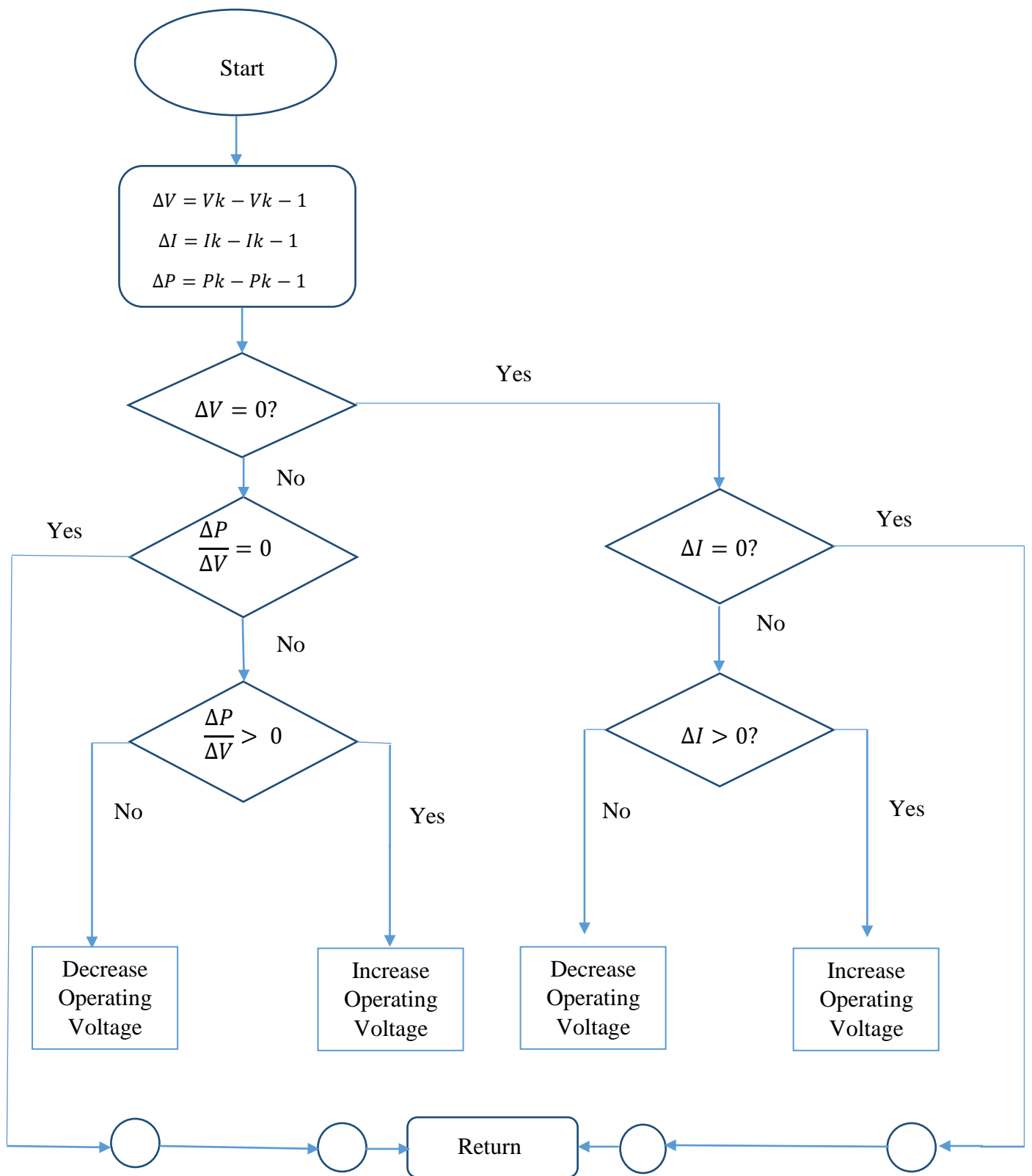


**Figure 3.3.5.1:** Flowchart of Incremental Conductance Method Algorithm

## Chapter 4

### System Overview

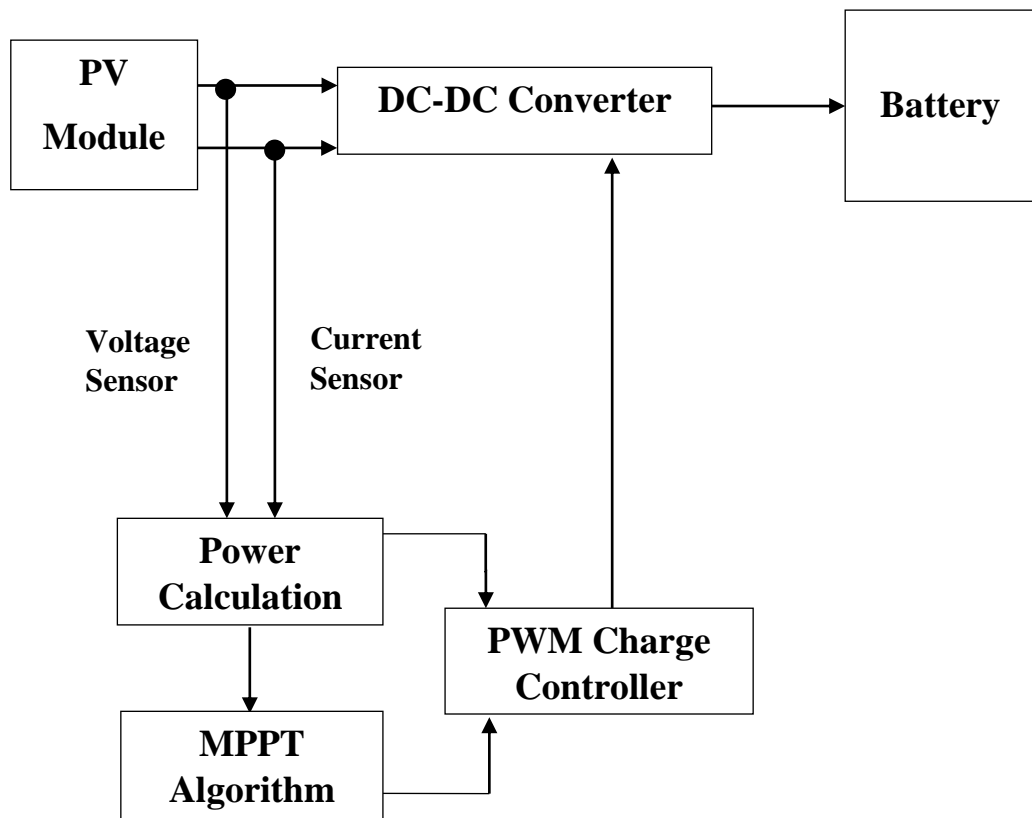


**Figure4.1:** Block Diagram of the system

## 4.1 Panel Specifications

The PV module we used is based on polycrystalline silicon diode. Usually, this type of PV module is used in home usage, project based work where the cost should be in a reasonable range. The specifications provided with our PV module are given below.

- Company : Power4U
- Cell type & efficiency: polycrystalline
- Dimensions: 1088mm\*540mm\*33mm
- Maximum Power : 65W
- Tolerance of  $P_{max}$ : 0-3%
- Rated Voltage( $V_{MPP}$ )- 17.8V
- Rated Current ( $I_{MPP}$ )- 3.66A
- Open circuit Voltage ( $V_{oc}$ )- 22.3V
- Short circuit current ( $I_{sc}$ ) – 3.94A
- Weight- 7.19Kg
- Manufacturer Company: NINGBO AIKE SOLAR LTD.

## 4.2 Voltage Sensor

The main target of charge controller is to charge up the battery by supplying it the required level of voltage. It is achieved by Arduino by the preset algorithm of MPP. Notably, Arduino microcontroller chip consists of a built-in analog to digital converter. By this conversion it enables the analog dc input voltage to convert into quantized digital values and then fed to the algorithm to compare the voltage level with previous output level.

A voltage divider circuit was used to sense the input voltage. Arduino can measure upto 5V DC voltage. Two resistors of value  $4.7\text{k}\Omega$  and  $1\text{k}\Omega$  were used. The ADC pin A0 was connected to the node between  $1\text{k}\Omega$  and  $4.7\text{k}\Omega$  resistor as shown in the figure below. The equation for voltage in A0 pin is-

$$V_o = \frac{R2}{R1+R2} Vin = \frac{1}{5.7} Vin$$

The maximum voltage supply from the solar panel is open circuit voltage 22.3V. For maximum voltage supply the ADC pin A0 is fed 3.912 V which is below the limit. The Arduino code then calculates the actual voltage by multiplying the measured voltage by 5.7.

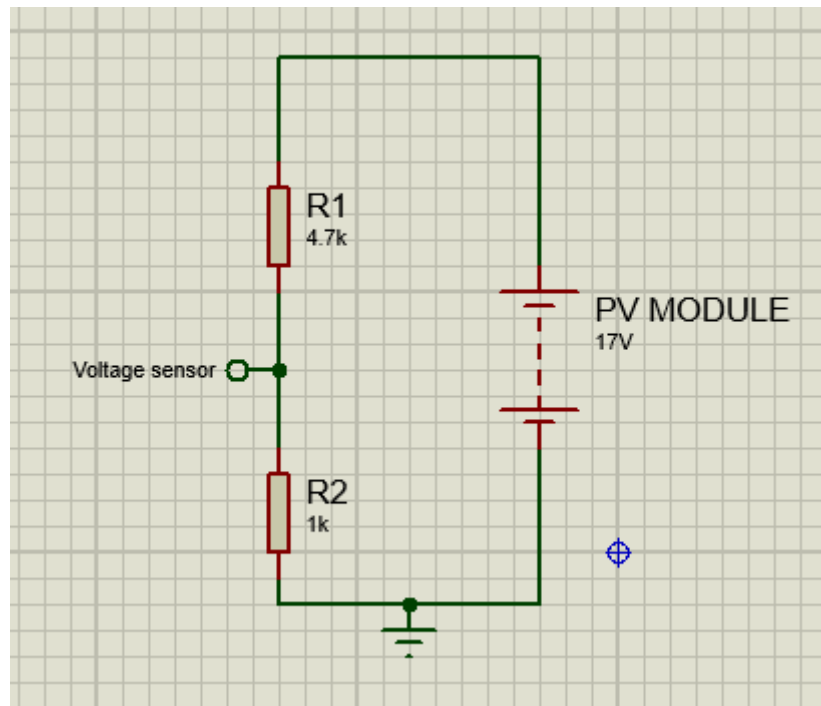


**Figure 4.2.1:** Voltage divider circuit for voltage sensing

### 4.3 Current Sensor

To sense the current generated by the PV module in different conditions a hall-effect current sensor ACS712 was used. The ACS712 Current Sensor is a product of Allegro MicroSystems that can be used for precise measurement of both AC and DC currents. This sensor is based on Hall Effect and the IC has an integrated Hall Effect device. Most importantly, it is the most preferable microchip assembled IC to be used with Arduino.

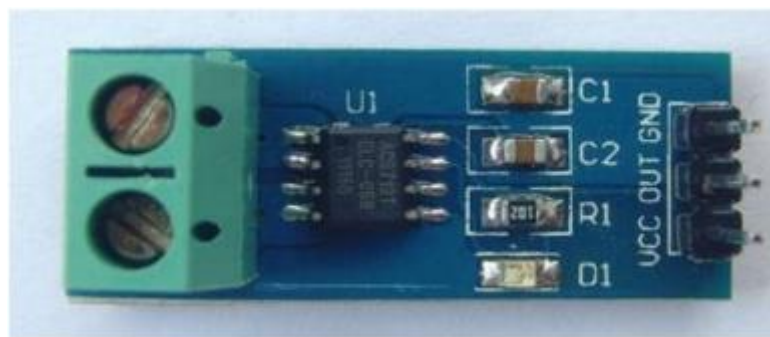


**Figure 4.3.1:** Hall Effect current sensor ACS712

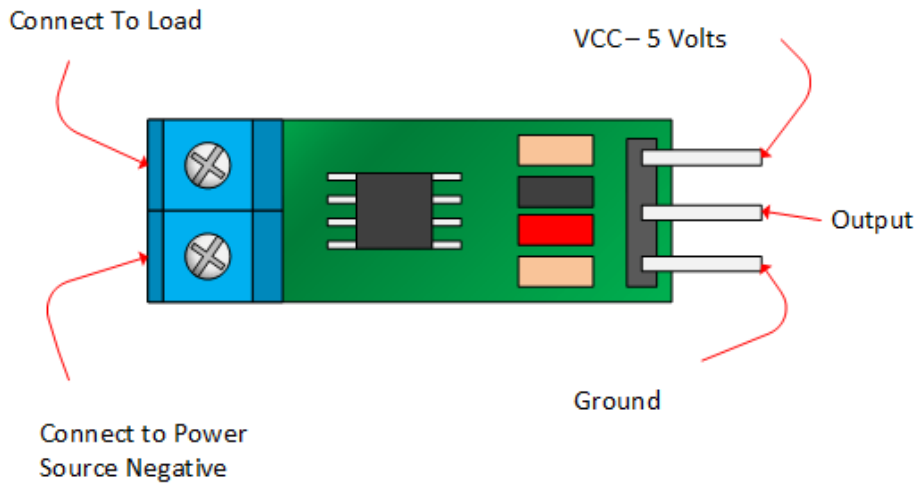


**Figure 4.3.2:** Pin configuration

A Current Sensor is an important device in power calculation and management applications. It measures the current through a device or a circuit and generates an appropriate signal that is proportional to current measured. The output signal of ACS712 is an analog voltage. The ACS712 IC is available in an 8-lead SOIC package and the following image shows its pin diagram.

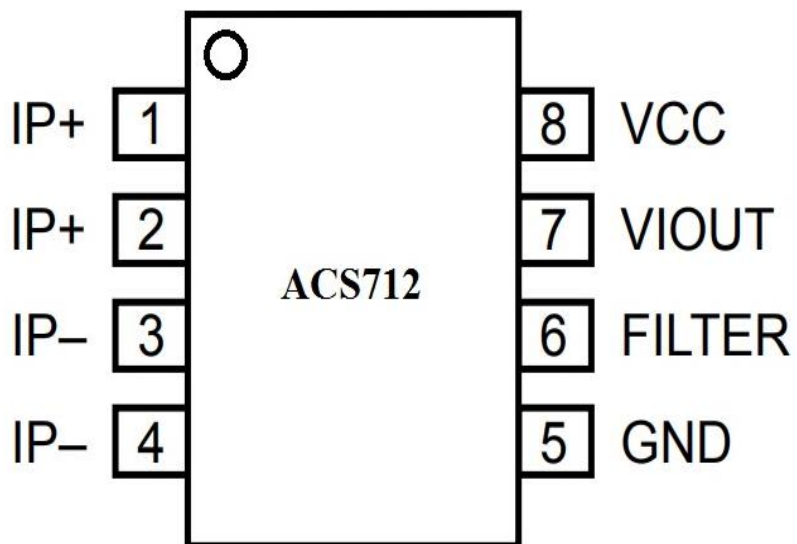


**Figure 4.3.3:** Pin out diagram of ACS712

The ACS712 is based on Hall Effect. There is a copper strip connecting the IP+ and IP- pins internally. When some current flows through this copper conductor, a magnetic field is generated which is sensed by the Hall Effect sensor. The Hall Effect sensor then converts this magnetic field into appropriate voltage. In this method, the input and the output are completely isolated.

For establishing the current sensing equation we tested the current sensor and gathered calibration data. The analog input was divided by 1024 and then scaled up by multiplying it by 5000. At 0A current the sensor has an offset value and after taking several analog input the average value of offset was determined 2500. The offset was deducted from the analog voltage value and divided by sensitivity to determine the current value. We used 5A current sensor and the sensitivity for it is 185mV/A. The connections were made as the pin outs configuration described above. With the help of the Arduino we ran the code and we varied the supplied current from a DC source. The actual value of current supplied by the DC source and the measured current by ACS712 is given below:

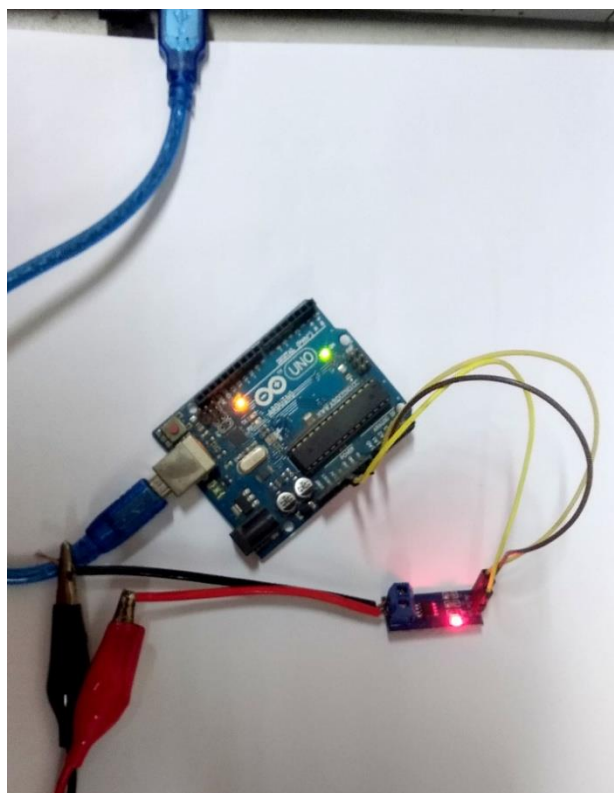


**Figure 4.3.4:** Testing Current Sensor ACS712

Supplied current from source(A)	Measured current with ACS712(A)
0	0.05
0.2	0.17
0.4	0.37
0.7	0.64
1.0	0.92
1.5	1.40
2.2	2.03
3.0	2.78
3.5	3.37

**Table 4.3.1:** Current sensor test results with comparison to actual value

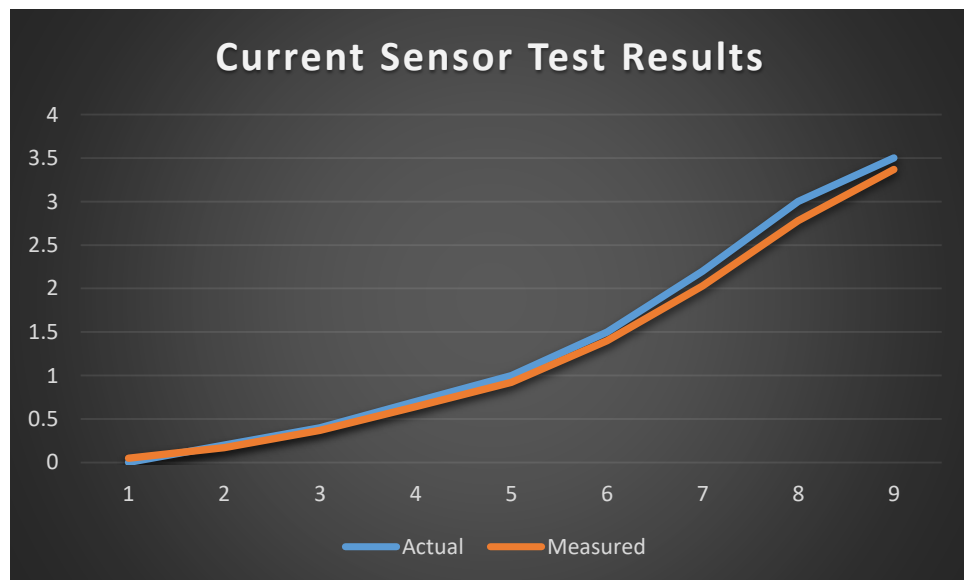


**Figure 4.3.5:** Test Results of ACS712

## 4.4 MOSFET Driver Circuit

TLP250 IC was used to build the MOSFET Driver Circuit. The TOSHIBA TLP250 (INV) consists of a GaAlAs light emitting diode and an integrated photo-detector. This unit is 8-lead DIP and is suitable for gate driving circuit of IGBT or power MOSFETs.

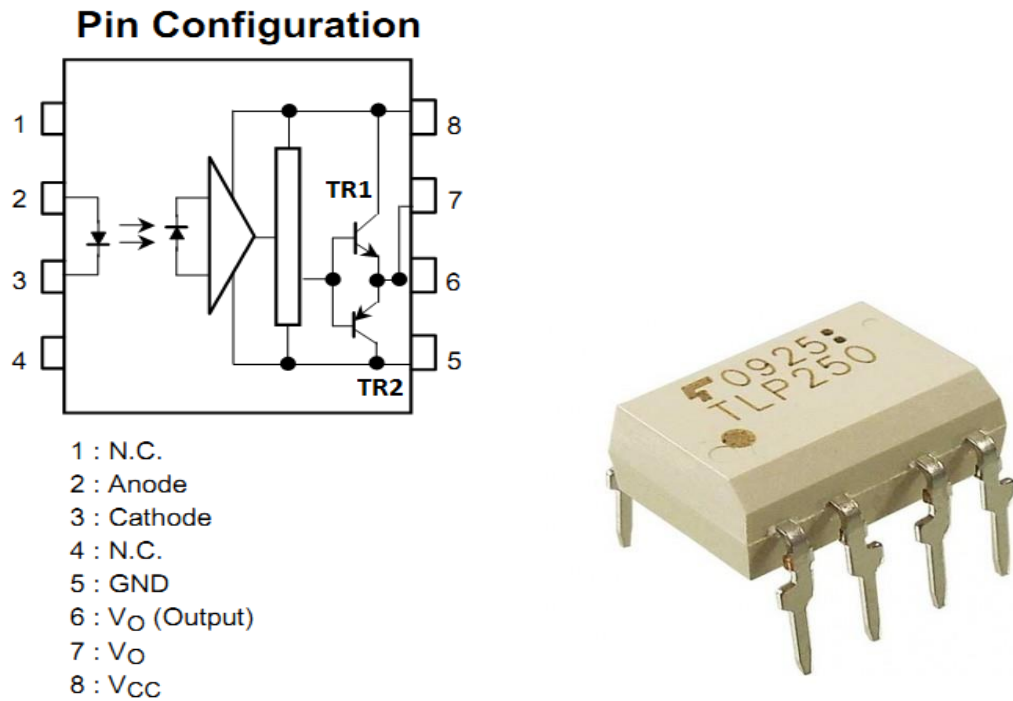


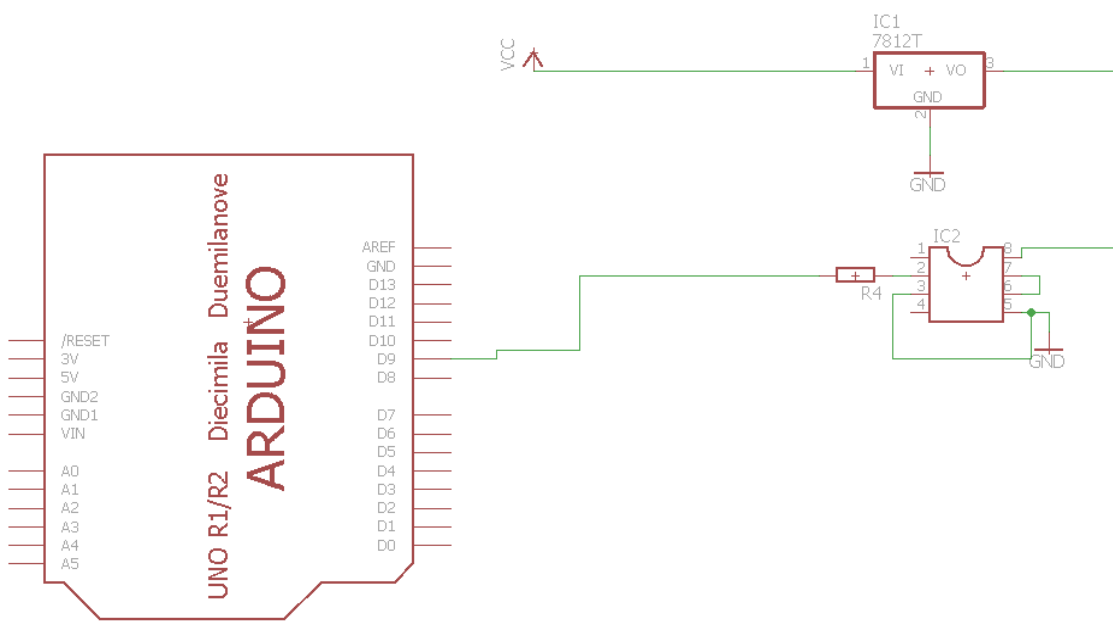
Figure 4.4.1: Pin out diagram of TLP250

Figure 4.4.2: TLP250 IC

The maximum gate threshold voltage of MOSFET IRF250 is 4V. The PWM signal supplied by Arduino is generally below 5V amplitude which is not sufficient to drive the MOSFET. Therefore TLP250 was used to generate PWM signal of the same duty cycle as supplied by Arduino but of 12V amplitude.

A PWM signal from Digital pin 9 was fed into pin 2 of TLP250 and pin 3 and 5 were grounded. An  $220\Omega$  input resistor was used to limit the input current to 22mA . A 12V was supplied from 7812 IC into the pin 8 of TLP250. The output PWM generated by TLP250 is fed into the gate pin of MOSFET from pin 8.

The frequency of PWM signal provided by Arduino is only of 1kHz whereas the switching frequency required for the boost converter is much higher. A library was built to enable arduino to supply PWM signal of 100kHz .



**Figure 4.4.3:** Schematic of MOSFET driver circuit

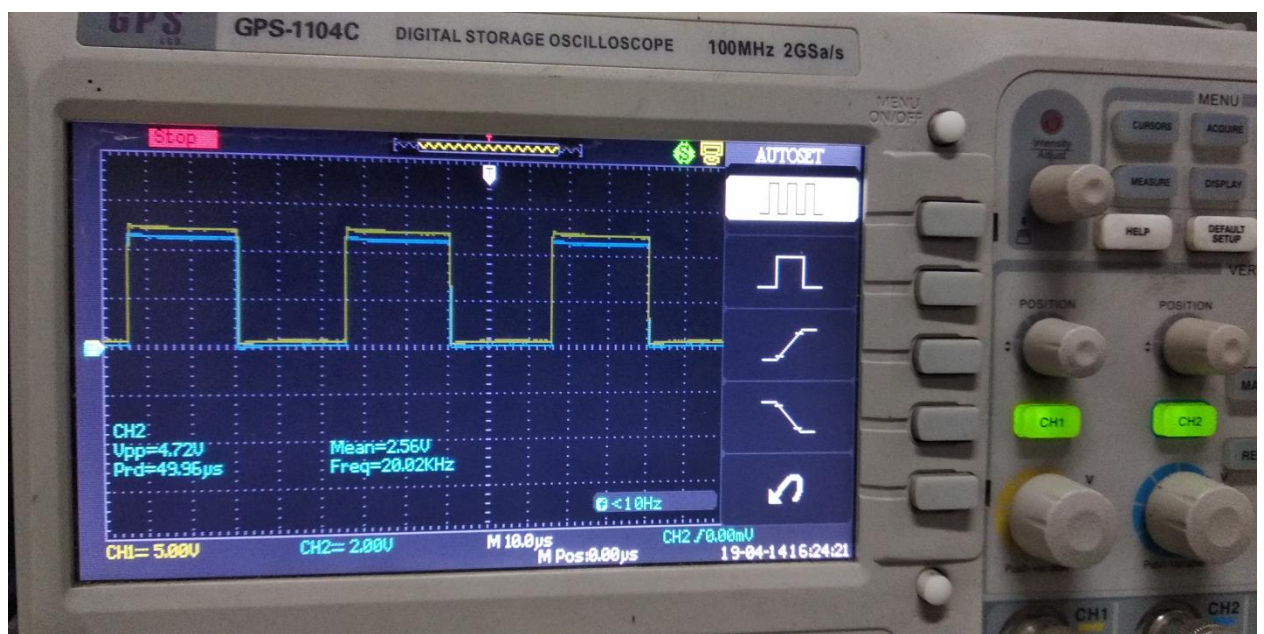


**Figure 4.4.4:** Input PWM Signal (5V Amplitude - blue) & Output PWM Signal ( 12V Amplitude -yellow)

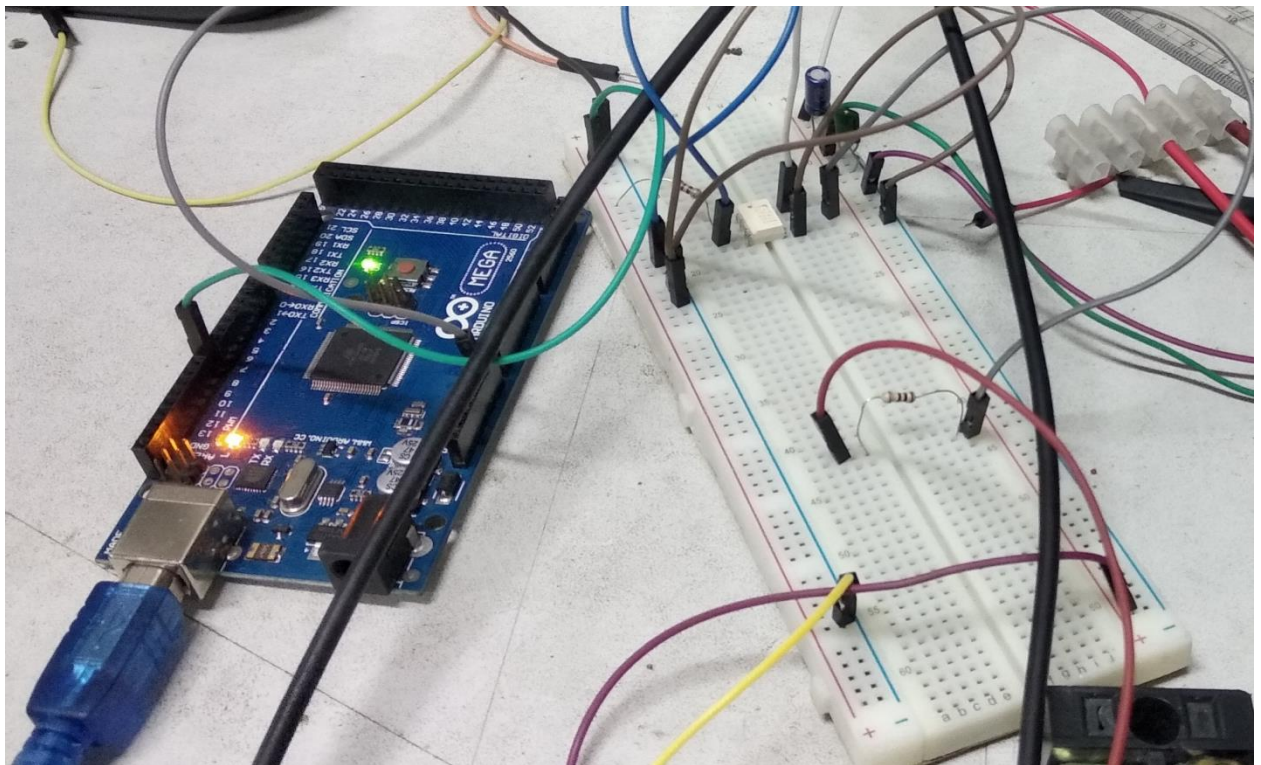


**Figure 4.4.5:** MOSFET Driver circuit during experimentation

## 4.5 Boost Converter

The boost converter is designed to increase a DC voltage from a lower voltage to a higher one .The boost converter consists of a inductor, a capacitor, a diode and a MOSFET. it uses a parallel connected switching transistor to control the output voltage from the switch mode power supply. As the transistor switch is effectively connected in parallel with the output, electrical energy only passes through the inductor to the load when the transistor is biased “OFF” (switch open).

In the *Boost Converter* circuit, when the MOSFET is fully-on, electrical energy from the PV module,  $V_s$  passes through the inductor and MOSFET and back to the supply. As a result, none of it passes to the output as the MOSFET effectively creates a short circuit to the output. This increases the current flowing through the inductor as it has a shorter inner path to travel back to the supply. Meanwhile, diode D becomes reverse biased as its anode is connected to ground via the MOSFET with the voltage level on the output remaining fairly constant as the capacitor starts to discharge through the load.

When the switch is on

$$V_S = V_L$$

$$I_{L.on} = \frac{V_S}{L} \int dt$$

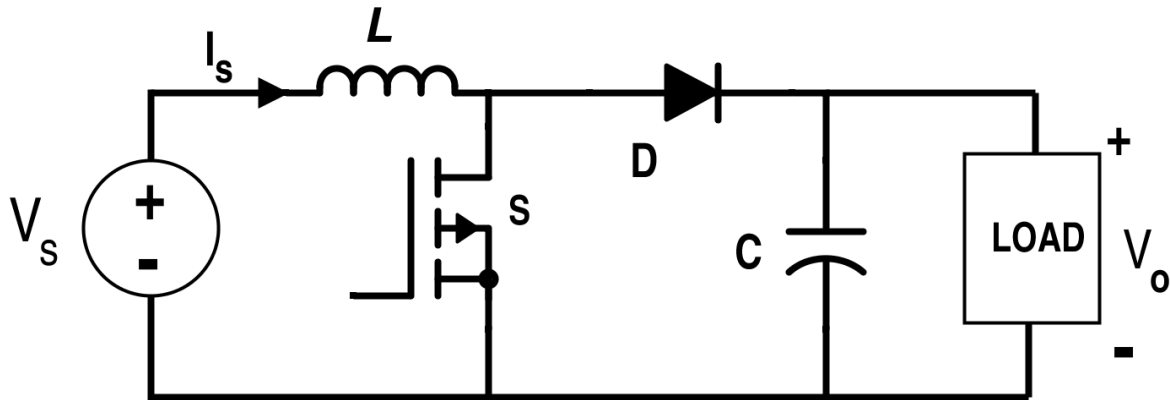


**Figure 4.5.1:** Circuit diagram of Boost Converter

When the MOSFET is switched fully-off, the input supply is now connected to the output via the series connected inductor and diode. As the inductor field decreases the induced energy stored in the inductor is pushed to the output by \$V\_s\$, through the now forward biased diode. The result of all this is that the induced voltage across the inductor \$L\$ reverses and adds to the voltage of the input supply as it now becomes –

$$V_S - V_0 = V_L$$

$$I_{L.off} = \frac{V_S - V_L}{L} \int dt$$

The ratio of output to input voltage is represented by

$$\frac{V_0}{V_S} = \frac{1}{1 - D}$$

$$\frac{I_0}{I_{in}} = (1 - D)$$

Where,

$D$  = Duty ratio

$V_o$  = Output voltage

$V_s$  = Input Voltage of PV module

$I_0$  = Output current

$I_{in}$  = Input current

The equation used to calculate minimum inductance is:

$$L_{min} > \frac{(1 - D)^2 DR}{2f}$$

Where,

$D$  = Duty cycle

$F$  = Switching frequency

$L_{min}$  = Minimum inductance

Component	Name/ Value
Inductor (L)	480uH
Capacitor (C)	68uF
Diode	MUR1560
MOSFET	IRF250

**Table 4.5.1:** The list of components

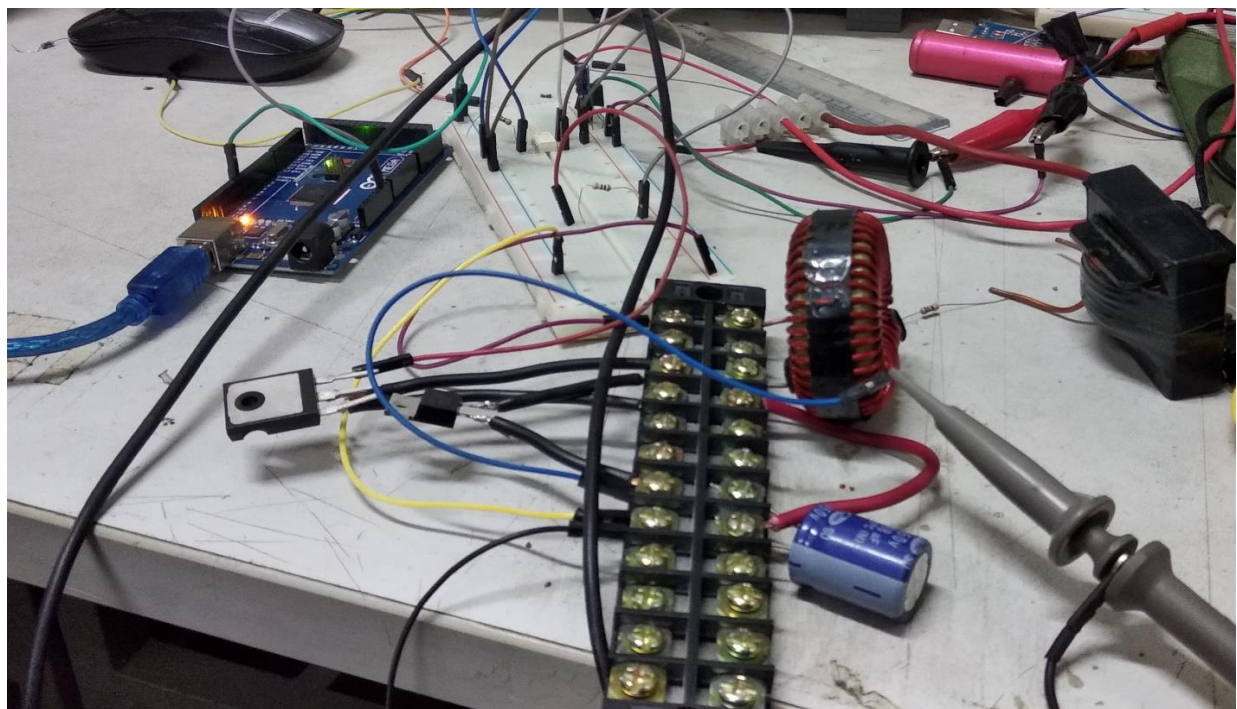


**Figure 4.5.2:** Boost converter circuit

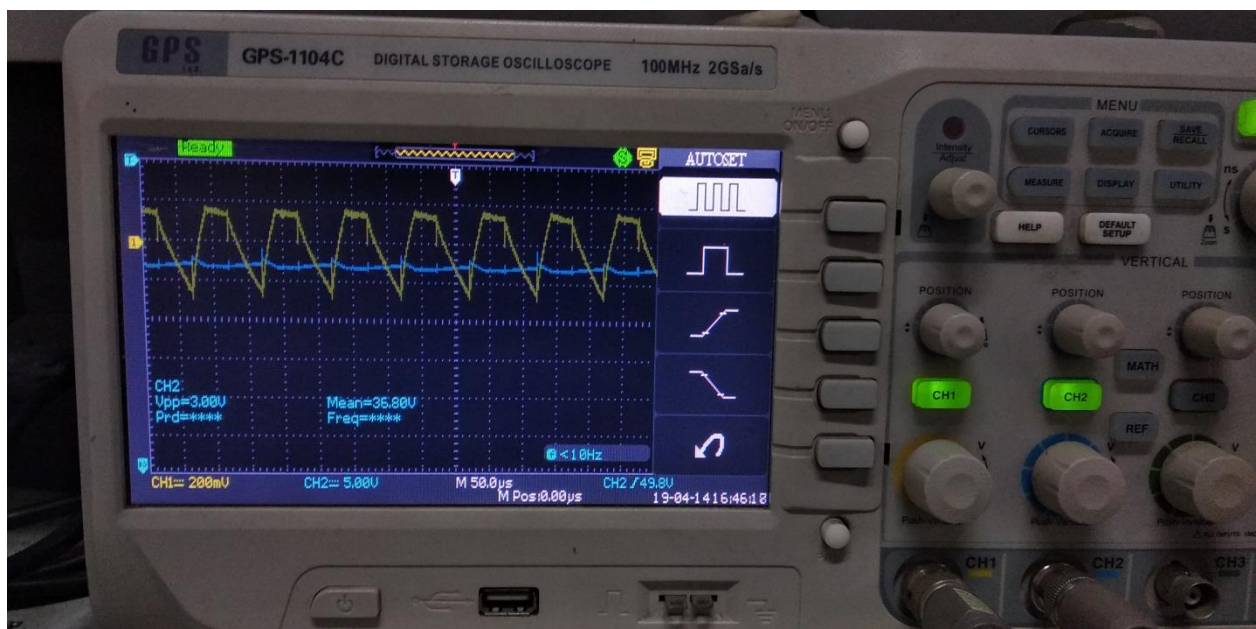


**Figure 4.5.3:** Output Voltage of Boost Converter (28V DC- blue line) when the input voltage was 12V and duty cycle 0.57

#### 4.5.1Inductor

Inductor is one of the most important part of boost converter circuit. Since making an inductor precisely by hand is very hard and the possibility of not getting the desired value because of the faulty position of wires in coil is very high. The inductor used in the boost circuit was obtained from an old circuit board. It is precisely coiled on a magnet core and the value ranges from 470 -480uH.The inductor was measured using a Digital LCR meter.



**Figure 4.5.1.1:** Measuring inductance using LCR meter

#### 4.5.2 Capacitor

A capacitor of 68uF of voltage rating 50V was used in the boost circuit.

#### 4.5.3 Diode

The switching frequency of the boost converter is 100kHz. Therefore the converter requires an ultra-fast rectifier diode with high voltage and current rating. MUR1560 diode was used which fulfills the requirements. MUR1560 is a switch mode power rectifier with ultrafast recovery time of 35 and 60 Nanosecond. It can handle 15A forward current and up to 600V.

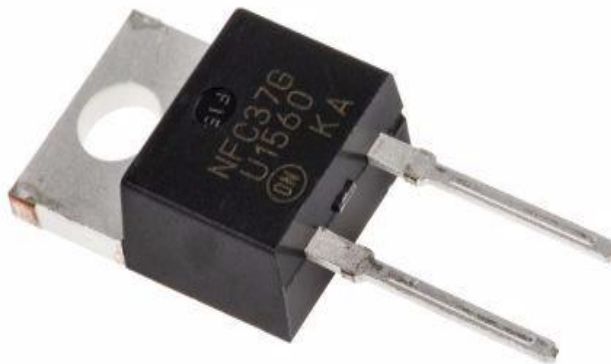


**Figure 4.5.3.1:** MUR1560 IC

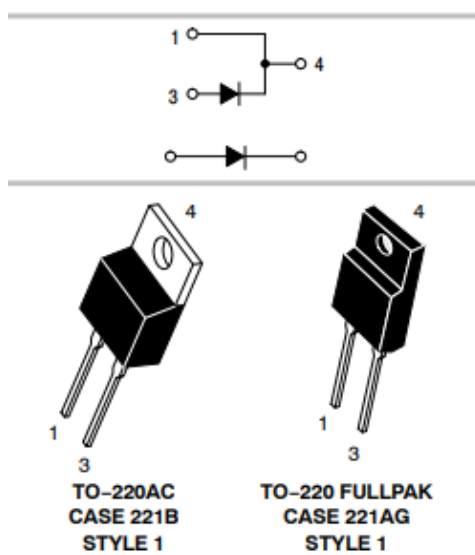


**Figure 4.5.3.2:** Pin out diagram of MUR1560

#### 4.5.4 MOSFET (IRF250)

MOSFET IRF250 was chosen for its high switching frequency and high power handling capacity. IRF250 is an n-channel MOSFET with a gate to source threshold voltage of 4V, maximum drain-source voltage of 200V and maximum drain current of 30A. It also has a low input capacitance, 10nS rise time and maximum power dissipation of 150W.

Therefore IRF250 is suitable for this boost converter where it operates at 100 kHz with a maximum drain to source voltage of 22.3V and maximum drain current of 3.94A.

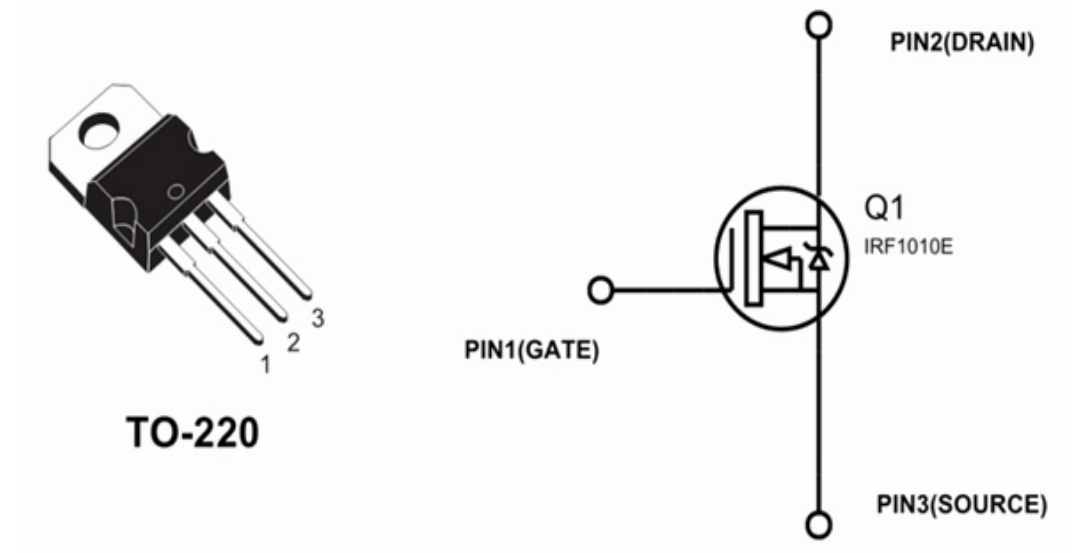


**Figure 4.5.4.1:** Pin out diagram of IRF250

## 4.6 Arduino Uno

Arduino Uno was used to measure voltage, current and to calculate power in order to apply MPPT algorithms by adjusting duty cycle of the boost converter.

Arduino Uno board has ATmega328 microcontroller. This is the most robust and documented board of the arduino family. The board is equipped with sets of digital and analog input/output (I/O) pins that may be interfaced to various expansion boards or breadboards and other circuits. The board feature serial communications interfaces, including Universal Serial Bus (USB) which is used for loading programs from personal computers. In addition to using traditional compiler toolchains, the Arduino project provides an integrated development environment (IDE) based on the Processing language project.



**Figure 4.6.1:** Arduino Uno board

### 4.6.1 Characteristics of Arduino Uno

- Microcontroller: ATmega328
- Supply Voltage in Vcc ( Recommended): 7-12V
- Minimum Supply Voltage: 6V
- Maximum Supply Voltage: 20V
- Digital I/O Pins: 14 ( 6 PWM pins)
- Analog Input Pins: 6
- DC Current per I/O Pin: 40mA

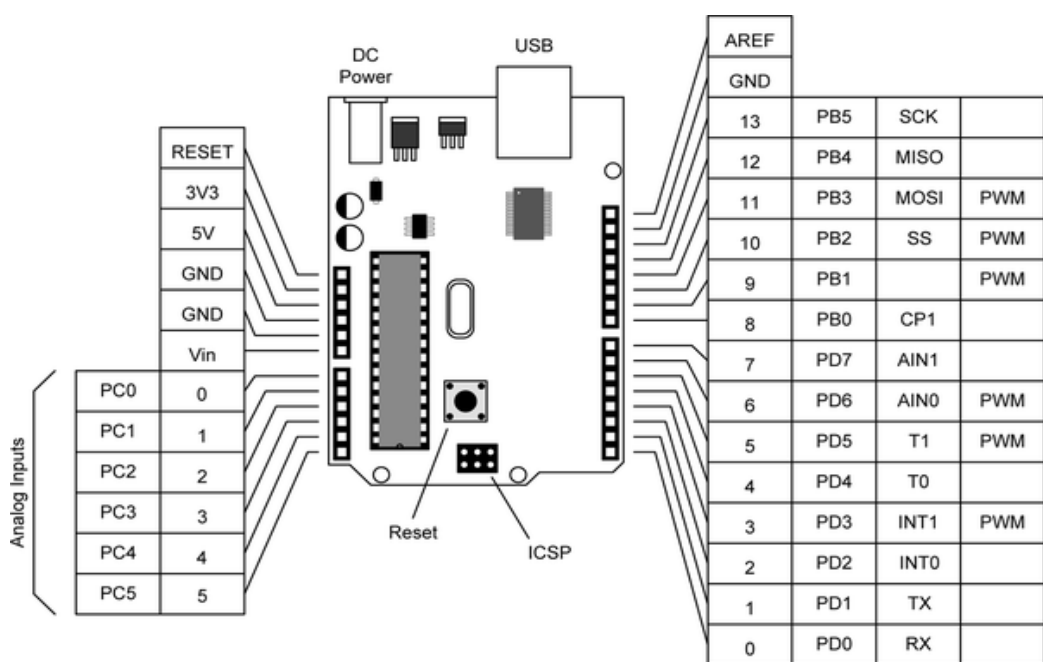


**Figure 4.6.2:** Pin out diagram of Arduino Uno board

## 4.7 Battery

In this thesis, two 12V batteries, connected in series, were used as load for the system. Each of the batteries is 12V,7Ah lead-acid battery made by ZIGOR Corporation S.A. Even though Li-ion batteries have some advantages over lead acid battery such as fast charging rate, high energy density, extended cycle life, low maintenance, lead acid batteries were used for its low capital cost.



**Figure 4.7.1:** 12V lead acid battery used in the thesis

From HOMER (micro-grid simulation software) it is found that instead of high cycle life and maximum depth of discharge (DOD) of Li-ion batteries than lead acid ones, NPC of SHS with Li-ion battery is higher than that of system with lead acid battery if project lifetime is less than 5 years.

## Chapter 5

### Experimentation for MPPT

#### **5.1 Searching MPP Using Nichrome Heater Coil**

We set up the system exactly before mentioned just replaced the rheostat with the nichrome wire. We found the resistance of such long wire to be 36ohm. Then we swept one pointer along the length of the wire in order to get different values of the resistance and recorded the corresponding reading of the ammeter and voltmeter in each step. Fortunately, the nichrome wire was able to provide us with very little resistance within the range of 0 to 1ohm. We generated the following graphs with the help of MATLAB.

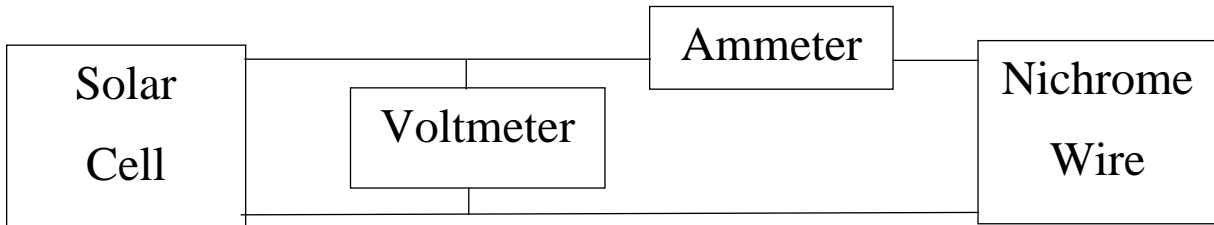


**Figure 5.1.1:** Block Diagram of Setup

We took several set of data in different part of the day with different intensity level of the sunlight. Nichrome wire gets heated too much upon flowing current for a long time and thus changes the value of the resistance which may corrupt the data we took. Considering this, we took the data very quickly avoiding the mere difference created by the contact resistance which is formed in the junction of the pointer and the wire.

From the graph, we can interrupt out maximum power point (MPP) is near around 18.5V and the current vs. voltage graph also matches with the theory we studied. And at the maximum power point we found the value of the current is near 3A.

This experiment was done to find out the maximum power point but we used resistance as a load. Our sole purpose is to track the MPP and recharge a hybrid battery. With a view to this we step into our next step where we purchased two 12V lead acid battery. Then we conducted our search for the MPPT using this battery as a load and varying the resistance of the nichrome wire to obtain different set of values.

**Date:** 19-10-2018

**Place:** Chatri Hall, BUET

**Temperature:** 33 degree to 36 degree

**Time:** 11am to 5pm

**Weather:** Sunny

Voltage (V)	Current (A)	Power (W)
1.3	2.71	3.523
1.4	2.94	4.116
1.6	3.00	4.8
2.2	3.02	6.644
2.7	2.84	7.668
3.1	2.72	8.432
4.0	2.74	10.96
5.4	2.78	15.012
6.9	2.82	19.458
9.4	2.64	24.816
10.6	2.56	27.136
11.2	2.44	27.328
12.4	2.41	29.884
13.5	2.30	31.05
15.1	2.18	32.918
15.4	1.88	28.952
15.8	1.82	28.756
16.2	1.62	26.244
16.5	1.22	20.13

**Table 5.1.1:** Data Sheet of MPPT testing using Nichrome Wire

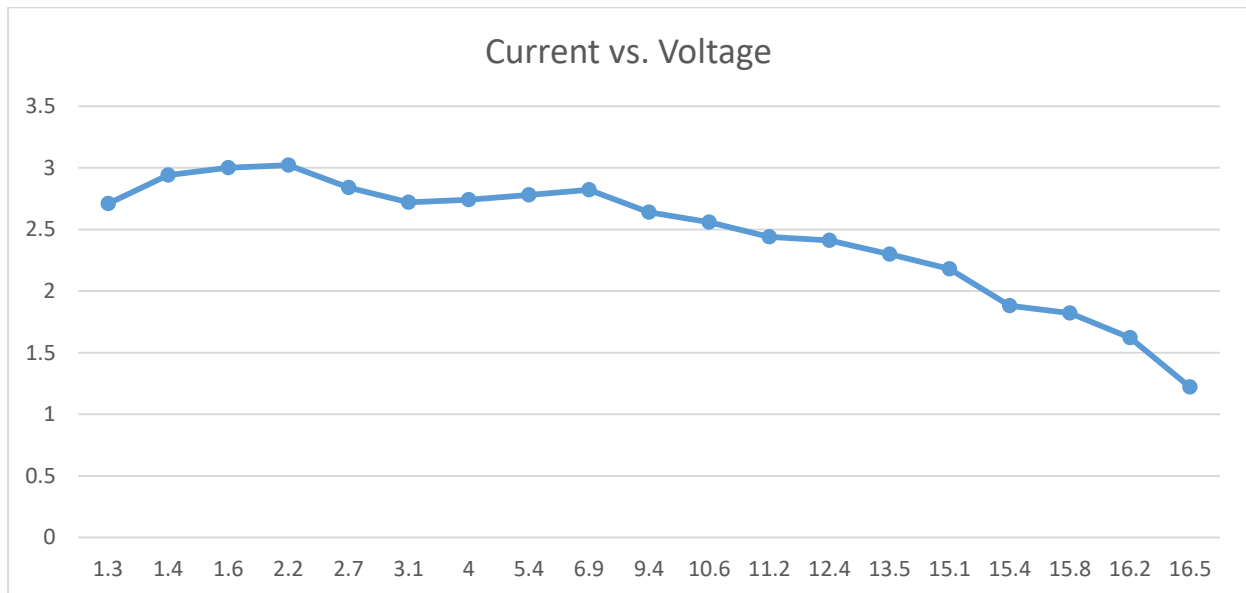


**Figure 5.1.2:** I-V graph of MPPT testing using Nichrome Wire.

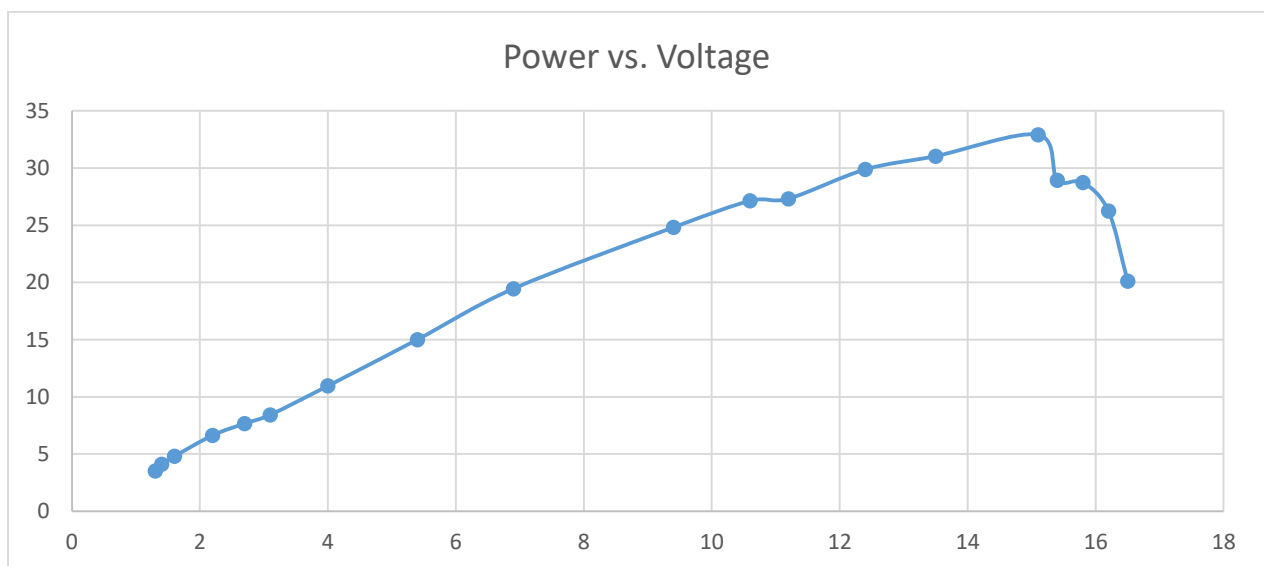


**Figure 5.1.3:** P-V Graph of MPPT testing using Nichrome Wire.

## 5.2 Searching MPP Using 24V Lead Acid Battery as a Load

Our prime objective of this step was finding out the MPPT using 24V battery load which in turn will be required once we design our desired processor. The experimental setup is represented in the form of a block diagram below.

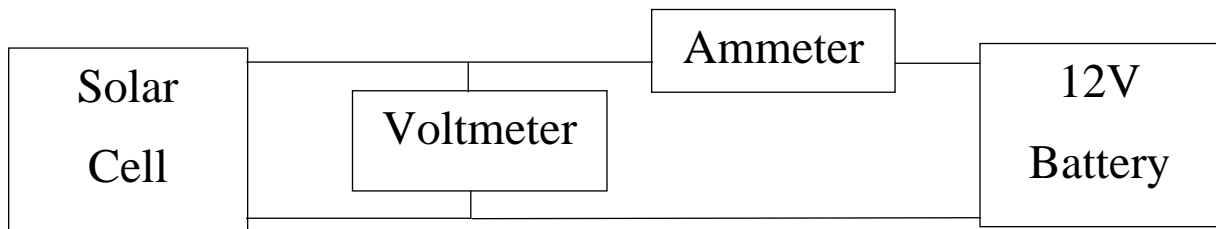


**Figure 5.2.1:** Block Diagram of Setup

**Date:** 26-10-2018

**Place:** Chatri Hall, BUET

**Temperature:** 33 degree to 36 degree

**Time:** 12pm to 4pm

**Weather:** Sunny and Partially Cloudy

Voltage (V)	Current (A)	Power (W)
17.1	2.91	49.761
17.35	2.89	50.1415
17.45	2.87	50.0815
17.70	2.86	50.622
17.90	2.83	50.657
18.15	2.81	51.0015
18.45	2.79	51.4755
18.66	2.76	51.5016
18.82	2.73	51.3786
19.07	2.71	51.6797
19.24	2.69	51.7556
19.39	2.64	51.1896
19.54	2.61	50.9994
19.90	2.58	51.342
20.13	2.52	50.7276
20.30	2.49	50.547
20.51	2.41	49.4291

**Table 5.2.1:** Data Sheet of MPPT testing using 24V Lead Acid Battery as a Load

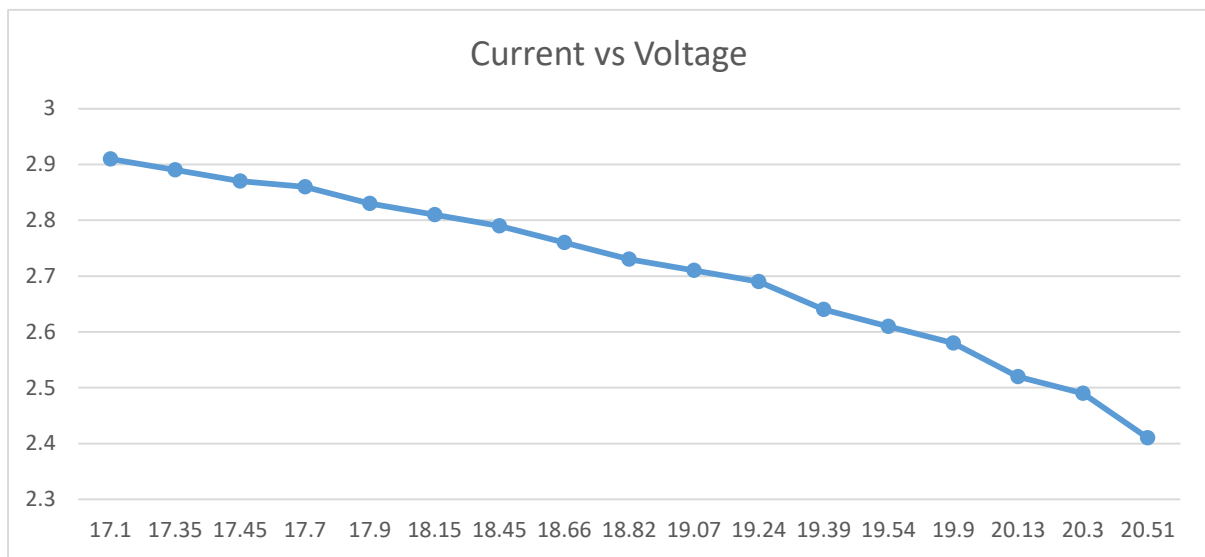


**Figure 5.2.1:** I-V Graph of MPPT testing using 24V Lead Acid Battery as a Load.

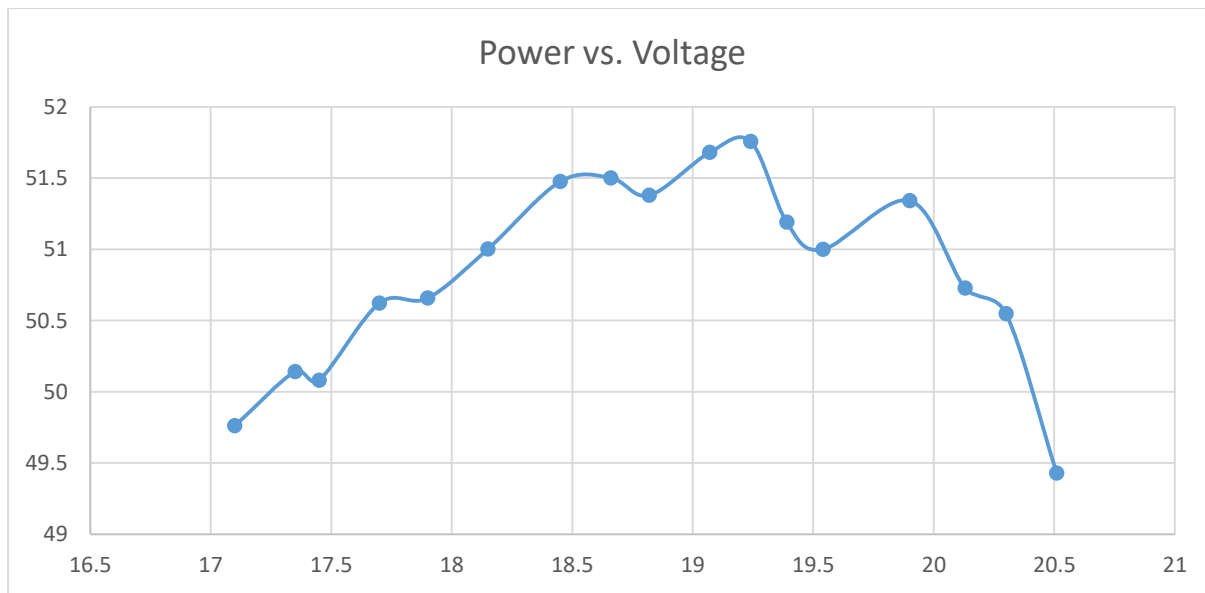


**Figure 5.2.2:** P-V Graph of MPPT testing using 24V Lead Acid Battery as a Load.

**Date:** 23-12-2018

**Place:** Chatri Hall, BUET

**Temperature:** 24 degree

**Time:** 3pm to 4pm

**Weather:** Sunny

Voltage (V)	Current (A)	Power (W)
15.6	0.52	8.112
15.8	0.55	8.69
16.1	0.57	9.177
16.4	0.6	9.84
16.9	0.62	10.478
17.2	0.69	11.868
17.3	0.69	11.937
17.8	0.68	12.104
18.3	0.55	10.065
19.2	0.5	9.6

**Table 5.2.2:** Data Sheet of MPPT testing using 24V Lead Acid Battery as a Load

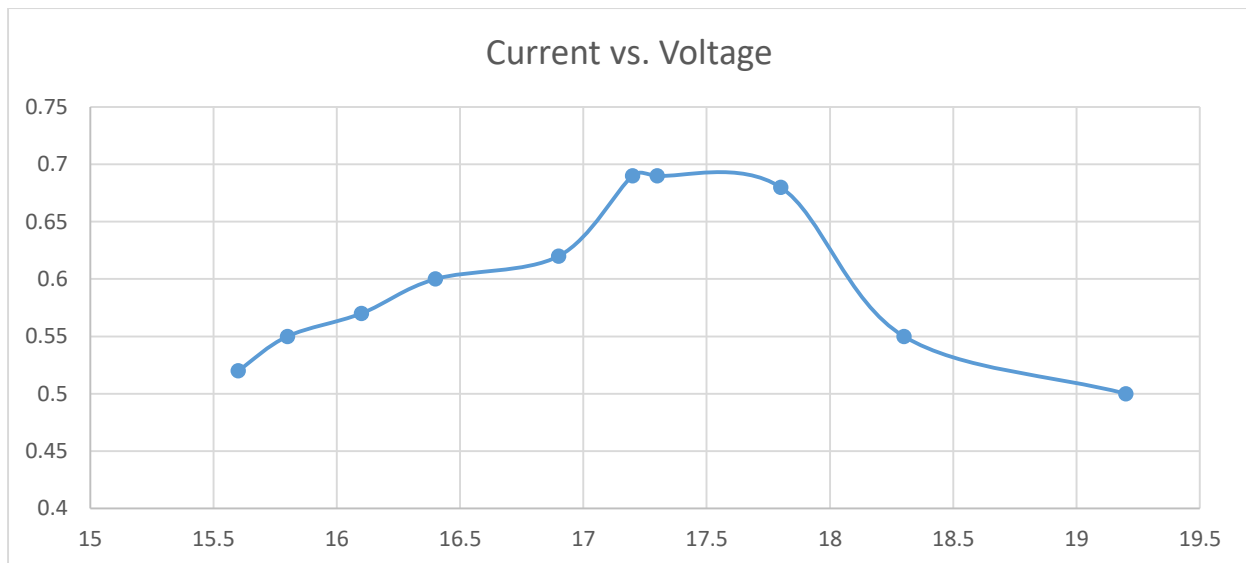


**Figure 5.2.3:** I-V Graph of MPPT testing using 24V Lead Acid Battery as a Load.

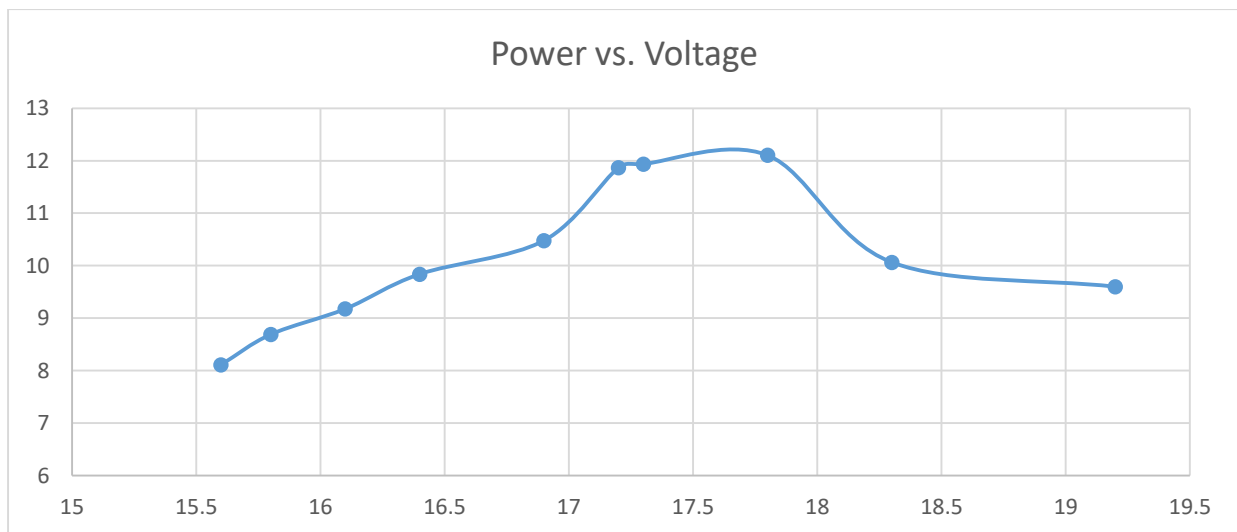


**Figure 5.2.4:** P-V Graph of MPPT testing using 24V Lead Acid Battery as a Load.

**Date:** 09-11-2018

**Place:** Chatri Hall, BUET

**Temperature:** 27 degree

**Time:** 12pm to 4pm

**Weather:** Sunny

Voltage (V)	Current (A)	Power (W)
18.1	0.86	15.566
18.2	0.91	16.562
18.6	0.97	18.042
18.8	0.98	18.424
18.9	1.02	19.278
19.0	1.03	19.57
19.2	1.05	20.16
19.4	1.10	21.34
19.9	1.23	24.477
20.5	1.28	24.395
20.8	1.31	23.92

**Table 5.2.3:** Data Sheet of MPPT testing using 24V Lead Acid Battery as a Load

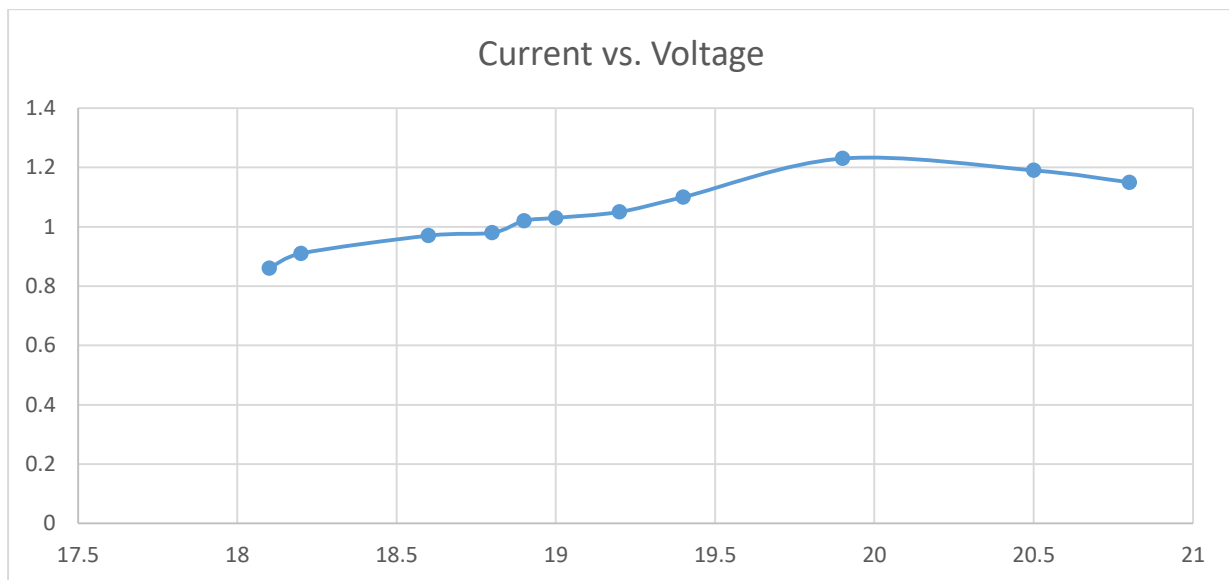


**Figure 5.2.5:** I-V Graph of MPPT testing using 24V Lead Acid Battery as a Load.

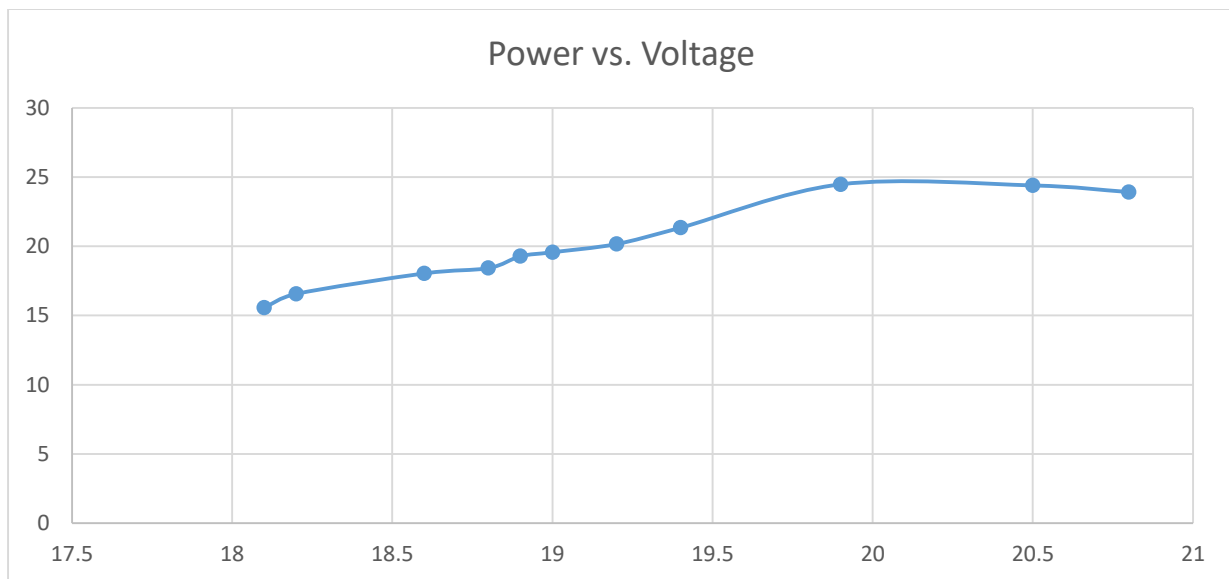


**Figure 5.2.6:** P-V Graph of MPPT testing using 24V Lead Acid Battery as a Load.

### 5.3 Full System Software Simulation

The full system was simulated in Proteus software to check the Incremental Conductance algorithm to track maximum power point. In figure 5.3.1 the solar panel was replaced by a fixed DC source. The PWM signals generated from Arduino pin 9 and MOSFET driver circuit output (Optocoupler pin 6) were plotted in two digital monitors and the Input current and output voltage of the Boost Converter were plotted in two separate analog monitors.

As we know the value of current and voltage of the solar panel depends on the solar irradiation, the fixed DC source was replaced by a current controlled voltage source to vary the input voltage and current as in the case of solar panels. Figure 5.3.3 shows the change of duty cycle to track maximum power point , as the incremental conductance algorithm was applied.

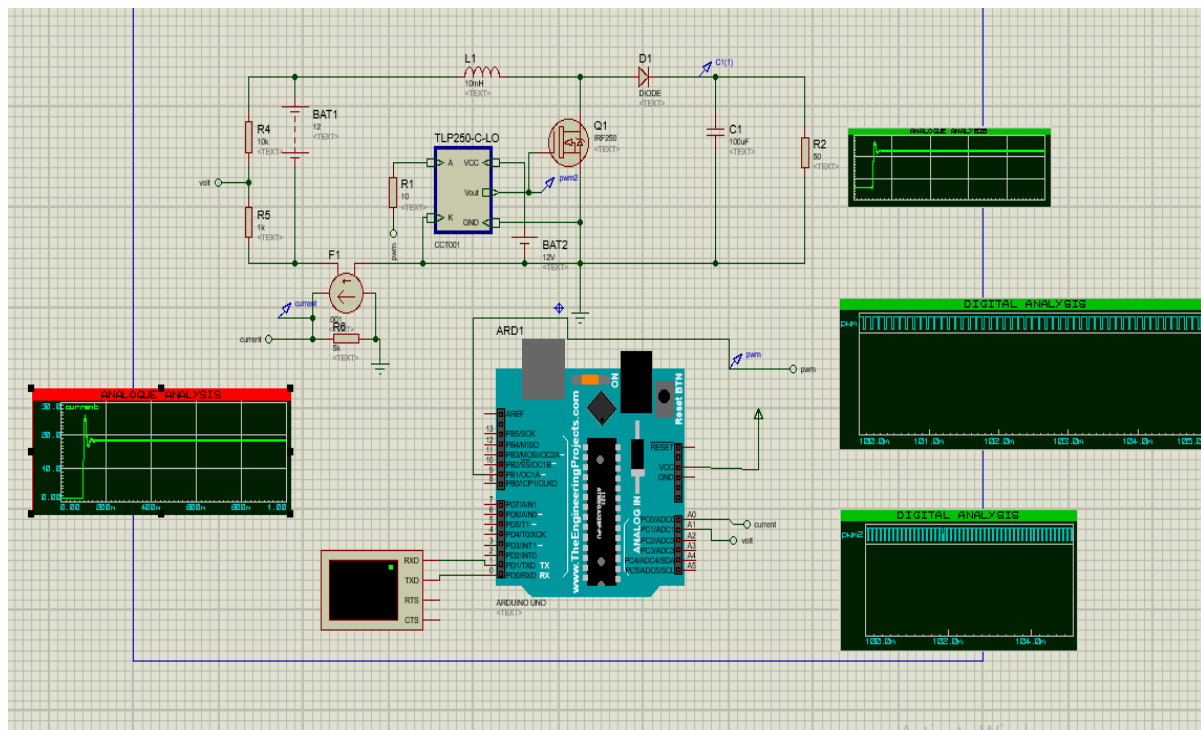


**Figure 5.3.1:** Schematic of the system using a fixed voltage DC source

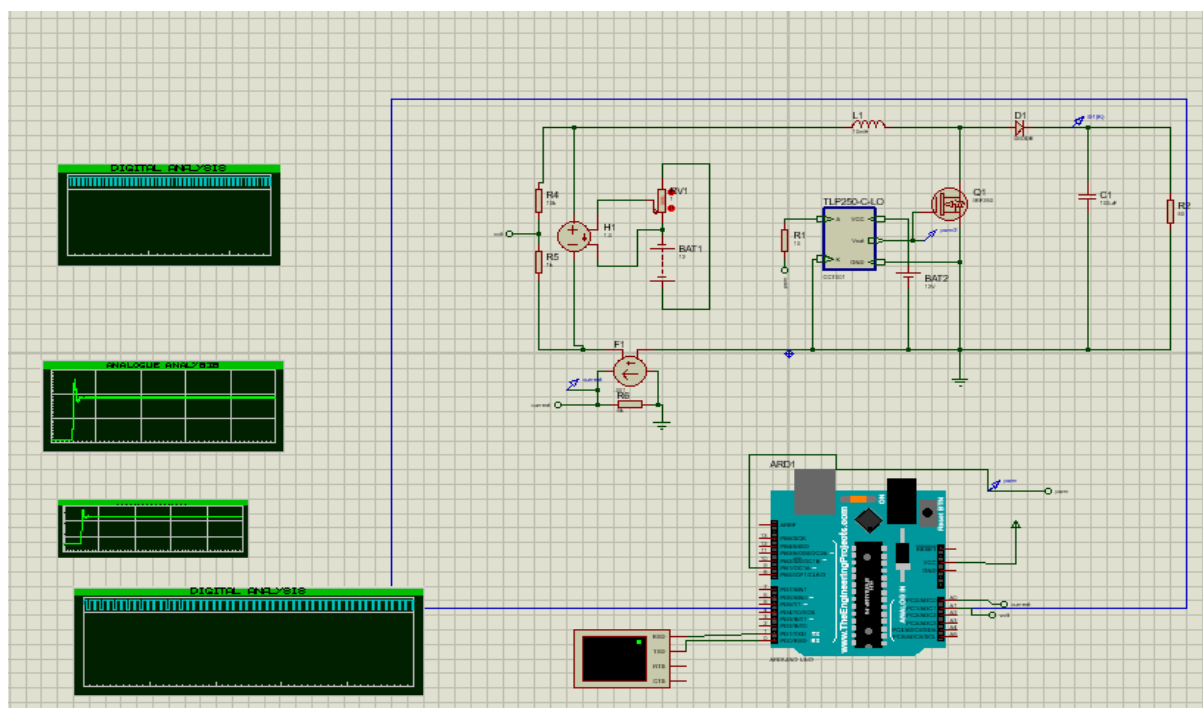


**Figure 5.3.2:** Schematic of the system with a current controlled voltage source

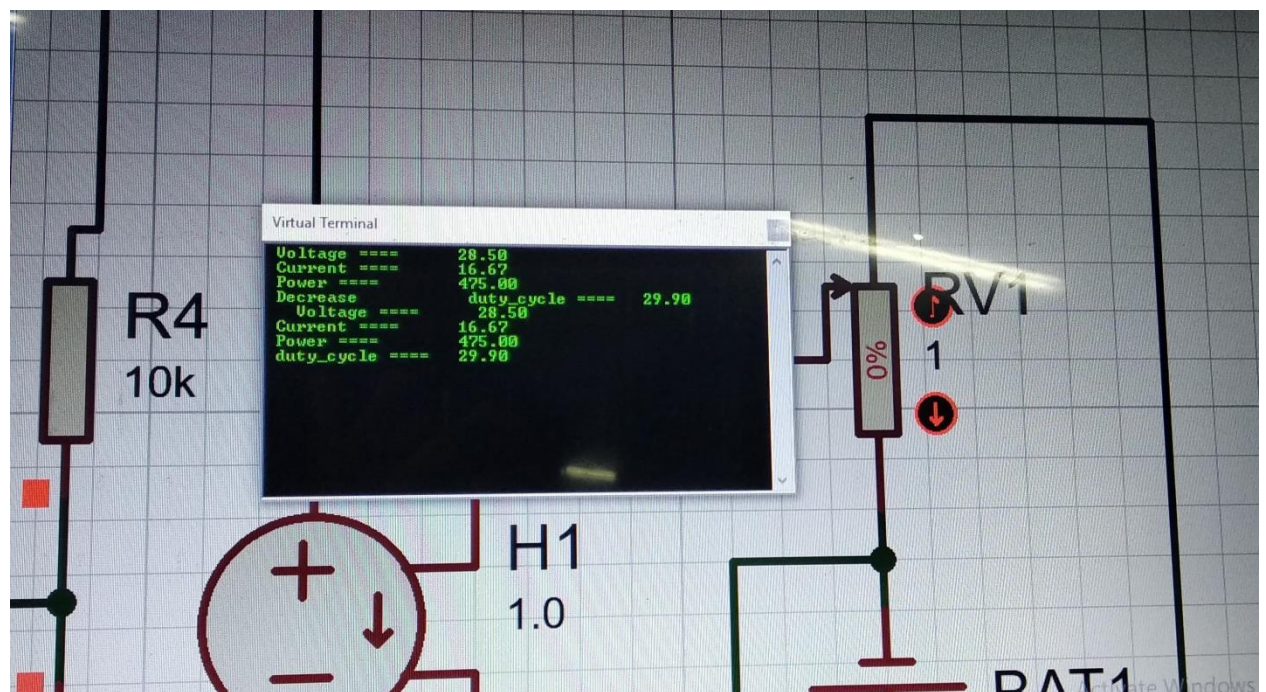


**Figure 5.3.3** Output of the Serial Monitor

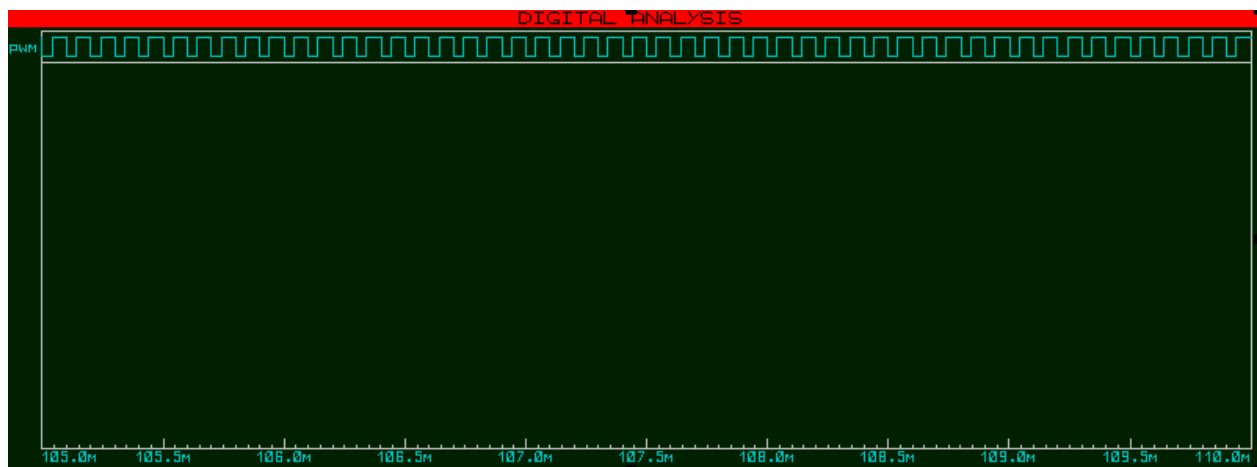


**Figure 5.3.4** Output of the PWM from Arduino UNO

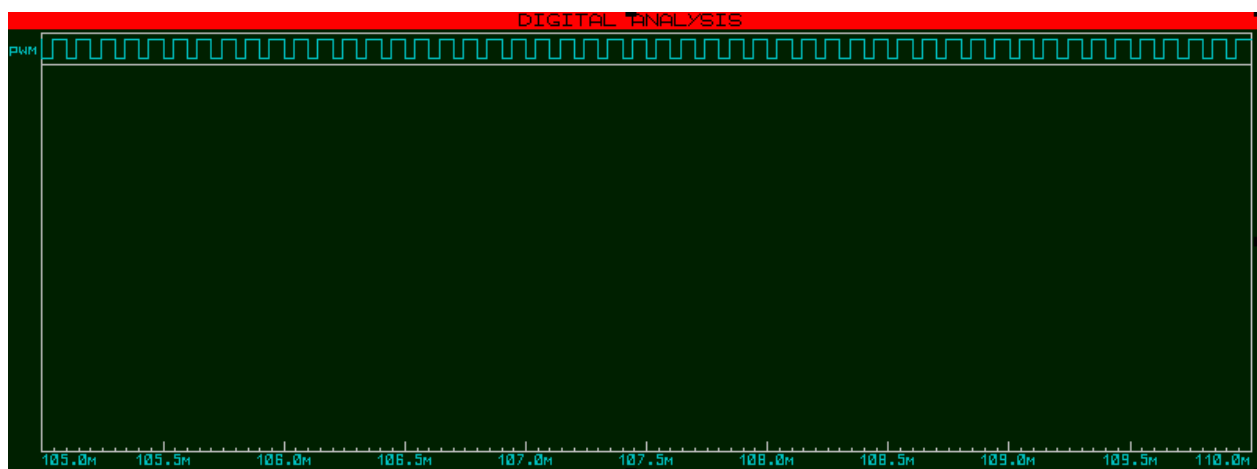


**Figure 5.3.5** Output of the PWM from Optocoupler

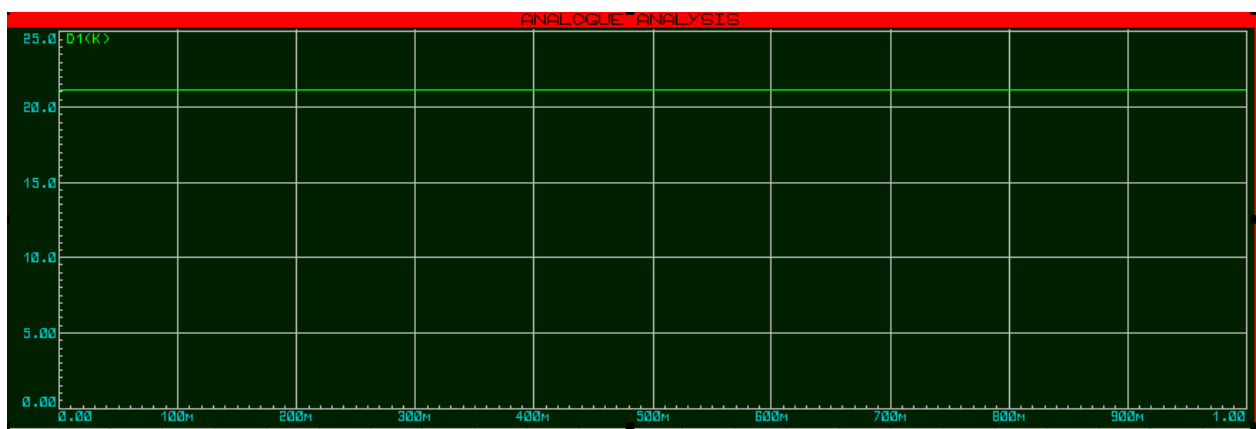


**Figure 5.3.6** Output Voltage

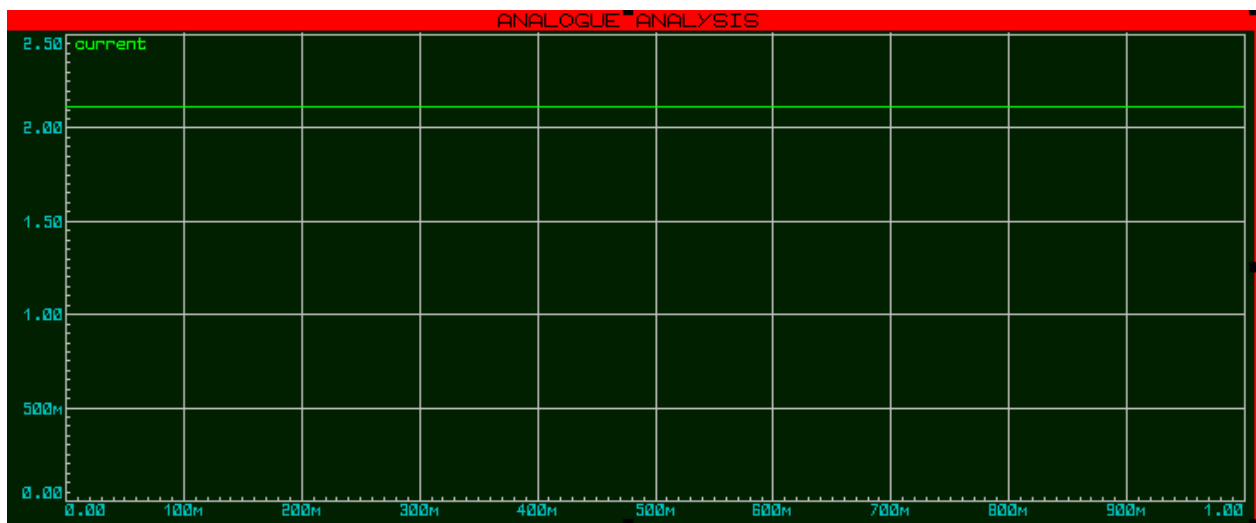


**Figure 5.3.7** Output of the Current from Current Transfor

## 5.4 Printed Circuit Board (PCB) Design

For making the system robust and having permanent solution we have designed a PCB board for hardware circuit. It gives less electronics noise and there is no chance of loose connections or short circuit. We can also achieve mass production at lower cost. For designing PCB, we have used Eagle software. The schematic and figure of printed board are given below.

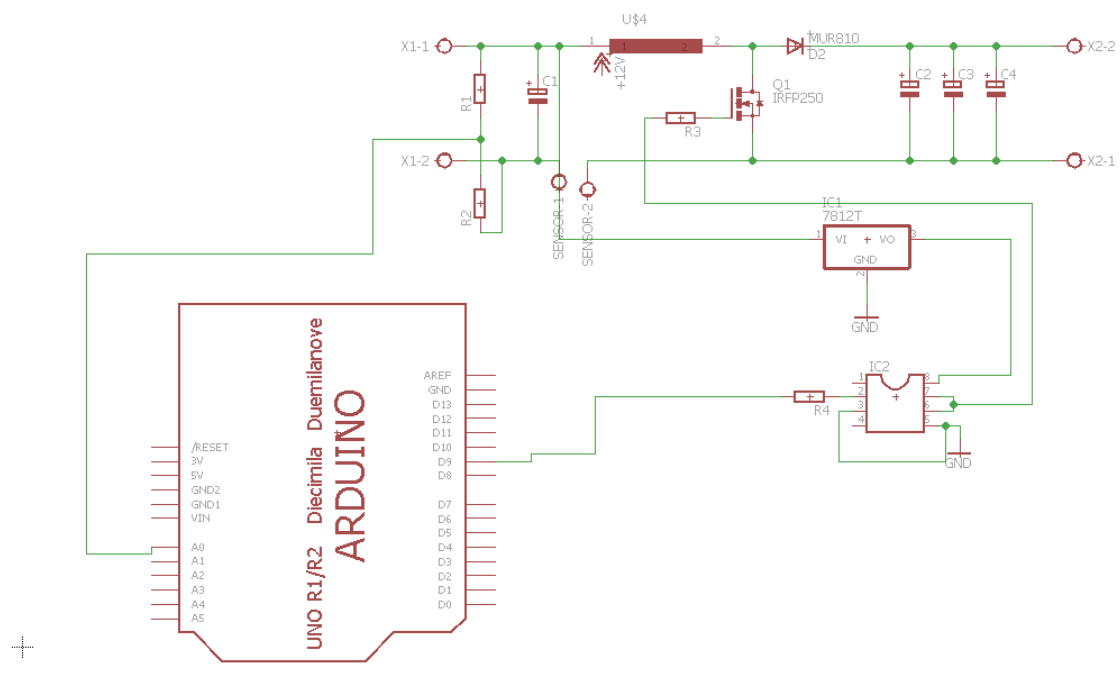


**Figure 5.4.1:** Schematic Design of PCB Board

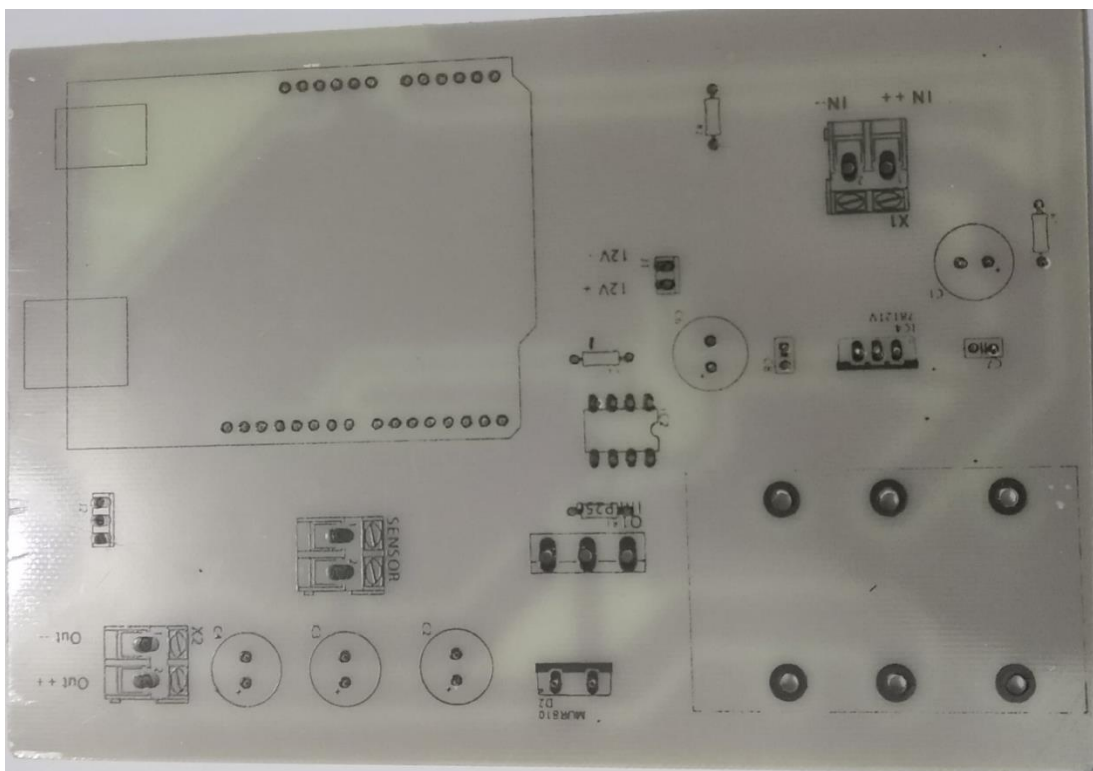


**Figure 5.4.2:** Top of the PCB Board

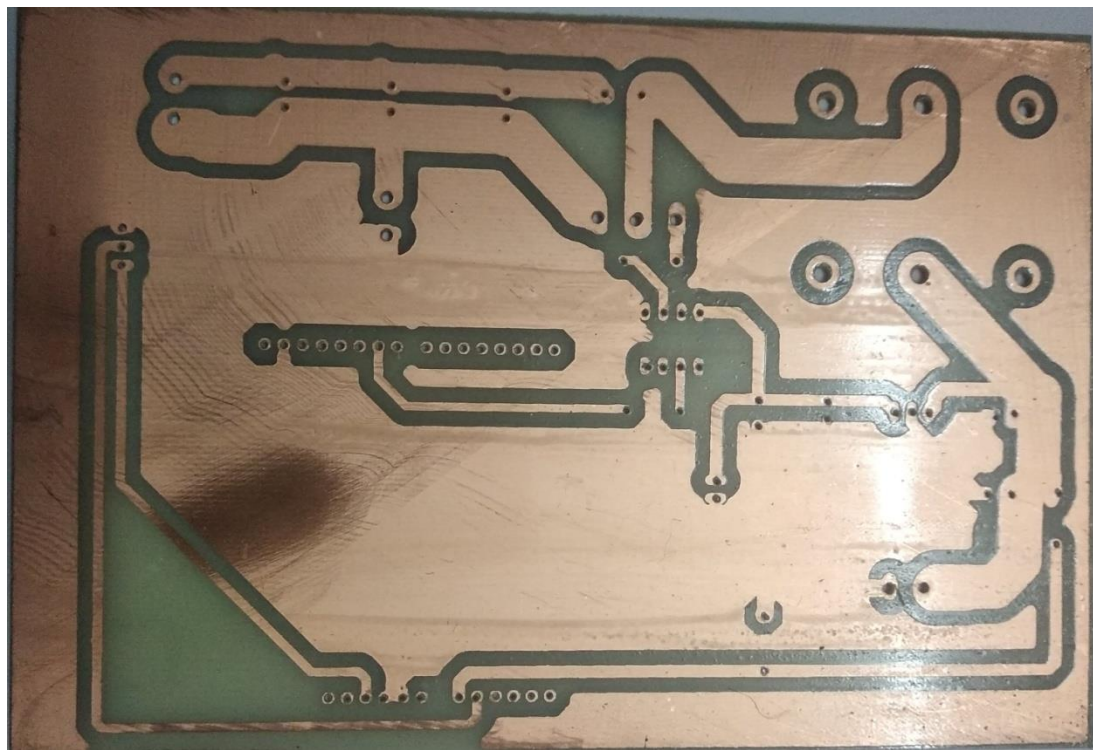


**Figure 5.4.3:** Bottom of the PCB Board

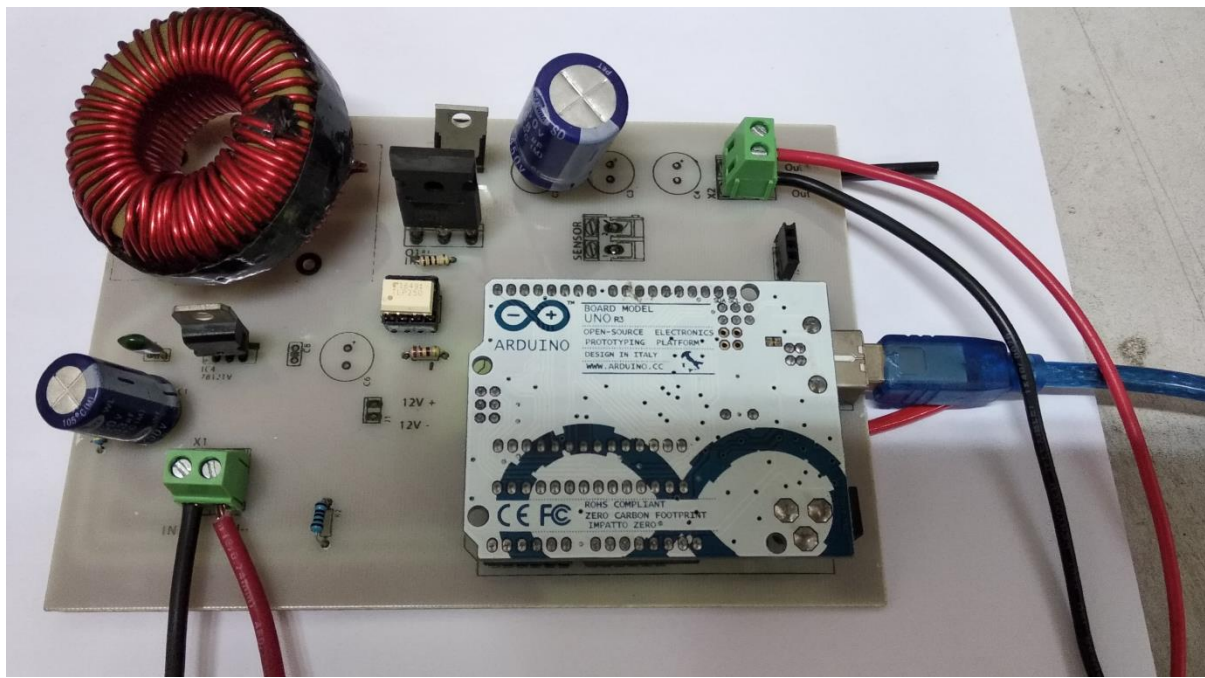


**Figure 5.4.4:** PCB Board with the components

## 5.5 Experimental Setup

In Figure 5.5.1, we connected all the parts and measured the voltage, current, power of the solar panel. Solar panel was continuously converting solar energy to the electrical energy and transferring this power to the batteries through Boost circuit. We were also logging the instantaneous data from Arduino UNO and precede the further calculation.



**Figure 5.5.1:** Full Experimental Setup

## 5.6 Result Analysis

We have recorded the data from Arduino UNO to Microsoft Excel through Teraterm software. There we have saved the voltage, current, power of the Solar panel and also the duty cycle. The tables and the graphs of the c are given below.

We have manually initialized the duty cycle and observed the output data of solar panel. Then varying the duty cycle (0%-100%) we could see that the current was increasing and so was the power. Then for initializing the duty cycle at 45% we have reached close to the maximum current (2.3A-2.4A) and found the maximum possible output power of the solar panel. Therefore, we chose 45% to be our base duty cycle.

For each initial value of duty cycle Arduino has calculated the next duty cycle observing the change of voltage and current according to the Incremental Conductance Algorithm.

### Initial duty cycle – 30%

Voltage	Current	Power	Calc. V <sub>out</sub>	Decision	Duty Cycle
17.09	0.35	6.02	24.38	Increase	30
17.14	0.37	6.28	24.48	Decrease	29.9
17.19	0.36	6.18	24.52	Increase	30
17.21	0.37	6.4	24.58	Decrease	29.9
17.23	0.37	6.39	24.57	Increase	30
17.27	0.37	6.46	24.67	Decrease	29.9
17.34	0.38	6.62	24.74	Decrease	29.8
17.43	0.39	6.84	24.83	Decrease	29.7
17.51	0.41	7.14	24.91	Decrease	29.6
17.58	0.39	6.94	24.97	Increase	29.7
17.62	0.38	6.76	25.06	Increase	29.8

**Table 5.6.1:** Collected data from full hardware when initial duty cycle was 30%

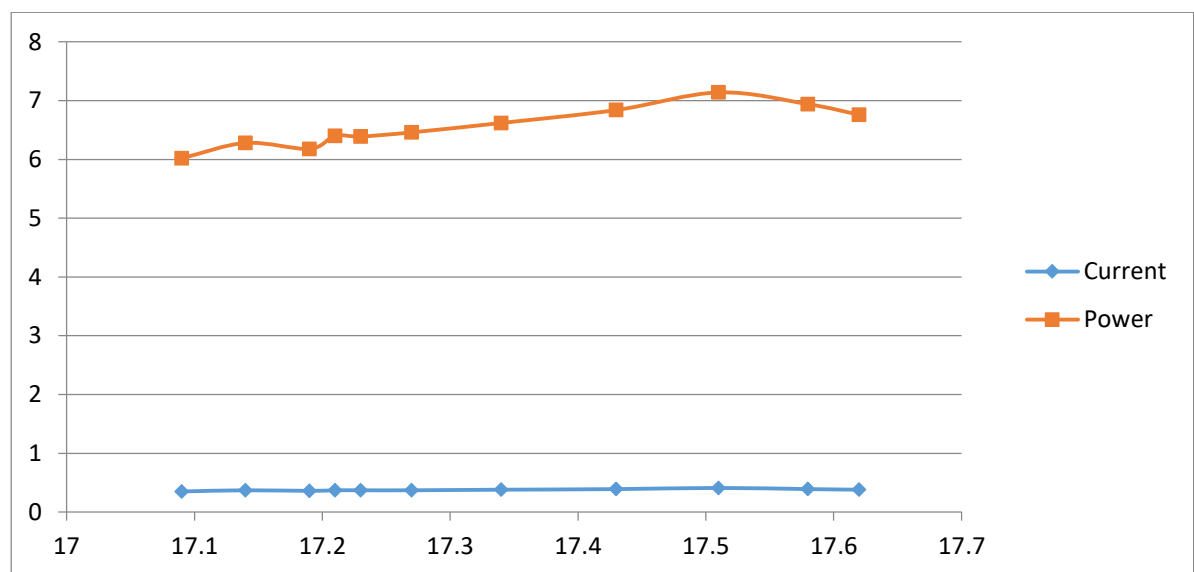


**Figure 5.6.1:** Current vs. Voltage (Blue) and Power vs. Voltage (Orange) Graph - Initial duty cycle – 30%

**Initial duty cycle – 35%**

Voltage	Current	Power	Calc. V <sub>out</sub>	Decision	Duty Cycle
16.99	0.93	15.83	26.29	No Change	350
16.98	0.9	15.32	26.29	No Change	35.0
16.99	0.96	16.3	26.29	Increase dellI	35.5
16.96	0.96	16.29	26.3	Decrease	35.4
16.98	0.94	16.05	26.29	Increase	35.5
16.96	0.96	16.36	26.3	Increase	35.6
16.95	0.95	16.1	26.32	Decrease	35.5
16.96	0.94	15.89	26.3	Increase	35.6
16.95	0.95	16.12	26.32	Increase	35.7
16.93	0.99	16.78	26.32	Increase	35.8
16.93	0.98	16.6	26.36	No Change	35.8
16.93	0.99	16.68	26.36	No Change	35.8
16.92	0.99	16.7	26.36	No Change	35.8
16.92	0.99	16.75	26.35	No Change	35.8
16.92	0.96	16.25	26.35	No Change	35.8
16.92	0.99	16.74	26.36	No Change	35.8
16.92	0.96	16.25	26.35	No Change	35.8
16.92	0.99	16.7	26.36	No Change	35.8
16.92	0.97	16.4	26.35	No Change	35.8
16.92	0.98	16.63	26.35	No Change	35.8

**Table 5.6.2:** Collected data from full hardware when initial duty cycle was 35%

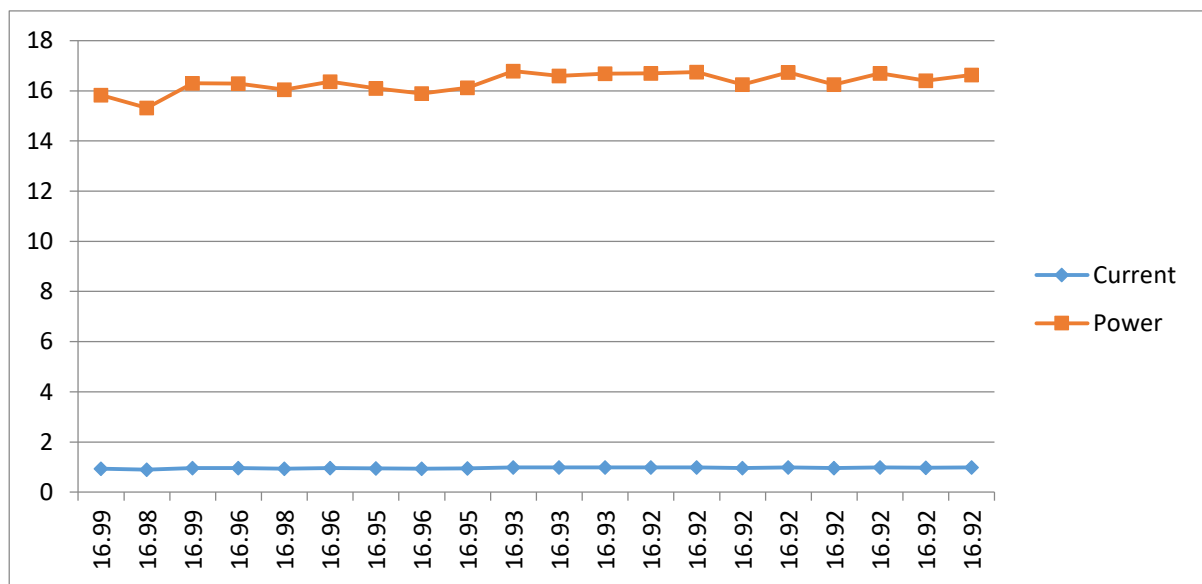


**Figure 5.6.2:** Current vs. Voltage (Blue) and Power vs. Voltage (Orange) Graph - Initial duty cycle – 35%

**Initial duty cycle – 40%**

Voltage	Current	Power	Calc. V <sub>out</sub>	Decision	Duty Cycle
16.12	1.66	26.81	26.86	Increase	40.1
16.09	1.67	26.81	26.87	Decrease	40
16.13	1.66	26.69	26.88	Increase	40.1
16.11	1.65	26.5	26.89	Decrease	40
16.13	1.61	25.92	26.89	Increase	40.1
16.11	1.67	26.97	26.89	Increase	40.2
16.08	1.68	27.04	26.89	Increase	40.3
16.09	1.68	27.05	26.95	No Change	40.3
16.09	1.73	27.84	26.95	No Change	40.3
16.08	1.72	27.73	26.94	No Change	40.3
16.08	1.7	27.33	26.94	No Change	40.3
16.08	1.68	27	26.94	No Change	40.3
16.08	1.69	27.18	26.93	No Change	40.3
16.08	1.65	26.56	26.93	No Change	40.3
16.08	1.68	27.01	26.93	No Change	40.3
16.07	1.7	27.26	26.92	No Change	40.3
16.08	1.67	26.82	26.93	No Change	40.3
16.08	1.68	27	26.93	No Change	40.3
16.08	1.68	26.96	26.93	No Change	40.3
16.07	1.66	26.62	26.92	No Change	40.3

**Table 5.6.3:** Collected data from full hardware when initial duty cycle was 40%

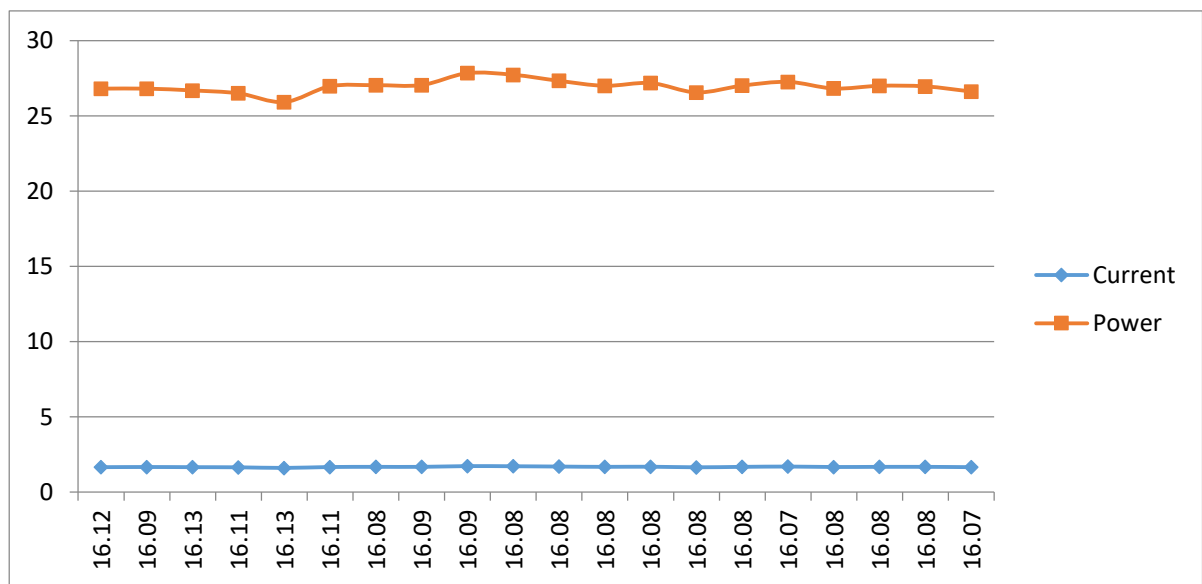


**Figure 5.6.3:** Current vs. Voltage (Blue) and Power vs. Voltage (Orange) Graph - Initial duty cycle – 40%

**Initial duty cycle – 45%**

Voltage	Current	Power	Calc. V <sub>out</sub>	Decision	Duty Cycle
15.02	2.35	35.28	27.47	Increase	45.4
15	2.38	35.64	27.48	Increase	45.5
14.97	2.33	34.91	27.47	Decrease	45.4
15	2.35	35.19	27.47	Decrease	45.3
15.03	2.35	35.37	27.47	Decrease	45.2
15.06	2.32	34.95	27.47	Increase	45.3
15.03	2.35	35.28	27.48	Increase	45.4
15	2.33	34.98	27.47	Decrease	45.3
15.03	2.36	35.49	27.47	Decrease	45.2
15.06	2.33	35.01	27.47	Increase	45.3
15.02	2.33	35.02	27.46	No Change	45.3
15.02	2.35	35.28	27.47	Increase	45.4
15	2.38	35.64	27.48	Increase	45.5
14.97	2.33	34.91	27.47	Decrease	45.4
15	2.35	35.19	27.47	Decrease	45.3
15.03	2.35	35.37	27.47	Decrease	45.2
15.06	2.32	34.95	27.47	Increase	45.3
15.03	2.35	35.28	27.48	Increase	45.4
15	2.33	34.98	27.47	Decrease	45.3
15.03	2.36	35.49	27.47	Decrease	45.2

**Table 5.6.4:** Collected data from full hardware when initial duty cycle was 45%

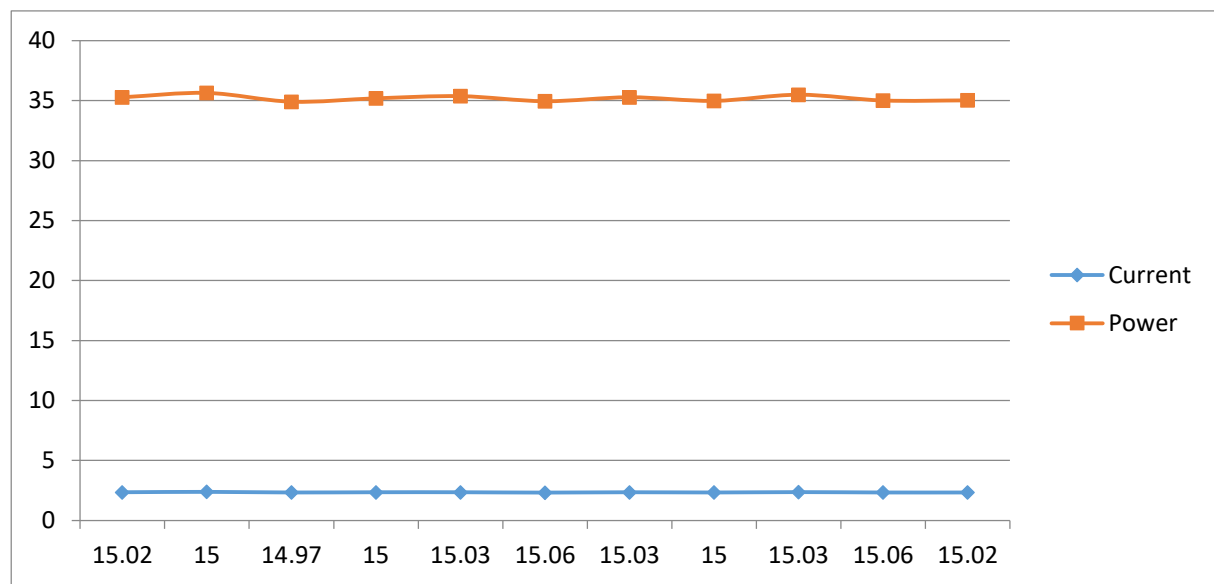


**Figure 5.6.4:** Current vs. Voltage (Blue) and Power vs. Voltage (Orange) Graph - Initial duty cycle – 45%

## **Chapter 6**

### **Conclusion**

#### **6.1 Summary**

In the final analysis, this thesis presents an efficient photo voltaic system with the capability of tracking the maximum power point using incremental conductance method. Each components of the system such as the solar panel, charge controller, DC-DC converter has all been discussed. The coding in terms of algorithm flowchart, proteus software simulation and Arduino code has been presented. Since the purpose of this thesis was to design an efficient MPPT solar charge controller using an Arduino, we have explained the maximum power point tracking and the procedure we have followed to achieve it. The use of an Arduino and its advantages has been provided along with the converter used for our design of the solar charge controller. We have later done the hardware implementation and matched the data we collected to support the incremental conductance method.

#### **6.2 Future Prospects**

Solar Energy is the ultimate source of ultra clean, sustainable and natural energy. Most importantly it is the most cost efficient energy source we can use in our favor and for securing financial benefits. In this regard developing more efficient charge controller is a progressive step to fulfill the need of power generation using green energy. For that purpose it is our wish to continue further study on making the PV module more efficient. To be specific, the charge controller can be improved by improving the algorithm. A better approach to the incremental conductance method is a variable step size incremental conductance algorithm, which automatically adjusts the step size to track the PV module's maximum power point. Compared with the implemented fixed step size method, this approach can effectively improve the MPPT speed and accuracy simultaneously. Furthermore, it is simple and can be easily implemented in digital signal processors. Another scope of future work is to implement the modified incremental conductance method for PV systems connected to grid.

## **Bibliography**

- choudhary, dhananjay and saxena, ammol ratna (2014) ‘DC-DC buck converter for MPPT of PV system’, *International Journal of Emerging Technology and Advanced Engineering*, 4(7).
- Kotak, V.C. and Tyagi, P. (2013) ‘DC To DC Converter in Maximum Power Point Tracker’, *International Journal of Advanced Research in Electrical, Electronics and Instrumentation Engineering*, 2(12).
- radio-electronis.com (no date)  
Available at: <http://www.radio-electronics.com/info/power-management/switching-mode-power-supply/step-down-buck-regulator-converter-basics.php>
- Harjai, A., Bhardwaj, A. and Sandhibigraha, M. (no date) ‘*STUDY OF MAXIMUM POWER POINT TRACKING (MPPT) TECHNIQUES IN A SOLAR PHOTOVOLTAIC ARRAY*’.
- utri, R.I., Wibowo, S. and Rifa’i, c M. (2015) ‘*Maximum power point tracking for Photovoltaic using incremental Conductance method ☆*’, Energy Procedia, 68, pp. 22–30. doi: 10.1016/j.egypro.2015.03.228.
- Kumari, S.J., Babu, C.S. and Professor, A. (2011) ‘*COMPARISON OF MAXIMUM POWER POINT TRACKING ALGORITHMS FOR PHOTOVOLTAIC SYSTEM*’, *International Journal of Advances in Engineering & Technology ©IJAET*, 1(5), pp. 133–148.
- Keeping, S. (2014) *Voltage- and current-mode control for PWM signal generation in DC-to DC switching regulators*.  
Available at: <http://www.digikey.com/en/articles/techzone/2014/oct/voltage-and-currentmode-control-for-pwm-signal-generation-in-dc-to-dc-switching-regulators>
- Pürschel, M. (2009) *Automotive Power*.  
Available at: <http://www.infineon.com/dgdl/Reverse-Battery-ProtectionRev2.pdf?fileId=db3a304412b407950112b41887722615>

- Rahman, S., Sultana, N. and Masud, Q. (2012) *Design of a Charge Controller Circuit with Maximum Power Point Tracker (MPPT) for Photovoltaic System*. Thesis Report, BRAC University (2012),  
Available at:  
<http://dspace.bracu.ac.bd/xmlui/bitstream/handle/10361/2389/Design%20of%20a%20Charge%20Controller%20Circuit.pdf.pdf?sequence=1&isAllowed=y>
- *News & analysis*  
Available at:  
[http://www.globalspec.com/learnmore/optics\\_optical\\_components/optoelectronics/optocouplers](http://www.globalspec.com/learnmore/optics_optical_components/optoelectronics/optocouplers) (Accessed: 12 August 2016).
- L.N.T, L., M.W.N.S, L., K.K, N. and W.M.W, W. (2014) *Development Of Smart Grid With Renewable Energy sources*.
- Hua, C., Lin, J. and Shen (1998) ‘*Implementation Of a DSP-Controlled Photo-voltaic System with Peak Power Point Tracker*’, IEEE TRANSACTIONS ON INDUSTRIAL ELECTRONICS, 45(1).
- Thenkani, A. (2011) ‘*Design Of Optimum Power Point Tracking Algorithm For Solar Panel*’, Tamilnadu, India: ICCCET

## Appendix A

### **Code implemented in Incremental Conductance Method**

#### **SignalGenerator Library (.h file):**

```
#ifndef SIGNALGENERATOR_h
#define SIGNALGENERATOR_h
#include <avr/io.h>
#include <avr/interrupt.h>
#include <avr/pgmspace.h>
#define RESOLUTION 65536 // Timer1 is 16 bit
#define TOTAL_SAMPLES 160

const uint16_t sinewave[] PROGMEM =
{0, 0, 10, 15, 20, 24, 29, 34, 39, 44, 49, 53, 58, 63, 68, 72, 77, 82, 86, 91, 95, 100, 104, 109,
113, 117,
122, 126, 130, 134, 138, 142, 146, 150, 154, 158, 162, 165, 169, 173, 176, 179, 183, 186,
189, 192, 196, 199,
201, 204, 207, 210, 212, 215, 217, 220, 222, 224, 226, 228, 230, 232, 234, 235, 237, 238,
240, 241, 242, 243,
244, 245, 246, 247, 247, 248, 248, 249, 249, 249, 249, 249, 249, 249, 248, 248, 247, 247,
246, 245, 244, 243,
242, 241, 240, 238, 237, 235, 234, 232, 230, 228, 226, 224, 222, 220, 217, 215, 212, 210,
207, 204, 201, 199,
196, 192, 189, 186, 183, 179, 176, 173, 169, 165, 162, 158, 154, 150, 146, 142, 138, 134,
130, 126, 122, 117,
113, 109, 104, 100, 95, 91, 86, 82, 77, 72, 68, 63, 58, 53, 49, 44, 39, 34, 29, 24, 20, 15, 0, 0};
```

```
class Timerone
{
public:
// properties
unsigned int pwmPeriod;
unsigned char clockSelectBits;
char oldSREG;      // To hold Status Register while ints disabled

void initialize(long microseconds=1000000);
void setPeriod(long microseconds);
void setPwmDuty(char pin, int duty);
void resume();
void pwm(char pin, int duty, long microseconds=-1);
void attachInterrupt();
};

extern Timerone timer1;

#endif
```

**SignalGenerator Library (.cpp file):**

```
#ifndef SIGNALGENERATOR_cpp
#define SIGNALGENERATOR_cpp
#include "SignalGenerator.h"

Timerone timer1;
int sample = 0;
bool channel = 0;

ISR(TIMER1_COMPA_vect)
{
    switch(channel)
    {
        case 0:
            OCR1A = pgm_read_byte(&sinewave[sample]);
            OCR1B = 0;

            break;
        case 1:
            OCR1B = pgm_read_byte(&sinewave[sample]);
            OCR1A = 0 ;
            break;
    }
    sample++;
    if (sample>=160)
    {
        sample=0;
        channel ^=1;
    }
}
```

```

void Timerone::initialize(long microseconds)
{
    TCCR1A = 0;
    TCCR1B = _BV(WGM13);
    setPeriod(microseconds);
}

void Timerone::setPeriod(long microseconds)
{
    long cycles = (F_CPU / 2000000) * microseconds;
    if(cycles < RESOLUTION)          clockSelectBits = _BV(CS10);
    else if((cycles >>= 3) < RESOLUTION) clockSelectBits = _BV(CS11);
    else if((cycles >>= 3) < RESOLUTION) clockSelectBits = _BV(CS11) | _BV(CS10);
    else if((cycles >>= 2) < RESOLUTION) clockSelectBits = _BV(CS12);
    else if((cycles >>= 2) < RESOLUTION) clockSelectBits = _BV(CS12) | _BV(CS10);
    else      cycles = RESOLUTION - 1, clockSelectBits = _BV(CS12) | _BV(CS10);

    oldSREG = SREG;
    cli();           // Disable interrupts for 16 bit register access
    ICR1 = pwmPeriod = cycles;
    SREG = oldSREG;

    TCCR1B &= ~(_BV(CS10) | _BV(CS11) | _BV(CS12));
    TCCR1B |= clockSelectBits;
}

```

```

void Timerone::setPwmDuty(char pin, int duty)
{
    unsigned long dutyCycle = pwmPeriod;

    dutyCycle *= duty;
    dutyCycle >>= 10;

    oldSREG = SREG;
    cli();
    if(pin == 1 || pin == 9)      OCR1A = dutyCycle;
    else if(pin == 2 || pin == 10) OCR1B = dutyCycle;
    SREG = oldSREG;
}

```

```

void Timerone::pwm(char pin, int duty, long microseconds)
{
    if(microseconds > 0) setPeriod(microseconds);
    if(pin == 1 || pin == 9) {
        DDRB |= _BV(PORTB1);
        TCCR1A |= _BV(COM1A1);
    }
    else if(pin == 2 || pin == 10) {
        DDRB |= _BV(PORTB2);
        TCCR1A |= _BV(COM1B1);
    }
    setPwmDuty(pin, duty);
    resume();
}

```

```

void Timerone::resume()
{
    TCCR1B |= clockSelectBits;
}

void Timerone::attachInterrupt()
{
    sei();      //global interrupt enable
    TIMSK1 |= 1<<OCIE1A; //Timer/Counter1, Output Compare A Match Interrupt Enable
}
#endif

```

### Main Code:

```
#include "SignalGenerator.h"
```

```

int analogPin0 = A1;
const int analogIn = A0;
int mVperAmp = 185;
int RawValue = 0;
double ACSoffest = 2500;
double Voltage = 0;
double Amps = 0;
//int ledPin = 13;
double duty_cycle1 = 70;
double vltg_i = 0;
double Amps_i = 0;
double pwr_i = 0;
int mltp = 5;
const int fanPin = 9;

```

```

void setup() {
    pinMode(13, OUTPUT);
    Serial.begin(9600);
    timer1.initialize(100); // 100 us = 10 kHz
}

void loop() {
    Amps = 0;
    double vltg = 0;
    for (int count = 1; count<=100; count++)
    {
        int vlt_rl = analogRead(analogPin0);
        int rfrnc = 5;
        double vltg1 = mltp * (vlt_rl * rfrnc) / 1023;
        vltg = vltg + vltg1;
        RawValue = analogRead(analogIn);
        Voltage = (RawValue / 1023) * 5000;
        double Amps1 = ((Voltage-ACSooffest) / mVperAmp);
        Amps = Amps + Amps1;
    }
    vltg = vltg / 100;
    Serial.print("\t Voltage ===== ");
    Serial.println(vltg);
}

```

```
double del_vltg = vltg - vltg_i;  
Amps = Amps / 100;  
double del_Amps = Amps - Amps_i;  
double pwr = vltg * Amps;
```

```
Serial.print("\t Current ===== ");  
Serial.println(Amps);
```

```
if(del_vltg== 0)  
{  
    if(del_Amps == 0)  
    {  
        duty_cycle1 = duty_cycle1;  
    }  
    else  
    {  
        if(del_Amps > 0)  
        {  
            duty_cycle1 = duty_cycle1 + 0.01;  
        }  
        else  
        {  
            duty_cycle1 = duty_cycle1 - 0.01;  
        }  
    }  
}
```

```

else
{
    double inc_cond = del_Amps / del_vltg;
    double ins_cond = Amps / vltg;
    if(inc_cond + ins_cond == 0)
    {
        duty_cycle1 = duty_cycle1;
    }
    else
    {
        if(inc_cond + ins_cond > 0)
        {
            duty_cycle1 = duty_cycle1 + 0.1;
        }
        else
        {
            duty_cycle1 = duty_cycle1 - 0.1;
        }
    }
}

vltg_i = vltg;
Amps_i = Amps;
Serial.print("\tPower === ");
Serial.println(pwr);
Serial.print("\tduty_cycle === ");
Serial.println(duty_cycle1);
Serial.print("\n \n \n \n");
timer1.pwm(fanPin, (duty_cycle1 / 100) * 1023);
delay(500);
}

```

## Appendix B

### Circuit implementation in PCB (Printed Circuit Board)

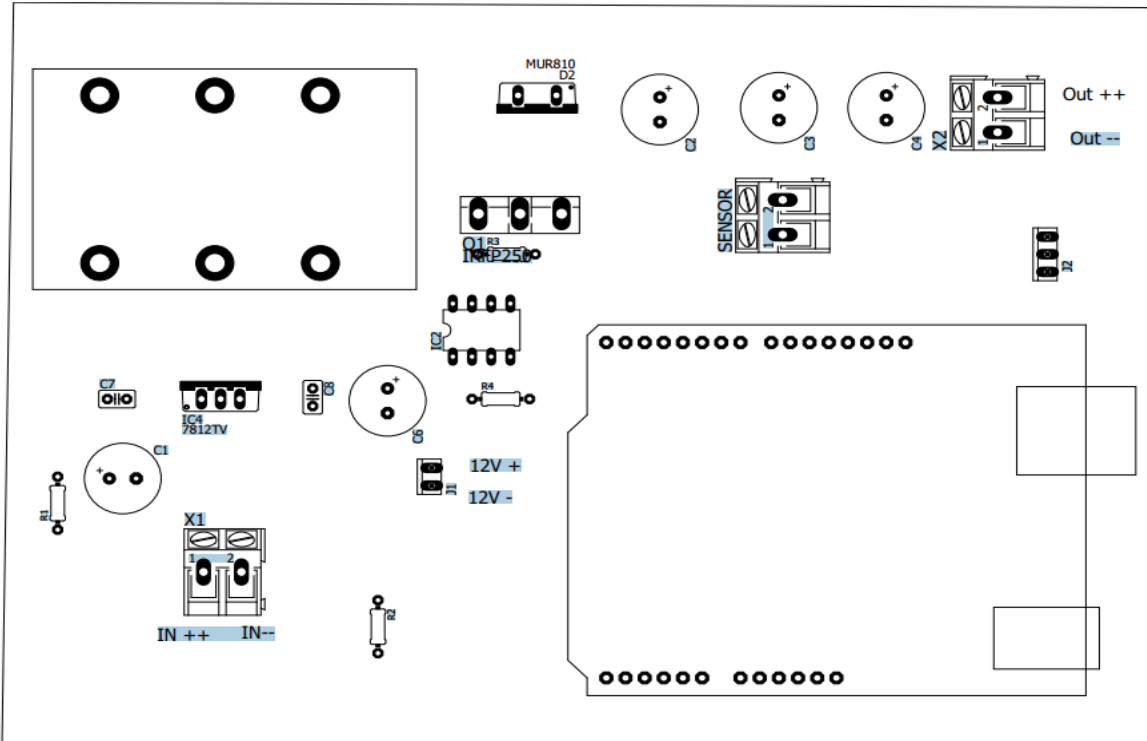


Figure B.1: Top Silk of PCB Board

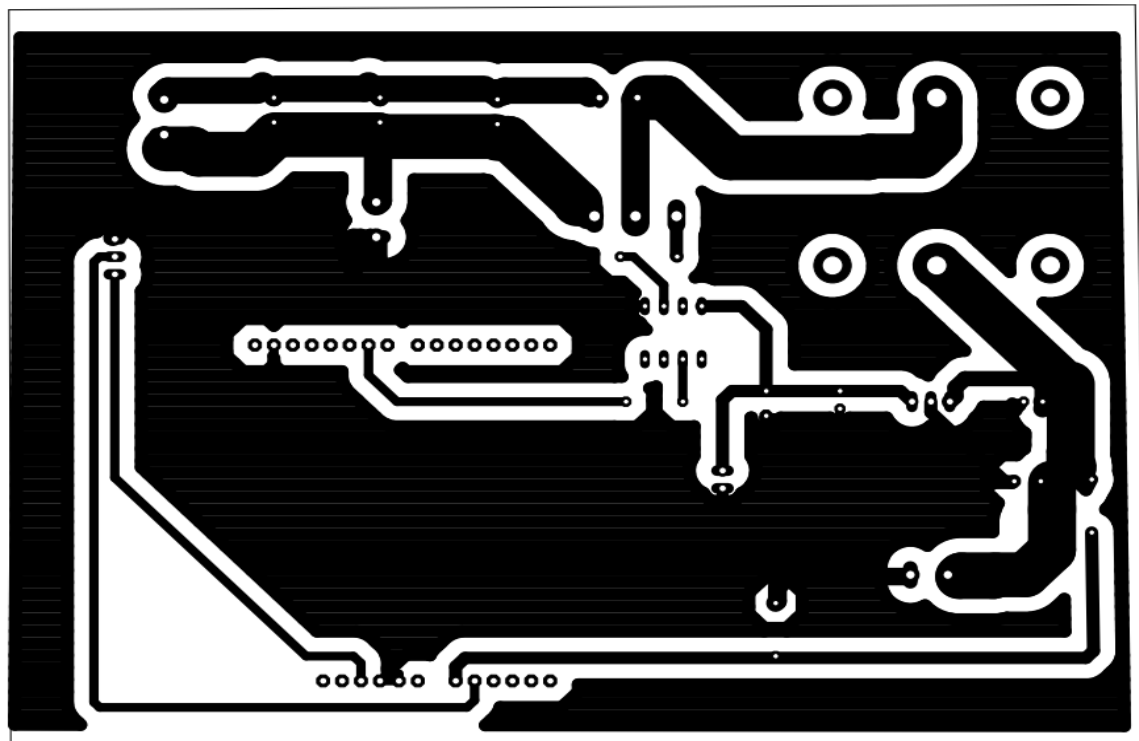


Figure B.2: Bottom Copper of PCB Board

## **Appendix C**

### **Abbreviations**

- PV – Photo Voltaic
- MPPT – Maximum Power Point Tracking
- AC – Alternating Current
- DC – Direct Current
- P&O Method – Perturb and Observe Method
- I&C Method – Incremental and Conductance Method
- LED – Light Emitting Diode
- SCR – Silicon Controlled Rectifier
- MOSFET – Metal Oxide Field Effect Transistor
- PCB – Printed Circuit Board

## **Appendix D**

### **Solar Panel Characteristics**

- Company – Power4U
- Dimension – 1088\*540\*33
- Maximum Power – 65W
- Tolerance of  $P_{max}$  – 0-3%
- Rated Voltage ( $V_{MPP}$ ) – 17.8V
- Rated Current ( $I_{MPP}$ ) – 3.66A
- Open Circuit Voltage ( $V_{OC}$ ) – 22.3V
- Short-Circuit Current ( $I_{SC}$ ) – 3.94A
- Maximum System Voltage – 1000V
- Weight – 7.19kg
- Manufacturer Company – NINGBO AIKE SOLAR CO. LTD
- Country - China